CHARLES UNIVERSITY

Faculty of Medicine in Hradec Králové

DISSERTATION

PharmDr. Natália Matyašovská **2024**

Doctoral Degree Programme

Clinical Biochemistry

Molecular profiling to reveal novel signatures in cancer

Molekulární profilování k odhalení nových signatur u nádorových onemocnění

PharmDr. Natália Matyašovská

Supervisor: prof. MUDr. Vladimír Palička, CSc., Dr.h.c.

Hradec Králové, 2024

Author‘s Declaration

Declaration:

I declare hereby that this dissertation thesis is my own original work and that I indicated by references all used information sources. I also agree with depositing my dissertation in the Medical Library of the Charles University, Faculty of Medicine in Hradec Králové and with making use of it for study and educational purpose provided that anyone who will use it for his/her publication or lectures is obliged to refer to or cite my work properly.

I give my consent to availability of my dissertation’s electronic version in the information system of the Charles University.

Hradec Králové, 2024 **Signature of the author**

Acknowledgments

Na tomto mieste by som chcela vyjadriť svoju úprimnú a srdečnú vďaku všetkým, ktorí ma podporovali a pomáhali mi počas môjho štúdia, výskumu a písania dizertačnej práce. Bez Vašej neoceniteľnej pomoci by táto práca nikdy nevznikla.

V prvom rade patrí moje najhlbšie poďakovanie môjmu školiteľovi, profesorovi MUDr. Vladimírovi Paličkovi, CSc., Dr.h.c. Vaša trpezlivosť, múdrosť a neustála podpora boli pre mňa nesmierne cenné. Vaše odborné vedenie, ústretovosť a schopnosť motivovať ma počas celého tohto náročného procesu, mi pomohli prekonať nemalé prekážky. Vaše dobré srdce, cenné rady a pripomienky ma nasmerovali správnym smerom a umožnili mi rásť nielen ako študent, ale aj ako človek.

Veľká vďaka patrí aj mojim kolegom a priateľom z Ústavu klinickej biochémie a diagnostiky, konkrétne Marcele Slavíčkovej, Ph. D, Helene Párovej, Ph. D, a Ivane Baranovej Ph. D, ktoré mi poskytovali nielen odbornú pomoc, ale aj morálnu podporu. Špeciálne ďakujem "Královi detekce", Martinovi Uhrovi, Ph.D. ktorý ma naučil najdôležitejšie základy multitaskingu, kritického myslenia, trpezlivosti a zodpovednosti v laboratóriu. S týmito pevnými základmi boli každé ďalšie metodiky či experimenty jednoduchšie. Taktiež moje ďakujem patrí aj jeho manželke, RNDr. Veronike Uhrovej (čoskoro PhD.), vďaka ktorej som sa mohla uchádzať o pozíciu vo výskume, s ktorou sme sa spoločne vybrali na túto náročnú cestu, prežili dlhé hodiny diskusií a experimentov, občas aj frustrácie, no neúnavne si pomáhali v čase, keď sme to najviac potrebovali. Ich podpora a priateľstvo boli pre mňa neoceniteľné a dodávali mi silu pokračovať.

Rada by som tiež vyjadrila svoju vďaku Univerzite Karlovej, Lekárskej Fakulte v Hradci Králové a Fakultnej Nemocnici v Hradci Královej, ktoré mi poskytli finančnú podporu nevyhnutnú pre môj výskum a možnosť vycestovať na zahraničnú vedeckú stáž.

Special thanks also goes to the entire scientific institution MultiplexDX in Bratislava, under the leadership of Pavol Čekan, PhD., where I had the opportunity to complete my internship. The internship at this institution was a great opportunity for me to gain invaluable experience and knowledge. Working in an international team of scientists allowed me not only to broaden my professional horizons, improve my English language, but also to establish valuable professional contacts. Your willingness and openness to share your knowledge and experience has been extremely inspiring and enriching for me. Furthermore, I would like to thank Professor Neil Renwick, MD, PhD. D., and Queen's University for their

significant collaboration and support. I would also like to thank the Ontario Biobank for providing me with the samples I needed for my research. "We gratefully acknowledge the Ontario Tumour Bank, which is supported by the Ontario Institute for Cancer Research through funding provided by the Government of Ontario for providing biological materials and associated clinicopathological data."

Poďakovanie patrí aj všetkým účastníkom môjho výskumu. Bez Vašej ochoty spolupracovať a zdieľať svoje skúsenosti by táto práca nemohla vzniknúť. V prvom rade ďakujem RNA-seq alias “Smart and funny” tímu. Vero moja, neskutočne som vďačná za Tvoje priateľstvo a Tvoje láskavé srdce. Ďakujem, že si mi vzorom ako vedeckým, tak ľudským. Ďakujem, že si ma motivovala a povzbudzovala a vždy tu bola pre mňa. Ďakujem Ti aj za cenné pripomienky, odborné rady a konštruktívnu kritiku, čo výrazne prispelo k vylepšeniu tejto práce. Ďakujem za nezabudnuteľné zážitky z worshopu tekutej biopsie v Dánsku, ktorého sme sa mohli so Silvi a Ivkou spoločne zúčastniť. Taktiež úprimné ďakujem patrí kolegyni Natálii Valkovej, PhD., ktorá ma naučila základy bioinformatiky, bola tímovou parťáčkou nie len v labáku či pri analýzach dát, ale aj pri svadobných plánovačkách, či pri každomesačných vínnych večeroch. Ženy moje, Vaše priateľstvo, vedomosti, ochota, dôvera a úprimnosť boli kľúčové pre dosiahnutie aj týchto výsledkov. Michal Gala PhD., bioinformatický, analytický a štatistický guru, Tebe chcem poďakovať za to, že si ma naučil pozerať sa na dáta iným, než biologickým pohľadom, a že si mi trpezlivo vedel zodpovedať na moje nekonečné štatistické či bioinformatické otázky. Vaša podpora a spolupráca boli pre mňa nesmierne cenné a prispeli k úspechu môjho výskumu.

Nemôžem zabudnúť na svoju rodinu. Mojej mamke a ockovi patrí moje nesmierne poďakovanie za ich nekonečnú lásku, trpezlivosť a povzbudenie. Mami, ďakujem za každú modlitbu či obetovanú svätú omšu za moje štúdium. Ďakujem, že si mi bola vzorom a motiváciou, že si vo mňa verila a podporovala ma v dobrých či zlých časoch. Ďakujem, že si prekonala aj nečakaná životné skúšky, aby si tu naďalej pre nás mohla byť. Verím, že čoskoro sa Ti splní jeden z mnohých snov, a to stáť v Karolinu spolu so mnou. Ocik môj, ďakujem Ti, že som mohla študovať, hoci Ťa to stálo dve práce a nekonečné hodiny nadčasov. Bez Vašej obety by som nedokázala dosiahnuť to, čo som dosiahla. Ďakujem Vám, že ste mi dali viac, ako ste mali Vy, aby som sa ja mohla mať lepšie. Vaša viera a podpora vo mňa mi dávala silu pokračovať aj v tých najťažších chvíľach. Ďakujem aj mojej sestre Simke a bratovi Maťkovi za ich neustálu podporu, za to, že ma od malička učili priebojnosti a za to, že vždy verili v môj úspech.

V neposlednom rade by som chcela vyjadriť svoju hlbokú vďačnosť aj môjmu manželovi Janíkovi. Ani nevieš aká som vďačná, že Boh mi Ťa poslal do cesty. Ty moja každodenná radosť, láska, trpezlivosť, povzbudenie, motivácia, pokora a vďaka. Ďakujem Ti, za Tvoju podporu a pomocnú ruku, ktorá ma dvíhala vždy, keď som bola v koncoch. Ďakujem, že si mi pomáhal nájsť vždy tú cestu, ktorou to pôjde, aj keď som ju ja nevnímala. Ďakujem, že si ma naučil, že je v poriadku zlyhať, alebo nenaplniť očakávania iných. Ďakujem za Tvoje pochopenie a lásku počas celého procesu tvorby tejto dizertačnej práce. Ďakujem Ti, že si ťahal domácnosť niekoľko týždňov sám, len aby som ja mohla písať. Som veľmi vďačná, že som mala práve Teba po svojom boku, lebo Ty sám vieš, aký to je proces, keďže si si tým sám prešiel. Rovnako by som chcela poďakovať aj tvojím milujúcim a fantastickým rodičom, a Miškovi s Majkou, za ich neustálu pomoc a záujem. Ich podpora a viera vo mňa boli pre mňa nesmierne dôležité a dodali mi silu pokračovať. Z celého srdca vám ďakujem.

Rovnako chcem poďakovať aj svojim priateľom, ktorí ma počas celého štúdia podporovali a dodávali mi energiu. Ďakujem Vám za vaše pochopenie, keď som nemohla tráviť s Vami toľko času, koľko by som si priala. Vaša trpezlivosť a povzbudenie boli pre mňa veľmi dôležité a vážim si, že ste vždy stáli pri mne.

Na záver by som chcela poďakovať všetkým, ktorí priamo alebo nepriamo prispeli k vzniku tejto práce. Vaša podpora, pomoc a povzbudenie boli pre mňa nesmierne cenné a som Vám za to veľmi vďačná.

The study was supported by the Ministry of Health of the Slovak Republic under registration number 2019/69 MXDX-1, by the Ministry of Health Czech Republic conceptual development of research organization (UHHK, 00179906), by the Charles University, project GA UK (SVV UK, LFHK, No. 260657), and by the program Cooperatio, research area DIAG.

Table of Contents

Acknowledgments 5

Summary CZE 10

Summary ENG 11

List of abbreviations 12

1 INTRODUCTION 15

1.1 Primary pancreatic tumors 15

1.2 Pancreatic neuroendocrine neoplasm (PanNEN) 16

1.2.1 Definition and epidemiology 16

1.2.2 Diagnosis, classification, and clinical presentation 17

1.2.4 The pathway-based landscape of PanNETs pathophysiology 22

1.3 Biomarkers of PanNENs 25

1.3.1 General biomarkers 26

1.3.2 Specific biomarkers 27

1.3.3 Immunohistochemical tissue biomarkers 29

1.3.4 Theranostic markers 31

1.3.5 Novel liquid biomarkers 32

1.4 miRNAs 33

1.4.1 miRNA biogenesis 34

1.4.2 miRNA and cancer 38

1.5 miRNA vs. mRNA expression profiling 49

1.6 miRNA target identification and prediction 50

2 OBJECTIVES 52

3 MATERIAL AND METHODS 53

3.1 Patient cohort/Study group 53

3.2 Total RNA isolation 56
3.3 RNA library preparation and sequencing 56
3.3.1 RNA sequencing data processing and differential expression analysis 58
3.3.2 Focused analysis of expression levels of key clinicopathological markers 59
3.3.3 Molecular subtyping of PanNETs 59
3.4 Small RNA library preparation and sequencing 60
3.4.1 Small RNA-seq data processing and differential expression analysis 61
3.4.2 Validation of miRNA expression 61
3.4.3 miRNA target identification and miRNA-mRNA interaction network 62
3.4.4 Correlation of the miRNA-mRNA predicted targets 63
3.4.5 GO term & KEGG pathway enrichment analysis 63
4 RESULTS 64
4.1 Differential expression analysis of mRNAs 64
4.1.1 Functional enrichment analysis of differentially expressed mRNAs 66
4.2 Assessment of expression levels of important clinicopathological markers 70
4.3 Molecular subtyping of PanNETs 71
4.4 Differential expression analysis of miRNAs 75
4.5 Validation of miRNA-seq results 79
4.6 Construction of the miRNA-mRNA interaction network 81
4.7 Correlation of the miRNA-mRNA predicted pairs 83
4.8 GO term & KEGG pathway enrichment analysis of target genes 89
5 DISCUSSION 92
6 CONCLUSIONS 100
7 LITERATURE 102

Summary CZE

Zatímco spolehlivé biomarkery pro personalizovanou léčbu neuroendokrinních nádorů slinivky břišní (PanNET) jsou stále omezené, transkriptomické profilování mikroRNA (miRNA) a mRNA se ukázalo jako slibné pro segregaci podtypů PanNET a předpovídání odpovědi na léčbu. Vzhledem k tomu, že miRNA jsou klíčovými posttranskripčními regulátory exprese mRNA, mohla by integrace údajů o dysregulovaných miRNA a mRNA poskytnout zásadní poznatky o molekulární patogenezi PanNEN.

Cílem této studie bylo prozkoumat úlohu exprese mRNA a miRNA v molekulární patogenezi, klinické prezentaci a prognóze PanNETů ve srovnání s kontrolními skupinami bez onemocnění. Bylo provedeno sekvenování RNA za účelem identifikace rozdílně exprimovaných mRNA se zaměřením na klinicko-patologické biomarkery. Vzorky PanNET byly také rozděleny do odlišných molekulárních podtypů na základě transkriptomických profilů. Sekvenování miRNA bylo provedeno za účelem detekce rozdílně exprimovaných miRNA, které byly validovány pomocí kvantitativní PCR v reálném čase a veřejných souborů dat. Poté byla provedena integrativní analýza interakcí miRNA-mRNA s cílem odhalit regulační sítě a funkční dráhy.

Výsledky odhalily významnou dysregulaci 715 upregulovaných a 702 downregulovaných genů v PanNET. Analýza drah umožnila nahlédnout do molekulárních mechanismů, které jsou základem patogeneze PanNET, včetně regulace transportu iontů, vývoje nervového systému a proteolýzy. Analýza exprese klinicko-patologických biomarkerů potvrdila potenciál RNA jako diagnostického zdroje se zvýšenou expresí *CHGA*, *SYP* a *SSTR2*. Vzorky PanNET byly na základě transkriptomických profilů rozděleny do molekulárních podtypů intermediárních nádorů a metastázám podobných/primárních nádorů. Sekvenování miRNA identifikovalo 41 upregulovaných a 19 downregulovaných miRNA u PanNET, přičemž byla potvrzena downregulace miR-216a-5p a miR-216b-5p. Integrační analýza sítě miRNA-mRNA ukázala, že došlo k dysregulaci drah zahrnujících buněčnou adhezi, metabolismus a biosyntézu mucinu.

Závěrem lze říci, že tato studie poskytuje komplexní pohled na molekulární krajinu PanNET a zdůrazňuje hodnotu integrovaného transkriptomického profilování pro lepší pochopení jejich patogeneze, klinické prezentace a potenciálních prognostických důsledků. Identifikované regulační sítě miRNA-mRNA si zaslouží další zkoumání jako potenciální diagnostické a terapeutické cíle pro léčbu PanNET.

Summary ENG

While reliable biomarkers for personalized management of pancreatic neuroendocrine tumors (PanNETs) remains limited, transcriptomic profiling of microRNAs (miRNAs) and mRNAs has shown promise in segregating PanNET subtypes and predicting treatment response. Since miRNAs are key post-transcriptional regulators of mRNA expression, integrating data on dysregulated miRNAs and mRNAs could provide critical insights into the molecular pathogenesis of PanNETs.

This study aimed to investigate the role of mRNA and miRNA expression in the molecular pathogenesis, clinical presentation, and prognosis of PanNETs compared to non-diseased controls. RNA sequencing was performed to identify differentially expressed mRNAs, with a focused analysis on clinicopathological biomarkers. PanNET samples were also classified into distinct molecular subtypes based on their transcriptomic profiles. miRNA sequencing was conducted to detect differentially expressed miRNAs, which were validated using quantitative real-time PCR and public datasets. An integrative analysis of miRNA-mRNA interactions was then performed to uncover regulatory networks and functional pathways.

The results revealed significant dysregulation, with 715 upregulated and 702 downregulated genes identified in PanNETs. Pathway analysis provided insights into the molecular mechanisms underlying PanNET pathogenesis, including ion transport regulation, nervous system development, and proteolysis. Expression analysis of clinicopathological biomarkers confirmed the potential of RNA as a diagnostic source, with increased expression of *CHGA*, *SYP*, and *SSTR2*. PanNET samples were classified into intermediate and metastasis-like/primary molecular tumor subtypes based on their transcriptomic profiles. miRNA sequencing identified 41 upregulated and 19 downregulated miRNAs in PanNETs, with validated downregulation of miR-216a-5p and miR-216b-5p. Integrative miRNA-mRNA network analysis implicated dysregulated pathways involving cell adhesion, metabolism, and mucin biosynthesis.

In conclusion, this study provides comprehensive insights into the molecular landscape of PanNETs, highlighting the value of integrated transcriptomic profiling to better understand their pathogenesis, clinical presentation, and potential prognostic implications. The identified miRNA-mRNA regulatory networks warrant further investigation as potential diagnostic and therapeutic targets for PanNET management.

List of abbreviations

18F-DOPA	18F- dihydroxyphenylalanine
18FDG	18F-fluorodeoxyglucose
5-HTP	5-hydroxytryptophan
68Ga	68Gallium
ACTH	Adrenocorticotropic hormone
AFP	Alpha-fetoprotein
AGO	Argonaute
ALT	Alternative Lengthening of Telomeres
antagomiRs	miRNA antagonists
AUC	Area under the receiver operating characteristic curve
BP	Biological process
CC	Cellular component
CCK-8	Cell Counting Kit-8
cfDNA	Cell-free DNA
CgA	Chromogranin A
CpG	Cytosine-guanine dinucleotide
CTCs	Circulating tumor cells
DAVID	Database for Annotation, Visualization, Integrated Discovery
DE	Differential expression
DEG	Differentially expressed gene
DEM	Differentially expressed miRNA
DGCR8	DiGeorge Syndrome Critical Region 8 protein
DOTA	Tetraxetane
EMT	Epithelial–mesenchymal transition
ENETS	European Neuroendocrine Tumor Society
EpCAM	Epithelial cell adhesion molecule
FC	Log2fold change
FDA	Food and Drug Administration
FDR	False discovery rate
FFPE	Formalin-fixed paraffin-embedded tissue
GAS	Gastrin
GCG	Glucagon

GEO	Gene Expression Omnibus
GEP-NETs	Gastroenteropancreatic neuroendocrine tumors
GHRH	Growth hormone-releasing hormone
GLUT1	Glucose transporter 1
GO	Gene ontology
hCG	Human chorionic gonadotropin
HE	Hematoxylin-eosin
HPF	High-power field
HR	Homologous recombination
IHC	Immunohistochemistry
INS	Insulin
IPNM	Intraductal papillary mucinous neoplasms
ISL1	Homeobox transcription factor Islet 1
IT	Islet/insulinoma tumors
KEGG	Kyoto Encyclopedia of Genes and Genomes
LNAs	Locked nucleic acids
MF	Molecular function
miRISC	miRNA-induced silencing complex
miRNA	microRNA
MLP	Metastasis-like/primary
mRNA	Messenger RNA
mTOR	Mammalian target of rapamycin
NECs	Poorly differentiated neuroendorcine carcinomas
NEN	Neuroendocrine neoplasm
NETest	Neuroendocrine neoplasms test
NETs	Well-differentiated neuroendocrine tumors
NF-1	Neurofibromatosis type 1
NGS	Next-generation sequencing
NSE	Neuron-specific enolase
PanNEC	Pancreatic poorly differentiated neuroendocrine carcinoma
PanNEN	Pancreatic neuroendocrine neoplasm
PanNET	Pancreatic well-differentiated neuroendocrine tumor
PARP	Poly(ADP-ribose) polymerase

PCA	Principal component analysis
PCSK9	Proprotein convertase subtilisin/kexin 9
PDAC	Pancreatic ductal adenocarcinoma
PET	Positron emission tomography
PP	Pancreatic polypeptide
PPGL	Pheochromocytomas/paragangliomas
PR	Progesterone receptor
PRRT	Peptide receptor radionuclide therapy
PTHrpP	Parathyroid hormone-related peptide
QC	Quality control
RanGTPase	RAS-related nuclear protein-guanosine-5'-triphosphate-ase
RISC	RNA-induced silencing complex
RNA-seq	RNA sequencing
RPPA	Reverse phase protein array
SCA	Serous cystadenomas
SPECT	Single-photon emission computed tomography
SPN	Solid pseudopapillary neoplasms
SRS	Somatostatin receptor scintigraphy
SST	Somatostatin
SSTR	Somatostatin receptor
SYP	Synaptophysin
TNM	Tumor-node-metastasis
TSC	Tuberous sclerosis complex
t-SNE	t-distributed stochastic neighbour embedding
TUNEL	TdT-UTP nick-end labeling
UMI	Unique Molecular Identifiers
UTR	Untranslated region
VIP	Vasoactive intestinal peptide
VST	Variance stabilizing transformation
WHO	World Health Organization
β-hCG	β subunit of human chorionic gonadotropin
δ	Delta

Gene symbols are not included in the list of abbreviations because they are commonly used.

1 INTRODUCTION

1.1 Primary pancreatic tumors

Primary pancreatic tumors are classified according to their histological origin, molecular characteristics, and function. The two most common subtypes are pancreatic ductal adenocarcinoma (PDAC) and pancreatic neuroendocrine neoplasm (PanNEN) [1]. PDAC originates from the ductal cells of the exocrine pancreas, which are responsible for the production of digestive enzymes. PDACs comprise approximately 90% of primary pancreatic tumors [2]. On the other hand, PanNENs, accounting for only 1-2% of pancreatic tumors, originate from the neuroendocrine islet cells of the endocrine pancreas, which produce hormones like insulin, gastrin, glucagon, and somatostatin (**Figure 1**.) [3].

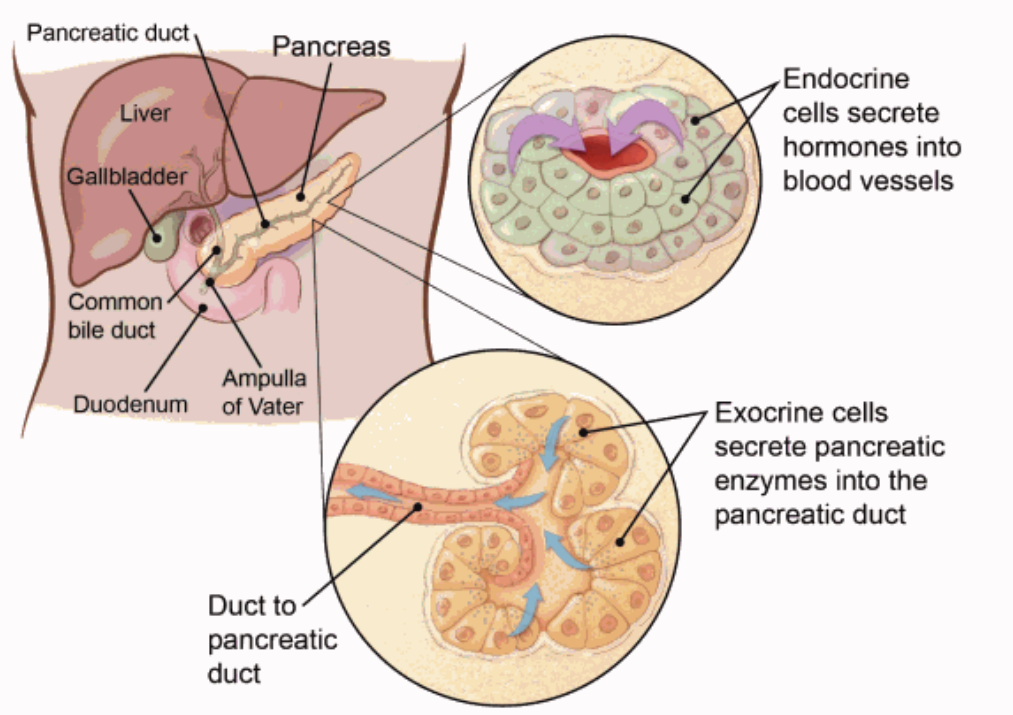

Figure 1. Anatomical illustration of primary pancreatic ductal adenocarcinoma and pancreatic neuroendocrine neoplasm (adopted from [4])]

According to epidemiological studies of all malignant types, PDACs have the lowest 5-year relative survival rate and the highest mortality rate, mainly due to their aggressive growth and frequent metastases [5]. Patients diagnosed in the early stages have a 5-year survival rate of approximately 20%, but in general, less than 5% of PDAC patients survive

after 5 years [6]. Up to 90% of cases of PDAC are caused by mutation in *KRAS*, *CDKN2A*, *TP53*, and *SMAD4* [7].

Even though PanNENs exhibit a more favourable prognosis compared to PDACs, they too are usually diagnosed at advanced stages due to asymptomatic or nonspecific clinical presentation. The only exception are functional PanNENs, which can present specific symptoms due to the overproduction of hormones or peptides. On the other hand, overall survival of PanNEN patients is closely linked with their classification into pancreatic well-differentiated neuroendocrine tumors (PanNETs) and pancreatic poorly differentiated neuroendocrine carcinoma (PanNECs) [1]. Similarly to PDACs, median overall survival (OS) of PanNECs is only 11 months [8]. Contrary, PanNETs are slow-growing (indolent) with 5- and 15-year OS rates of 85.4% and 55%, respectively [1]. There are many differences between PanNEC and PanNET tumors, in addition to their distinct clinicopathological characteristics and prognosis. *MEN1* (multiple endocrine neoplasia type 1), *DAXX* (death-domain-associated protein)/*ATRX* (alpha thalassemia/mental retardation syndrome X-linked), and mTOR (mammalian target of rapamycin) pathway mutations are examples of common somatic mutations in PanNETs. However, mutation of *TP53*, *RB1*, and *KRAS,* occurring in PanNECs, are making this subclass more comparable to PDACs (6).

Immunohistochemical markers can also differentiate between PDAC and PanNETs. PDAC usually expresses markers such as CA19-9, and MUC1, while PanNETs often express neuroendocrine markers such as chromogranin A, synaptophysin, and CD56. The Ki-67 index can also be very useful. PDAC generally has a higher proliferation rate (over 20%) compared to PanNETs, which typically have a lower rate (less than 3% for low-grade tumors). Understanding these differences and finding specific biomarkers is crucial for accurate diagnosis and optimal treatment management of patients with pancreatic tumors [9].

1.2 Pancreatic neuroendocrine neoplasm (PanNEN)

1.2.1 Definition and epidemiology

While tumors arising from neuroendocrine cells can occur throughout the body, they most commonly arise in the lungs, gastrointestinal tract, and pancreas [10,11]. PanNENs represent a rare heterogenous group with an incidence ~ 1:100 000 [12]. Several studies described an increasing incidence over the past few decades, which makes it imperative to better understand their molecular, clinical, and pathological characteristics [13,14]. This

increasing incidence can be explained by the improvement of imaging and radiological techniques, which leads to more accurate detection of even small tumors. Further explanation may be a discovery and validation of new biomarkers for diagnosis [15]. PanNENs usually occur in patients in the fifth or sixth decade of life, men are affected slightly more frequently than women. Associated risk factors include smoking, alcohol and tobacco consumption, being overweight, *diabetes mellitus*, and a positive family history which is a component of some inherited syndromes, such as Multiple Endocrine Neoplasia type 1 (MEN1) and Von Hippel Lindau (VHL) syndrome [16–18].

The majority of PanNENs are sporadic; however, approximately 10-15% of all PanNENs develop as part of familial syndromes linked to particular germline mutations such as multiple endocrine neoplasia type 1 syndrome (MEN-1 syndrome) caused by *MEN1* gene mutation, von Hippel-Lindau syndrome (VHL syndrome) caused by *VHL* gene mutation, neurofibromatosis type 1 (NF-1 or von Recklinghausen disease) caused by *NF1* gene mutation, and tuberous sclerosis complex (TSC) caused by mutation in *TSC* or *TSC2* gene [19,20]. Additionally, whole genome sequencing efforts have recently shown that 17% of PanNETs that seemed to be sporadic, carried germline mutations, including previously unreported mutations involved in DNA repair genes (e.g., *MUTYH*, *CHEK2*, *BRCA2*) [21].

1.2.2 Diagnosis, classification, and clinical presentation

To guide the overall management of patients diagnosed with the disease, a well-defined classification system is necessary, due to the heterogeneity of the clinical and biological characteristics of PanNETs. Tissue morphology, grading, and the tumor-node-metastasis (TNM) pattern are used to characterize the pathophysiology of all PanNENs. All patients must have a histological diagnosis, which can be performed on core biopsies in cases of advanced disease or on resection material. On hematoxylin-eosin (HE)-stained tissue, the diagnosis of a neuroendocrine neoplasm (NEN) is based on histomorphological growth pattern and cytology. The neuroendocrine markers released from neurosecretory granules produced by neuroendocrine cells, synaptophysin (SYP), and/or chromogranin A (CgA) can be detected via immunohistochemistry, which confirms the neuroendocrine phenotype. It rarely happens that both markers are absent in a subset of poorly differentiated PanNECs. Apart from CgA and SYP, neuron-specific enolase (NSE) and CD56 markers are often positive in gastroenteropancreatic neuroendocrine neoplasms, but their lack of specificity makes them less reliable diagnostic markers [22].

Introducing the use of the differentiation status of tumor cells as a predictor of their behaviour was first presented in 2000 by World Health Organization (WHO) categorization system [23]. Differentiation is a term used to refer to the resemblance of the neoplastic tissue to its tissue of origin and for PanNETs, the endocrine islets of Langerhans. Traditionally, "well-differentiated tumors" (NETs) and "poorly differentiated carcinomas" (NECs) categories have been used to classify PanNENs into two different entities differing in aggressiveness and malignant potential. A neuroendocrine neoplasm with well-differentiated characteristics exhibits minimal to moderate cellular atypia, expression of markers of neuroendocrine differentiation, and hormone production. The size and nuclear morphology of poorly differentiated tumor cells will differ, while neuroendocrine differentiation markers will be less prominently expressed [23].

A new classification was developed in 2010 [24], in response to a suggestion submitted by the European Neuroendocrine Tumor Society (ENETS) to add a TNM-based classification system for gastrointestinal NETs. Moreover, the growth patterns of the cancerous cells are graded by counting the number of cells undergoing division using Ki-67 immunohistochemistry staining. Tumor grade refers to their growth rate (proliferation) and ability for spreading and metastasis. Based on the staining, neuroendocrine tumors are categorized into three grades: G1 (NET), G2 (NET), and G3, which also includes poorly developed G3 carcinomas (NEC). Specifically, G1 tumors have a proliferation rate of less than 2%, G2 tumors range from 2% to 20%, and G3 (NEC) tumors have a proliferation rate of over 20% (**Table 1**.) [25].

Table 1. **Classification of PanNENs based on the WHO 2010 grading system**

	Well-differentiated (NET)		Poorly differentiated (NEC)
Tumor grade	1	2	3
Ki-67 Index (%)	<3	3-20	>20
Mitotic count (per 10 HPF)	<2	2-20	>20

HPF, high-power field

Clinically, this staging/grading system is relevant in distinguishing low-grade from high-grade tumors and tailoring their respective management strategy, but intermediate-grade

lesions remain difficult to accurately identify (e.g. the prediction of G2 tumor survival remains challenging) [26]. Furthermore, there is uncertainty surrounding G3 tumors, specifically regarding the assessment of their level of differentiation and histological grading. Since these features impact the clinical management, further clarification is warranted.

When cancer cells show well-differentiated phenotype, but have a high proliferative index, accurate diagnosis becomes problematic, as it is still unclear if these cases should be included in the G3 class [27]. In these cases, a deep molecular characterization can help with correct classification, since the molecular profile of well-differentiated neuroendocrine neoplasms (NENs) differs from aggressive poorly differentiated tumors that are characterized by loss of *p53* and *Rb1* with mutations in *MEN1* and *DAXX/ATRX* (**Table 2**.) [18].

Table 2. Clinical utility of biomarkers in PanNEN diagnostics and prognostics (adopted from ESMO guidelines[18])

Biomarker	Method	Use
Ki-67	IHC	Prognostic relevance, essential component of the WHO grading for NENs
SSTR-2/5	IHC	Detection of somatostatin receptors when no functional imaging is possible
DAXX/ATRX	IHC	Prognostic relevance for PanNETs; distinction from NEC
TP53/pRb	IHC	Classification of poorly differentiated NECs or distinction from NET G3
MGMT	IHC, promoter methylation assay	Predictive value for temozolomide response

MGMT, O6-methylguanine-DNA methyltransferase; NEC, neuroendocrine carcinoma; NEN, neuroendocrine neoplasm; NET, neuroendocrine tumour; Pan-NET, pancreatic neuroendocrine tumour; p53, tumour protein; pRb, retinoblastoma protein; SSTR, somatostatin receptor; WHO, World Health Organization (adopted from ESMO guidelines)

Indeed, depending solely on Ki-67 immunostaining or mitotic index for NENs, classification may result in suboptimal treatment choices. According to the revised WHO classification introduced in 2019, the heterogeneous NENs G3 of PanNETs is further split into well-differentiated NET G3, and poorly differentiated NEC G3 (**Table 3.**) [18].

Table 3. **Classification of PanNENs based on the WHO 2019 grading system**

Morphology	Grade	Mitotic count (2 mm^2)[a]	Ki-67 Index (%)[b]
Well-differentiated NETs	G1	<2	<3
Well-differentiated NETs	G2	2-20	3-20
Well-differentiated NETs	G3	>20	>20
Poorly differentiated NECs	G3	>20	>20

[a] 10 HPF (high-power field) = 2 mm^2, at least 40 fields (at ×40 magnification) evaluated in areas of highest mitotic density.
[b] MIB1 antibody; percentage of 500–2000 tumour cells in areas of highest nuclear labelling.

Other feature of PanNENs with diagnostic implication is the hormonal secretion. PanNENs are a clinically heterogeneous group of tumors and depending on their ability to show symptoms due to hormone production, they are divided into functioning and non-functioning PanNENs. While non-functioning tumors account for 70-90%, and do not show clinical symptoms until the disease has advanced to a late stage, functioning tumors (10-30%) are associated with hormonal syndromes due to the active secretion of biological amines and hormones including insulin (17%), gastrin (15%), glucagon (1%), vasoactive intestinal peptide (VIP) (2%), and somatostatin (1%) [18,28,29].

Common symptoms of non-functioning PanNENs are unspecific abdominal pain, nausea, rarely jaundice, and weight loss. Patients with functioning PanNENs often present with characteristic symptoms dependent on the hormones produced, such as hypoglycemia (insulin in insulinoma), heartburn (gastrin in gastrinoma), necrolytic migratory erythema (glucagon in glucagonoma), watery diarrhea (vasoactive intestinal peptide in VIPoma) and others (**Table 4**.) [18].

Table 4. Clinical classification of PanNENs based on their site of origin and hormonal secretion
(adopted from ESMO guidelines[18])

PanNETs	Frequency	Symptoms	Secretory product
Functioning	10%–30%	Zollinger-Ellison syndrome	Gastrin
		Hypoglycaemia	Insulin
		Necrolytic erythema hyperglycaemia	Glucagon
		WDHA syndrome	VIP
		Diabetes, gallstones, diarrhoea	Somatostatin
		Cushing syndrome	CRH, ACTH

		Acromegaly	GHRH, GH
		Hypercalcaemia	PTHrP
		Flushing Diarrhoea	Calcitonin, Serotonin, CgA
Non-functioning	70%–90%	Unspecific abdominal pain, rarely jaundice, weight loss	CgA, PP

ACTH, adrenocorticotropic hormone; CgA, chromogranin A; CRH, corticotropin- releasing hormone; CS, carcinoid syndrome; GH, growth hormone; GHRH, growth hormone-releasing hormone; PP, pancreatic polypeptide; PTHrP, parathyroid hormone-related peptide; VIP, vasoactive intestinal peptide; WDHA syndrome, watery diarrhoea, hypokalaemia, achlorhydria.

1.2.3 Molecular subtyping of PanNETs

A recent cross-species study has identified previously unrecognized subtypes of PanNETs in both mice and humans [30]. These tumor subtypes have different mutations, phenotypic characteristics, clinical characteristics, and pathological properties, indicating the heterogeneous background biology. Dual messenger RNA (mRNA) and microRNA (miRNA) transcriptome profiling analysis combined with assessment of known biomarkers in human PanNET identified three distinct molecular subtypes, termed "islet/insulinoma tumors"(IT), "metastasis-like/primary" (MLP), and "intermediate" tumors [30]. PanNETs of the IT subtype consist primarily of less-aggressive, non-metastatic insulinomas that express genes such as *INS*, *IAPP*, and *INSM1* associated with insulinomas and differentiated/mature β-cells. On the other hand, MLP tumors are invasive/metastatic and show a gene signature that is enriched for genes associated with immature, nonfunctional cells, epithelial–mesenchymal transition (EMT), fibroblasts, and stem cells, indicating that they originate from progenitor cells. The majority of PanNETs in the intermediate subtype are nonfunctional; they share several genes with the IT subtype and have a moderate association with metastasis. The newly defined transcriptional subtypes of human PanNETs were also correlated with the WHO classification of NET grades. G1 and G2 PanNETs are heterogeneous, associating with a variety of transcriptome subtypes, whereas high-grade G3 tumors are exclusively associated with the MLP subtype (**Figure 2.**) [30,31].

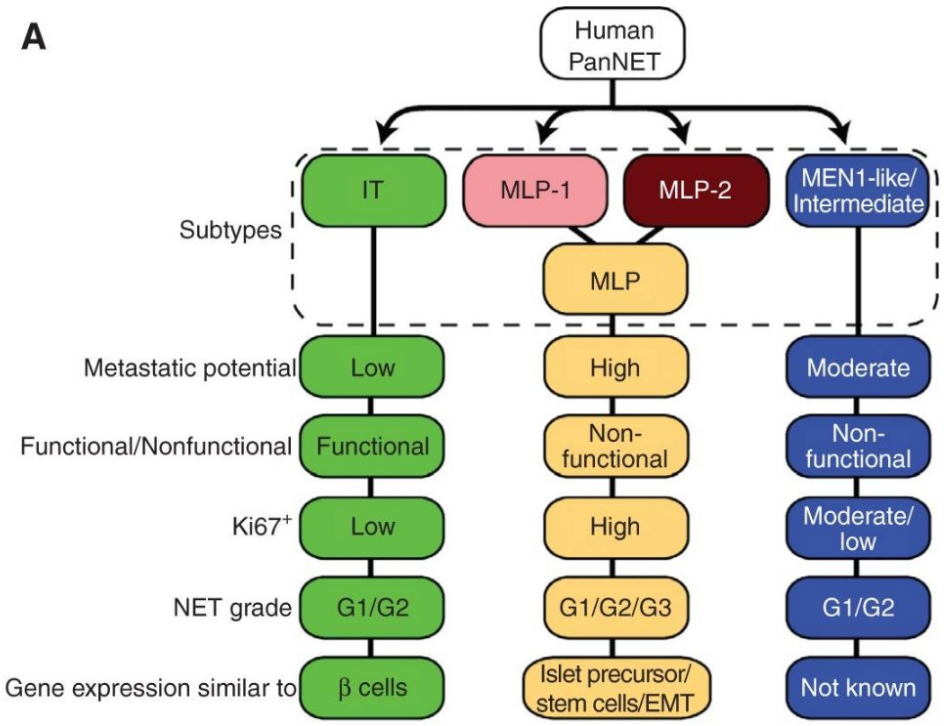

Figure 2. Summary of the different human PanNET subtypes and their defining characteristics (adopted from [30])

1.2.4 The pathway-based landscape of PanNETs pathophysiology

The complexity of PanNET pathogenesis is further evidenced by dissection of aberrant interactions among multiple signalling pathways driving their emergence and progression. Cell processes such as angiogenesis, migration, survival, and cell proliferation are all crucial to tumor development and affect many signalling pathways. Together, these pathways form a complex network, the disruption of which can lead to uncontrolled tumor growth and metastasis [32].

In a recent largest whole-genome sequencing effort encompassing 102 primary PanNETs, the driver pathways crucial to the disease were identified. These include: (I) DNA Damage Repair Pathway, (II) Chromatin Remodelling Pathway, (III) Telomere Alteration Pathway, (IV) PI3K/mTOR Signalling Pathway, (V) Cell Cycle Regulation Pathway and (VI) Wnt Signalling Pathway (**Figure 3.**) [21].

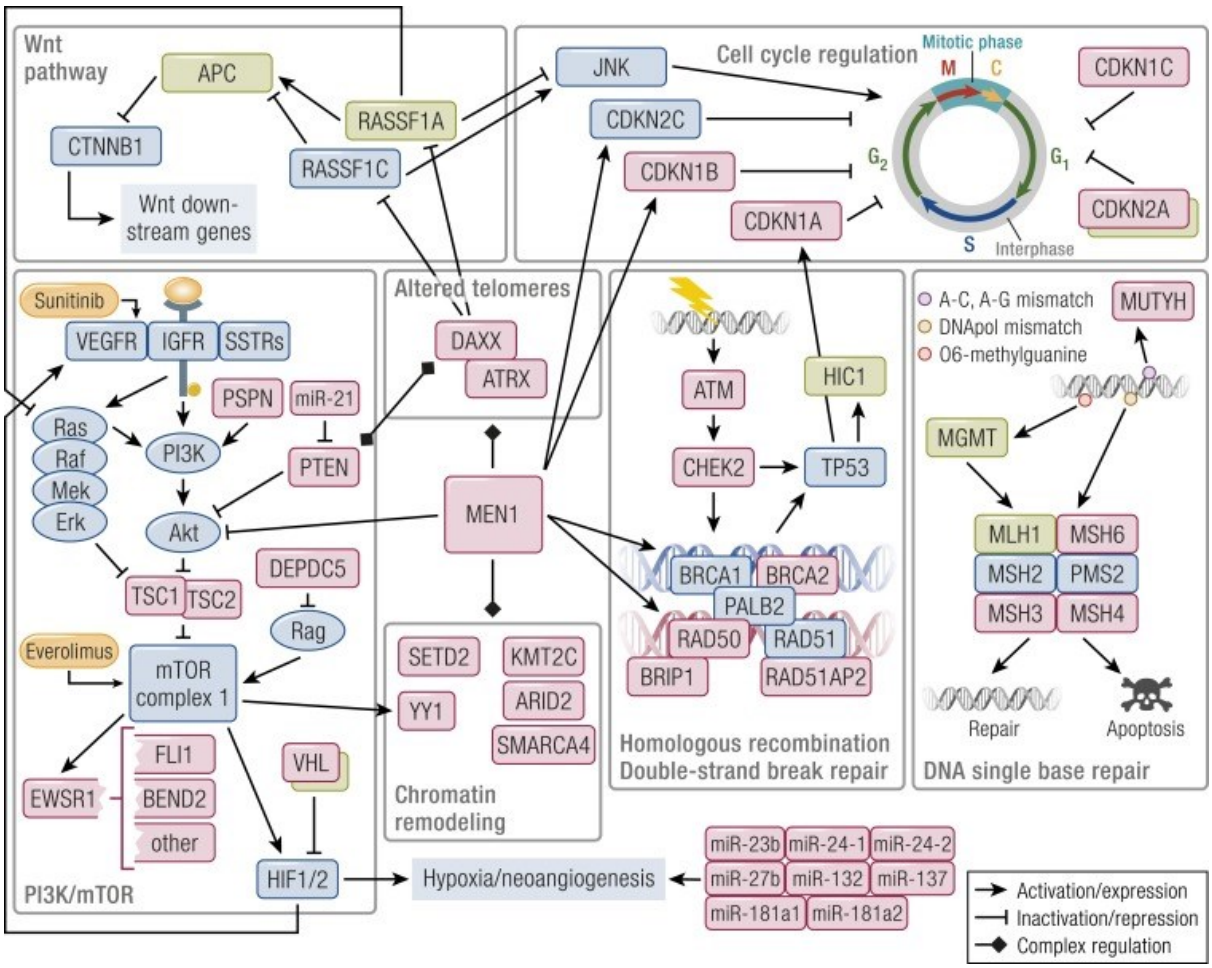

Figure 3. Summary of the crucial altered pathways in PanNETs (adopted from [33])

DNA Damage Repair Pathway

The alteration of DNA damage repair pathway is a hallmark of PanNET. Both germinal mutations (affecting e.g. *MUTYH*, *CHEK2*, *BRCA*), somatic mutations and even epigenetic alterations (e.g. *MGMT* hypermethylation) have been described to be involved in knocking out the single-base repair system and homologous recombination (HR) double-strand break repair. These alterations have been associated with the efficacy or response to certain treatment options like temozolomide, alkylating agents in *MGMT*-deficient PanNETs [34], platinum derivates, or poly(ADP-ribose) polymerase (PARP) inhibitors in HR-deficient tumors [33,35].

Chromatin Remodelling Pathway

Chromatin remodelling plays a crucial role in gene expression regulation and genomic stability. The role of the chromatin remodelling genes still needs to be further

investigated [36]. Besides the ALT phenomenon (Alternative Lengthening of Telomeres), *ATRX/DAXX* alterations directly affect genes like *RASSF* and *PTEN* through methylation or direct regulation [37,38]. Other mutations present among PanNET cases (e.g. *MEN1*, *SETD2*, *ARID1A* and *MLL3)* have also been reported to dysregulate chromatin remodelling [21].

Telomere Alteration Pathway

TERT upregulation and telomere lengthening is a well-established survival mechanism in solid tumors. MEN1 binds the *TERT* promoter and affects the mechanism that controls telomere integrity [39]. PanNETs with inactivating mutations in *DAXX* or *ATRX* correlated strongly with somatic telomere repeat content and telomere length, consistent with previous reports. Additionally, tumors with *DAXX* or *ATRX* mutations were associated with poor prognosis in the G2 subgroup and significantly correlated with mutations in mTOR regulators. Cases with unchanged telomere length had a better outcome [21].

PI3K/AKT/mTOR Signalling Pathway

The role of PI3K/AKT/mTOR Signalling Pathway in PanNETs has been well-established. This pathway leads to the activation of mTOR, which has positive effects on cell cycle progression, cell survival, and cell proliferation. Several gene expression profiling studies confirmed the role of *PTEN*, *TSC1*, *TSC2*, and *PIK3CA,* key players in the PI3K/Akt/mTOR pathway, in the disease [40,41]. Downregulation of *TSC2* and *PTEN* was associated with poor survival [42]. Of note, these mutations may represent putative biomarkers for mTOR inhibitor treatment selection [43]. Recently, three novel mechanisms were discovered to activate the mTOR pathway using whole genome sequencing. Firstly, inactivating mutation of the tumor suppressor *DEPDC5*, a subunit of the *GATOR1*; secondly, an mTOR activation mechanism involving the *EXSR1* fusion gene and thirdly, amplification of the RET receptor link *PSPN* [21].

Cell Cycle Regulation Pathway

Dysregulation of the cell cycle machinery contributes to uncontrolled cell growth and tumor progression in PanNETs. Cell cycle regulation in PanNETs is impacted by changes in cell cycle regulatory genes, such as mutations in *RASSF1A* and *CDKN1B*. Other alterations, including hypermethylation of *CDKN2A* and inhibition of *CDKN1B* and *CDKN2C,* may influence cell proliferation and differentiation [33,44–46]. Determination of interactions

between cell cycle dysregulation and other pathways is essential for understanding PanNET biology and identification of therapeutic targets.

Wnt Signalling Pathway

Activation of the WNT pathway leads to stabilization and accumulation of β-Catenin in the cytoplasm, its translocation into the nucleus for interaction with T-cell factor and lymphoid enhancer factor (Tcf/Lef) transcription factors, and transcriptional activation of target genes that promote cell proliferation, e.g. c-Myc or Cyclin D1 [47]. As a result of β-Catenin degradation, PanNETs are associated with increased proliferation and abnormal chromosome segregation, contributing to the chromosomal instability in PanNENs [48]. In PanNETs, this cascade is often maintained by loss or inhibition of *RASSF1A* and *APC* genes [33]. Hypermethylation of *APC* was detected in 21% to 48% of PanNETs and its expression was lost in 59% [49]. *RASSF1A* is a known tumor suppressor whose inactivation can elevate WNT activity (34,46).

1.3 Biomarkers of PanNENs

According to the definition of biomarkers, these are characteristics that can be objectively measured and serve as indicators of normal and pathogenic processes, as well as the response to therapeutic interventions. These can be assessed in biological fluids, tissue, and cells. Ideally, a biomarker should be able to diagnose NENs with high sensitivity and specificity, predict tumor aggressiveness (prognostic biomarker), and predict treatment response (predictive biomarker) in a rapid, cost-effective, and robust manner [51,52]. The biomarkers utilized in clinical practice to diagnose PanNENs can be classified into several groups: (I) Serum biomarkers, which can be further subdivided into general, which practically all PanNENs produce, and specific biomarkers, that are primarily produced by functional PanNENs [53]; (II) tissue biomarkers detectable immunohistochemically; and (III) theranostic biomarkers identified through imaging techniques (**Figure 4**.) [15,52,53].

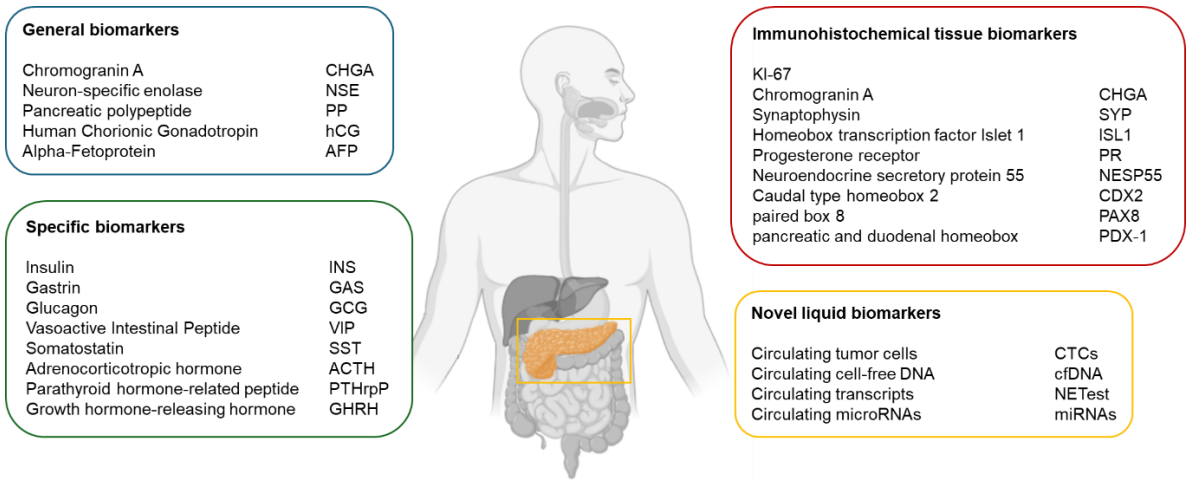

Figure 4. Schematic illustration of PanNEN biomarkers (adjusted from [15])

1.3.1 General biomarkers

General biomarkers used to assess PanNENs involve chromogranin A (CHGA), Neuron-specific enolase (NSE), Pancreatic polypeptide (PP), Human chorionic gonadotropin (hCG) and Alpha-fetoprotein (AFP). Measurement of these biomarkers is routinely performed in the serum or plasma of patients with suspected PanNEN. Abnormal levels of general markers would lead to further diagnostic investigations to gain a deeper understanding of the disease [15,54].

Chromogranin A

CHGA is the most widely used monoanalytical marker for the diagnosis and monitoring of neuroendocrine tumors with high sensitivity (73%) and specificity (95%) [55]. It is a glycoprotein secreted by neurons and neuroendocrine cells, belonging to the granin family, and is a precursor of bioactive substances such as pancreatin, catestatin, and vasostatins. Although it is the most widely used biomarker, not only in diagnostics, but also during the follow-up of PanNEN patients, its specificity can be reduced by comorbidities such as cardiovascular disease, renal cell failure, colorectal cancer, or the use of proton pump inhibitors, by up to 50% [15,55]. Circulating CHGA has been reported to correlate with tumor progression, presence of metastasis, and response to treatment in PanNENs [56,57].

Neuron-specific enolase

NSE represents a glycolytic cytoplasmic enzyme produced by neurons and neuroendocrine cells. Although it has low sensitivity and specificity, its levels have been

directly linked to tumor differentiation, aggressiveness, and tumor size [58]. NSE levels were also found to inversely correlate with overall survival and progression-free survival in the advanced stage [57,59,60]. NSE alone is rarely used for diagnostic purposes or to differentiate NEN from non-endocrine tumors, but the use of NSE with CHGA increases the reliability of the diagnosis. However, due to its non-specificity, it cannot be used for disease localization [54].

Pancreatic polypeptide

PP is secreted by the cells of the islets of Langerhans, but its role is not well understood. It is thought to regulate pancreatic secretion and hepatic glycogen levels. In general, PP is considered a marker of neuroendocrine differentiation with low and inconsistent sensitivity, but good specificity. Increased sensitivity for PanNEN is suggested by the detection of high levels of circulating PP in association with CHGA [61]. In all cases of sporadic and hereditary gastrinomas, PP and/or CHGA production is noted [62]. On the other hand, decreasing PP levels during patient monitoring are considered a favourable prognostic marker [57].

Human Chorionic Gonadotropin and Alpha-Fetoprotein

Although their use in PanNENs is limited, hCG and AFP may also be considered in biochemical evaluation [54]. hCG is a glycoprotein composed of α and β subunits that is physiologically synthesized by syncytiotrophoblastic cells of the placenta during pregnancy [55]. As tumour cells usually lack a mechanism to link the α and β subunits, increased secretion of the β subunit (β-hCG) is specific for pancreatic and PanNEN tumors. AFP is a peptide hormone produced during development. In the serum of adults an increase in AFP has been reported for NENs [63,64]. AFP-producing PanNENs are rare and often coexist with other malignancies [65,66]. However, it is the sensitivity and specificity of hCG and AFP that limits their use in NENs [67].

1.3.2 Specific biomarkers

Biomarkers encompassing bioactive peptides for prognosis and prediction of disease outcomes have been discovered in blood samples from functioning PanNEN patients [54]. However, hormones are not always released into the bloodstream. Assessing expression within the neoplastic tissue remains the gold standard for diagnosis. Also, symptoms

associated with elevated levels of specific bioactive compounds may help to diagnose and identify the primary site of the disease [68]. Functioning PanNENs are named according to the hormones that they produce, e.g. insulinomas, glucagonomas, gastrinomas, somatostatinomas, and VIPomas [15].

Insulin (INS)

INS is a dimeric peptide hormone secreted by the beta cells of the pancreatic islets. Insulinomas are the most common functional PanNENs, characterized by the best prognosis among functional and non-functional PanNEN [69]. Due to abnormal insulin secretion, hypoglycemia is an essential clinical symptom and should by diagnosed using Whipple's triad: (1) Low glucose level (40 md/dl or less); (2) symptoms and signs of hypoglycemia, (3) symptoms are relieved after glucose administration. The gold standard remains biomechanical diagnostics consisting of 72h fasting with serial measurements of blood glucose, insulin, C-peptide, proinsulin, and beta-hydroxybutyrate levels [55,57,70].

Gastrin (GAS)

GAS is a hormone consisting of linear peptides that are released by G-cells in the pyloric antrum, duodenum, and pancreas. It is involved in regulating the release of hydrochloric acid from parietal cells in the stomach, as well as gastric motility and pancreatic secretion [55]. Gastrinomas or Zollinger–Ellison syndrome caused by hypersecretion of gastrin are characterized by peptic ulcers in an atypical location, diarrhea, and dysphagia. Laboratory diagnosis consists of evaluation of fasting serum gastrin level > 1,000 pg/ml (normal level <100 pg/ml) and secretin stimulation test for patients with mildly elevated serum gastrin levels [71,72].

Glucagon (GCG)

An important function of GCG is to increase catabolism by mobilizing energy reserves to free glucose molecules through gluconeogenesis and glycogenolysis [73]. Glucagonoma arise from the pancreatic α-cells and clinical symptoms referred to as the 4D syndrome; dermatitis (necrolytic migratory erythema), diabetes, deep vein thrombosis, and depression [74]. Laboratory diagnosis consists of measurement levels of fasting glucagon. Usually, the level of fasting glucagon is elevated more than 10-20 times, but in patients with

levels only 4 times above the reference (normal: 0–150 pg/ml), it is key to correlate these findings with clinical symptoms mentioned above [57].

Vasoactive Intestinal Peptide (VIP)

VIP released by pancreatic and brain cells is a neurotransmitter and vasodilator regulating epithelial cell secretion, gastrointestinal blood flow, and muscle activity. The result of VIP oversecretion is severe diarrhea, resulting in achlorhydria hypokalemia. VIPoma secreting tumor or Verner-Morisson Syndrome is diagnosed by serum concentration of VIP above 200pg/dl with secretory diarrhea usually greater than 3.0 liters per day [15].

Somatostatin (SST)

SST represents a peptide hormone that arises in delta (δ) cells of the pancreatic islet cells. Somatostatin inhibits the intestinal absorption and gut motility and release of insulin, glucagon, gastrin, and pancreatic enzymes. Oversecretion of somatostatin induces unspecific clinical symptoms such as diarrhea, cholelithiasis, steatorrhea, diabetes mellitus, hypochlorhydria, and weight loss. Laboratory diagnosis of somatostatinoma includes fasting serum somatostatin levels > 14 mmol/l [75]. High somatostatin level is also associated with Neurofibromatosis type 1 and MEN - 1 syndrome, therefore SST level alone is insufficient for diagnosis [15,76].

Ectopic hormones

Less frequently, hypersecretion of ectopic hormones such as Adrenocorticotropic hormone (ACTH), Parathyroid hormone-related peptide (PTHrpP), and Growth hormone-releasing hormone (GHRH) has been described in PanNENs. Their circulating level with the clinical symptoms is highly specific for the corresponding neoplasms [28,53].

1.3.3 Immunohistochemical tissue biomarkers

Histological diagnosis is usually assessed on endoscopic or surgical biopsies, where immunohistochemistry (IHC) is used for morphological and distributional analysis of markers. PanNENs can produce hormones that are not released into the bloodstream. Specific positive markers such as GAS, INS, and SST can confirm clinical symptoms even without

biochemical elevation in serum. However, IHC for hormones and bioactive peptides cannot determine the site of origin and functionality of NENs [77].

Ki-67

Ki-67 is the most widely used cell proliferative marker, which plays a crucial role in tumor classification, grading, prognosis, and tumor aggressiveness of PanNENs [78]. This nuclear antigen is expressed in all cell cycle phases (G1, S, G2, and mitosis) except G0, which makes it a useful marker for measuring cellular proliferation [79]. The Ki-67 labelling index is an important factor in determining the aggressiveness and prognosis of PanNETs. It measures the percentage of tumor cells that are positive for Ki-67. A higher Ki-67 index indicates a more aggressive tumor and a worse prognosis according to the World Health Organization classification system [80].

Chromogranin A and synaptophysin

Currently, CHGA and SYP are considered to be the most specific markers in immunohistochemistry for the differentiation of NEN [81]. CHGA is a glycoprotein precursor of several functional peptide hormones. Besides diagnosis, it is also used for differentiation of NENs, since CHGA is highly expressed in well-differentiated tumors compared to low expression levels in poor differentiated tumors [82]. SYP is a glycoprotein expressed in neuroendocrine cells and neurons involved in synaptic transmission. Their combined assessment represents the first step in confirmation of the PanNENs diagnosis [15,83].

Homeobox transcription factor Islet 1 (ISL1)

ISL1 is a transcription factor crucial for endocrine pancreatic cell development. Despite its high sensitivity in identifying metastatic neuroendocrine tumors of pancreatic origin, it does not distinguish pancreatic NENs from duodenal and colorectal NENs [84,85].

Progesterone receptor (PR)

PR represents a well-studied nuclear receptor, which inhibits cell proliferation in PanNENs [86]. Different PR isoforms, namely PRA and PRB, have distinct roles and prognostic significance in the disease. Recent studies confirmed that up to 75% of PanNENs

expressed PRB, which promotes overexpression of cyclin-D1 (*CCND1*) and thus induces proliferation and tumorigenesis via c-Fos and C-Jun signalling [15,87].

Other markers

Immunohistochemical panels which include other transcription factors such as neuroendocrine secretory protein 55 (NESP55), caudal type homeobox 2 (CDX2), paired box 8 (PAX8), pancreatic and duodenal homeobox (PDX-1) can provide insight to PanNENs differentiation and tumor's origin. Overlapping pancreatic expression of these markers could improve diagnosis, classification, prediction of tumor behaviour, and assessment of prognosis [15,57,88].

1.3.4 Theranostic markers

Imagining techniques use radiological tracers to evaluate specific molecular markers present on or in neoplastic cells. The somatostatin receptor (SSTR) has emerged as a key diagnostic marker of NETs. The SSTR family consists of five types (I-V) of G-coupled transmembrane receptors that are predominantly found on the surface of NETs. Somatostatin receptor scintigraphy (SRS), also referred to as Octreoscan®, can be used to selectively target SSTR types II, III, and V using a radiolabelled somatostatin analogue 111-pentetreotide. This imaging technique uses single-photon emission computed tomography (SPECT) and has demonstrated the ability to detect the target in more than 80% of patients with an impressive sensitivity ranging from 92% to 100% and a specificity of 91% [57,89].

SRS can detect the functional status of the lesions based on the SSTR expression level. As a result, SRS has a higher diagnostic value for certain types of NEN, such as gastrinomas and VIPomas, compared with insulinoma, which expresses less SSTR2. Nevertheless, the detection of cancers smaller than 2 cm demonstrated the limitations of SRS [90].

Advances in positron emission tomography (PET) have led to the development of 68Gallium (^{68}Ga)-labelled somatostatin analogues that are conjugated to the DOTA (tetraxetane) molecule [91]. This innovative PET imaging offers better spatial resolution compared to SPECT and shows excellent sensitivity (93 %) and specificity (96 %) and an impressive AUC (area under the receiver operating characteristic curve) value of 0.98. The

increased affinity of this PET tracer for SSTR translates into improved detection rates compared to traditional SRS [92].

In contrast, 18FDG (^{18}F-fluorodeoxyglucose) positron emission tomography is used to assess metabolic activity in NEN based on the metabolism of radiolabelled glucose for diagnosis and staging of various cancers. Tumors are localized using the increased uptake of 18FDG compared to normal tissue background levels due to increased glycolytic activity of neoplastic cells [93].

In addition, GLUT1 (glucose transporter 1) expression in tumors correlates with tumor grade, Ki67 proliferation index, mitotic index, and tissue hypoxia, thus serving as a potential surrogate marker for FDG-PET-based prognosis. The diagnostic sensitivity of FDG PET ranges from 32% to 72%, which limits its effectiveness in detecting NEN. Nevertheless, FDG PET in conjunction with somatostatin receptor imaging may increase diagnostic accuracy and facilitate more precise therapeutic strategies for aggressive NENs [57].

Other imaging biomarkers, including amines (serotonin/5-HTP (5-hydroxytryptophan) and 18F-DOPA (^{18}F- dihydroxyphenylalanine) (precursors) as well as surface receptors (e.g., glucagon-like peptide receptor 1/GLP1R and CXC-chemokine receptor 4/CXCR4), have been identified. However, these markers exhibit lower diagnostic sensitivity, radiotracer complexity, increased radiation exposure, and higher associated costs compared with ^{68}Ga PET imaging, limiting their widespread clinical use [57,94].

1.3.5 Novel liquid biomarkers

Circulating tumor cells (CTCs)

CTCs may become useful biomarkers for cancer diagnosis and prognosis. The size of tumor cells and the presence of epithelial cell adhesion molecule (EpCAM) are two features of CTCs that have been utilized for this purpose [95]. Using the Food and Drug Administration (FDA) approved CellSearch platform, circulating tumor cells were detectable in only 21% of patients with PanNETs. These low detectable levels of circulating PanNET cells make diagnosis, accuracy, and correlation with treatment response difficult [96,97]. Their promising prognostic role was studied in a prospective study of 176 patients, where the presence of CTCs was associated with a higher tumor grade, tumor burden, an increased circulating CgA concentration, and a higher Ki-67 index [98].

Cell-free DNA (cfDNA)

The role of cfDNA in PanNENs remains questionable. Next-generation sequencing (NGS) was recently used to reveal tumor-associated genetic alterations such as *MEN1*, *DAXX*, *ATRX*, and *TSC2* mutations in 66% of cfDNA samples of metastatic PanNENs samples [99].

Neuroendocrine neoplasms test (NETest)

A recently developed innovative approach, termed NETest, allows the detection of multiple circulating mRNA transcripts in gastroenteropancreatic NETs (GEP-NETs). Liquid biopsy test based on the assessment of the expression levels of 51 different transcriptome signatures with high sensitivity (99%) and specificity (95%) in diagnosing PanNETs represents a novel and useful tool for NENs, outperforming monoanalyte-based methods [100]. NETest is also valuable in the prediction of clinical response to treatment (resection, peptide receptor radionuclide therapy (PRRT)) and in prognosis [101,102]. NETest score below 40% correlated with stable disease, while scores over 80% indicated progressive disease in a cohort of GEP-NETs [103]. This molecular approach provides a non-invasive, cost-effective, reproducible, and easy clinical-use method for early detection, monitoring, and personalized treatment of NETs [15,57,104].

microRNAs (miRNAs)

Several studies have investigated tissue-specific miRNA signatures to distinguish PanNEN patients from healthy individuals and the primary tumor from metastatic disease with a prognostic and/or predictive role (14, 105–107). Their biogenesis and role in the disease will be further explored in the next chapters.

1.4 miRNAs

miRNAs are small RNA molecules with lengths of approximately 22 nucleotides. They are important endogenous regulators of gene expression at the post-transcription level due to their abundance and their important function in proteosynthesis repressing [105,106]. A single miRNA molecule can have up to hundreds of target mRNAs, and a single mRNA can be regulated by several miRNAs, thus forming a complex regulatory network in the organism [107]. They are involved in physiological functions such as stem cell differentiation, cell division, signal transduction, and cell death, as well as pathological

processes such as tumorigenesis. Therefore, miRNAs are currently the research focus of many laboratories due to their possible utility as new diagnostic, prognostic, and predictive biomarkers, in particular for cancer, as well as potential therapeutic targets [108–110].

There are more than 1,000 miRNA genes encoded in the human genome. The positions of miRNA genes relative to known transcription units in the genome are diverse. Most are located intergenically between coding sequences, some miRNA transcripts may be monocistronic with their promoter, while about a half are polycistronic arising in the form of clusters [111–113]. The second most common case is the location of miRNA genes in the intron regions of coding or non-coding RNA genes. There are other possible positions, but these are distinctly a minority. Thus, a miRNA can be transcribed from its gene as a separate transcriptional unit with its promoter, or the miRNA gene can be transcribed with the help of the promoter of the host gene, if it is nearby or directly part of a gene coding a protein [114,115].

1.4.1 miRNA biogenesis

miRNAs play an intricate role in gene regulation and understanding their biogenesis and expression patterns is important in defining their biological functions. Biogenesis of miRNA begins in the nucleus, and can be canonical, which is by far the most predominant, or non-canonical [105,113]. In the canonical pathway, as illustrated in **Figure 5**., the gene for the miRNA has its promoter and is therefore capable of autonomous transcription as an independent unit. Transcription of the gene occurs in the cell nucleus by RNA polymerase II or RNA polymerase III, as appropriate, to produce a primary pri-miRNA transcript, which can be post-transcriptionally edited by the addition of 7-methyl-guanosine at the 5′ end and polyadenylation at the 3′ ends [113,116]. Pri-miRNAs are subsequently converted to pre-miRNAs by a microprocessor complex consisting of the RNA-binding protein DGCR8 (DiGeorge Syndrome Critical Region 8 protein) and the ribonuclease III enzyme named Drosha [117]. DGCR8 recognizes certain patterns in the pri-miRNA, such as a GGAC sequence with N6-methyladenylation, whereas Drosha cuts the pri-miRNA at the bottom of its hairpin structure, resulting in a 3' overhang of 2 nucleotides on the pre-miRNA [118]. These pre-miRNAs are escorted from the nucleus to the cytoplasm by a complex involving Exportin-5 and RAS-related nuclear protein-guanosine-5’-triphosphate-ase (RanGTPase) [117,119]. Once in the cytoplasm, Dicer then processes the pre-miRNAs by cutting off the terminal loop, resulting in a mature miRNA duplex. The two strands of this duplex are (I) 5p,

which arises from the 5′ end of the pre-miRNA hairpin and (II) 3p, originating from the 3′ end. Both strands can attach to the Argonaute (AGO) protein family (specifically AGO1-4 in humans) in an ATP-dependent manner [120]. The decision of whether to incorporate 5p or 3p strand into AGO is based on factors such as thermodynamic stability and the presence of a 5′ uracil at position 1 [121]. The strand that is less stable or contains a 5′ uracil usually becomes the guide strand, while the other strand becomes the passenger strand. The passenger strand is then cleaved by Argonaute 2 (AGO2) and subsequently degraded, and the guide strand is incorporated into the RNA-induced silencing complex (RISC) [116]. The target structure for miRNA-induced silencing complex (miRISC) is the 3′ UTR (untranslated region) on the coding mRNA, which carries binding sites for many regulatory molecules important in controlling mRNA metabolism, such as localization, transport, translation efficiency, and stability [122].

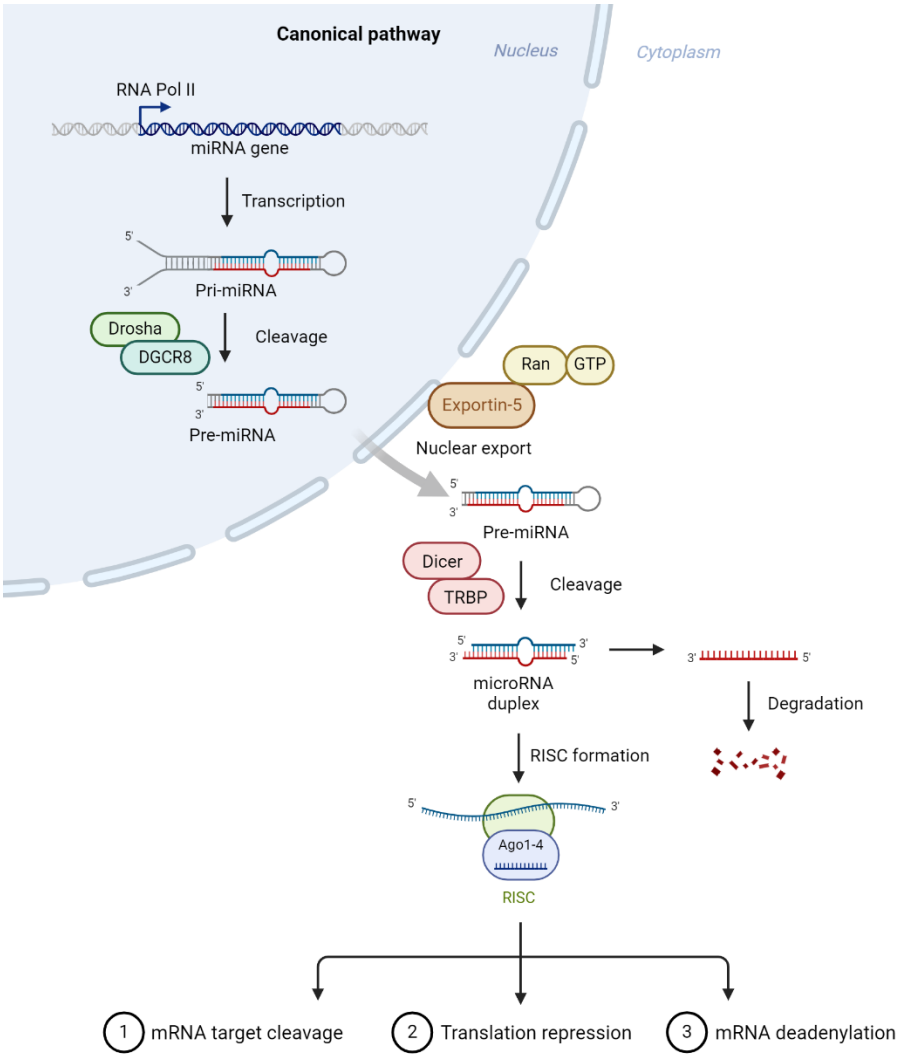

Figure 5. Canonical pathway of miRNA biogenesis (created with BioRender.com)

The degree of complementarity between miRNA and mRNA determines which of the three regulatory mechanisms the miRISC complex applies. This determination is based on the complementarity of seven nucleotide-long region, known as the seed sequence, located at the 5' end of miRNAs and complementary areas in the 3' UTRs of mRNAs [123]. The most common is imperfect pairing in the seed region, which directs the miRISC complex to target's deadenylation or translation inhibition. mRNA deadenylation leads to 5' end decapping and degradation of target mRNA. Less common is the perfect pairing leading to target degradation via endonucleolytic cleavage, and finally, extensive pairing leads to miRNA degradation and occurrs more frequently in plants [124].

The non-canonical pathway of miRNA biogenesis differs from the canonical pathway in various steps and mechanisms (**Figure 6**.). In contrast to the canonical pathway, which involves miRNAs transcribed from long primary transcripts (pri-miRNAs) that Drosha-DGCR8 then processes into shorter precursors (pre-miRNAs), the noncanonical pathway involves miRNAs encoded in introns (mirtrons) which are processed during splicing without Drosha involvement. Alternative pathways can export these pre-miRNAs to the cytoplasm and process them by enzymes other than Dicer. RISCs incorporate mature miRNAs using alternative complexes, which may affect their efficiency and specificity. In this way, the non-canonical pathway increases the complexity of post-transcriptional regulation of gene expression [113,125].

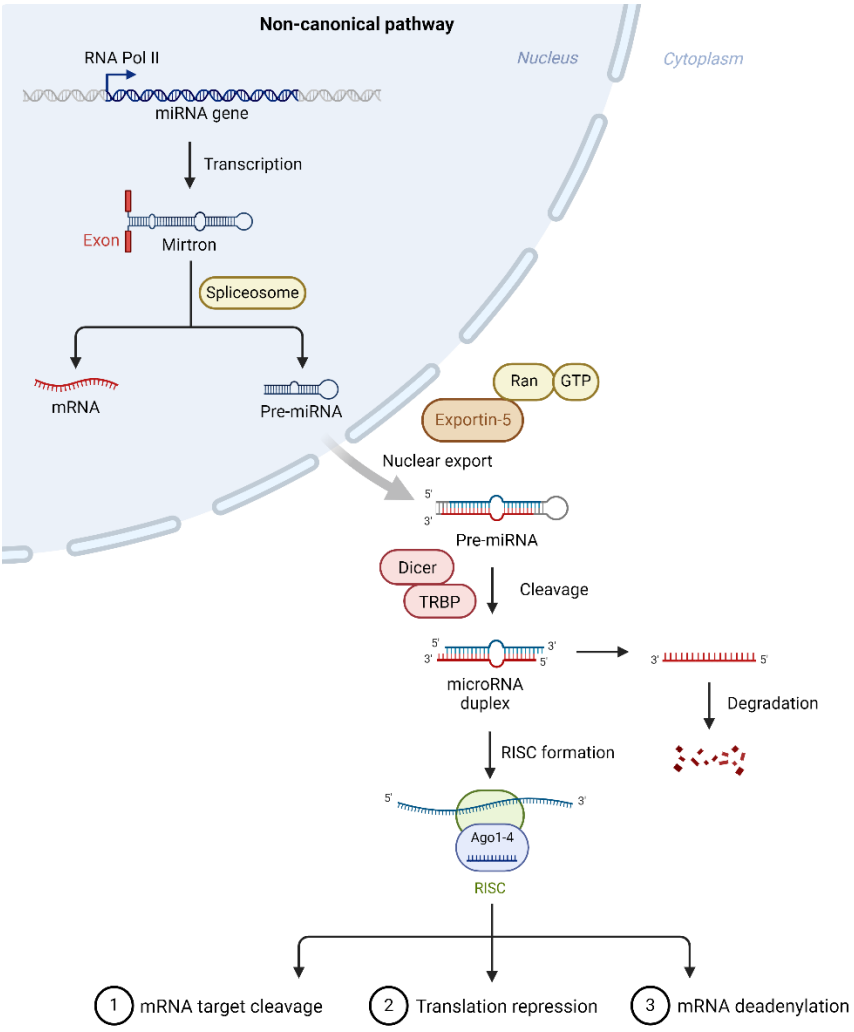

Figure 6. Non-canonical pathway of miRNA biogenesis (created with BioRender.com)

Although the mechanisms of miRNA biogenesis have been studied in detail, the same cannot be claimed for the degradation of these regulators. It is a well-known fact that miRNAs are highly stable molecules, but their half-life varies depending on the molecule type and localization. It was found that the half-life of miRNAs in organs such as the liver or heart reached hours to days, contrary to miRNAs in neurons that showed much shorter lifetimes and were more rapidly degraded [126–128]. Sequencing techniques have demonstrated that miRNAs with longer half-lives are modified by adding adenosine or uracil residues to their 3′ end, which protects them from exonuclease cleavage. miRNAs appear to have a very flexible and dynamic metabolism that has no universal rules, but is highly related to miRNA function and localization [124].

1.4.2 miRNA and cancer

miRNAs modulate the expression of more than 30% of genes and are involved in several processes ensuring homeostasis. It has become increasingly evident that miRNA dysregulation plays a significant role in carcinogenesis [129]. Human cancer is characterized by six biological capabilities acquired during tumor growth, according to Hanahan and Weinberg [130]. These abilities include maintaining proliferative signalling, evading growth suppressors, resisting cell death, enabling replicative immortality, activating invasion and metastasis, and inducing angiogenesis. Due to abnormal miRNA expression in tumors, the dysregulated miRNAs may affect one or more cancer hallmarks for tumor initiation and progression. [131].

In the process of carcinogenesis, miRNAs can act as an oncogene or a tumor suppressor. If expression is elevated in malignant cells, miRNA has oncogenic effect increasing tumor growth and metastatic potential. Increases in oncogenic miRNA levels can result from amplification, deregulation of transcription factors, or demethylation of cytosine-guanine dinucleotide (CpG) islands of gene promoters. Its role is then to regulate tumor suppressor target mRNA genes by downregulating their expression. In the case of tumor suppressor miRNAs, these are downregulated in malignant cells by deletion, DNA hypermethylation, or loss of transcription factors, while their target oncogenes are upregulated [132,133].

miRNAs can be detected in various biological samples including tissues and biological fluids such as blood, saliva, urine, cerebrospinal fluid, peritoneal and pleural fluids, and many others [133]. Using quantitative real-time PCR, microarrays, next-generation sequencing, and *in situ* hybridization, miRNAs can be quantified and could be used as minimally invasive biomarkers [134]. Although there are only a few studies on the role of miRNAs in PanNETs, they are evidently implicated in their oncogenesis. miRNA signatures could help differentiate between different pancreatic lesions as well as differentiate tumor samples from healthy tissues. Furthermore, miRNAs could provide prognostic information to enable improved patient management. Regarding the treatment of PanNETs, miRNAs may serve not only as biomarkers for treatment selection or response assessment but may also serve as potential therapeutic targets. However, despite their enormous potential, further research is needed in the areas of bioinformatics, miRNA profiling, and *in*

vitro/*in vivo* preclinical research models to better understand the various pathways of dysregulation in which miRNAs are involved [134].

1.4.2.1. miRNA as a diagnostic marker in PanNETs

miRNAs may help in the diagnosis of PanNET. From the expression profiling studies, various miRNAs have been highlighted (**Table 5**.). After examining the expression patterns of 754 miRNAs, Thorns et al. discovered a signature consisting of 13 miRNAs that allowed them to differentiate between PanNETs and healthy volunteers; only the expression of miR-193b changed significantly. Additionally, several miRNAs provided additional predictive data, indicating that miR-210 was associated with the prevalence of metastatic disease and miR-642 was correlated with Ki-67 [135]. Similar results were achieved by Roldo et al. [136], who showed that tumors may be distinguished from normal tissue by the expression of miR-103, miR-107, and the lack of miR-155. They also discovered a 10-miRNA signature that effectively distinguished between acinar and endocrine cancers. Comparably, 140 plasma and tissue samples from patients with different pancreatic lesions, such as pancreatic ductal adenocarcinoma, PanNETs, intraductal papillary mucinous neoplasms, and ampulla of Vater carcinomas, were subjected to exosomal miRNA profiling in a recent study [137]. The findings showed lesion-specific miRNA signatures that might be used to differentiate between various pancreatic lesions. Notably, miR-30a-3p, along with miR-24, miR-18a, miR-92a, miR-342-3p, miR-99b, miR-106b, miR-142-3p, and miR-532-3p, made it easier to distinguish between low-risk pancreatic cysts, where it would be enough to keep the patients under observation, and high-risk PanNETs that required surgery and/or further treatment. On the other hand, the diagnostic accuracy of chromogranin A was improved by a miRNA signature that included let-7b-5p, let-7i-5p, miR-143-3p, miR-30d-5p, miR-451a, and miR-486-p [138,139]. Furthermore, Panarelli et al. verified that miRNA expression profiling might help with the differentiation diagnosis of neuroendocrine tumors. PanNETs were classified as appendiceal, ileal, or rectal neuroendocrine tumors based on the expression patterns of miR-429, miR-487b, miR-615, and miR-92b [140].

Table 5. The diagnostic role of miRNAs in PanNETs (adjusted from [134])

miRNA	Expression	Function	Sample	Sample size	Method	Diagnostic Implication	Ref. No.
miR-193b	↑	Oncogenic	Serum, FFPE	37	TaqMan miRNA Arrays, qRT-PCR	Healthy vs. PanNETs	[135]
miR-103	↑	Oncogenic	FFPE	96	miRNA Microarray	Healthy vs. tumor	[136]
miR-107		Oncogenic					
miR-155	↓	Tumor suppressive					
miR-99a, 99b, 100, 125a, 125b-1, 125b-2, 129-2, 130a, 132, 342	↑	N/A				PanNETs vs. pancreatic adenocarcinoma/normal pancreas	
miR-451a, 372-3p, 106a-5p, 17-5p, 25-3p, 644a	↑	Oncogenic	Serum, FFPE	140	NanoString, qRT-PCR, miRNA *in situ* hybridization analysis	PanNETs vs. chronic pancreatitis	[137]
miR-22-3p, 1246, 4454, 7975, 320e	↓	Tumor suppressive					
miR-451a, 26b-5p, 25-3p, 16-5p	↑	N/A				PanNETs vs. pancreatic adenocarcinoma	
miR-1322, 1285-5p, 320e	↓	N/A					

miR-24, 30a-3p, 18a, 92a, 342-3p, 99b, 106b, 142-3p, 532-3p	N/A	N/A	FFPE	120	TaqMan miRNA Arrays, qRT-PCR	High-grade IPMNs, cystic PanNETs, and SPN vs. low-grade IPMN, SCA	[138]
let-7b-5p, let-7i-5p, miR-143-3p, miR-30d-5p, miR-451a, miR-486-p	⬇	N/A	Serum	75	Small RNA sequencing, qRT-PCR	PanNETs vs. PPGL	[139]
miR-615 and 92b	⬇	N/A	FFPE	81	Small RNA sequencing, qRT-PCR	midgut (ileum, appendix) vs. non-midgut (rectum, pancreas) NETs	[140]
miR-429 and 487b	⬆	N/A				PanNETs vs. rectal neuroendocrine tumors	

IPNM, intraductal papillary mucinous neoplasms; SPN, solid pseudopapillary neoplasms; SCA, serous cystadenomas; FFPE, formalin-fixed paraffin-embedded tissue; PPGL, pheochromocytomas/paragangliomas

1.4.2.2. miRNA as a prognostic marker in PanNETs

Recent studies have identified several miRNAs as potential prognostic biomarkers for PanNETs (**Table 6**.); some of them act as oncogenes, tumor suppressors, or modulators of metastasis [135,136,141–146]. Zimmerman et al. [141] analysed tissue samples from 37 PanNETs and found metastatic disease to be associated with miR-30a-5p, miR-210, miR-339-3p, miR-345, and miR-660 overexpression; in addition, miR-150, miR-21, and miR-660 levels correlated with proliferation index. Another study described that upregulation of miR-21, a miRNA involved in the regulation of *PTEN* and thus of the PI3K/mTOR pathway, was also associated with metastatic disease and proliferation activity [136,142] in PanNETs. miR-3653 hints to a poor prognosis, as its upregulation is associated with metastatic PanNETs through interaction with *ATRX* and the alternate lengthening of the telomeres pathway [143]. Cavalcanti et al. [144] demonstrated that high levels of miR-96-5p and miR-130b-3p expression were linked to higher tumor grade of GEP-NETs. On the other hand, higher miR-194-5p levels were associated with lower tumor grades, indicating that miRNAs may assist in histopathological analysis and clinical decisions in PanNET patients [144]. It was also shown that miR-196a was associated with worse survival rates for patients with PanNETs; eight miRNAs were examined in 37 resected PanNETs, and miR-196a was positively correlated with higher tumor size, node status, Ki-67, and mitotic counts [145]. An analysis of 57 PanNETs correlated miR-183-5p with increased tumor size, grade, and serotonin levels, as well as lower somatostatin receptor 2 expression and superior survival. Additionally, the study found a correlation between miR-183-5p and higher tumor size, grade, and serotonin levels; it also showed a correlation between reduced expression of somatostatin receptor 2 and better survival. The same study examined miR-132-3p, miR-145-5p, miR-34a-5p, and miR-449a. It similarly found a correlation between vascular invasion, low-grade malignancies, and elevated somatostatin expression with miR-132-3p. Hormone expression and miR-34a-5p were found to be related. miR-449a and miR-145-5p were linked to a worse prognosis [146].

Table 6. The prognostic role of miRNAs in PanNETs (adjusted from [134])

miRNA	Expression	Function	Sample	Sample size	Method	Clinical Implication	Ref. No.
miR-660, 30a-5p, 339-3p, 345	⬇	Tumor suppressive	FFPE	121	TaqMan miRNA Arrays, qRT-PCR	Metastatic disease	[141]
miR-21	⬆	Oncogenic	FFPE	121	TaqMan miRNA Arrays, qRT-PCR	Tumor grade	[141]
			FFPE	96	MicroRNA Microarray	Proliferative activity, Metastatic disease	[136]
miR-21, 10a, 106b	⬆	Oncogenic	FFPE	103	miRNA microarray, qRT-PCR	Proliferative activity	[142]
miR-3653	⬆	Oncogenic associated with ATRX mutations	FFPE	37	MicroRNA Microarray	Metastatic disease	[143]
miR-96-5p	⬆	Oncogenic, FoxO1a inhibition	FFPE	90	miRNA microarray, qRT-PCR	High tumor grade	[144]
miR-130b-3p	⬆	N/A					
miR-194-5p	⬇	N/A					

miR-196a	↑	N/A	FFPE	37	NanoString, qRT-PCR, miRNA *in situ* hybridization analysis	Advanced tumor Lymph-node invasion High mitotic and proliferative activity Recurrence	[145]
miR-183-5p	↑	Tumor suppressor	FFPE	57	qRT-PCR, IHC	High tumor grade Tumor size Somatostatin-receptor expression	[146]
miR-34a-5p	↑	N/A				Somatostatin, gastrin, and serotonin expression	
miR-145-5p	↑	N/A				High tumor grade Lymphatic invasion Serotonin expression	

miR-449a	↑	Oncogenic via histone deacetylases 3/4	FFPE	57	qRT-PCR, IHC	High tumor grade, mitotic and proliferative activity, lymph-node invasion	[146]
miR-132-3p	↑	Tumor-suppressing and tumor-promoting function				Low tumor grade	
						Vascular invasion	
						Somatostatin expression	
miR-210	↑	Oncogenic	Serum, FFPE	37	TaqMan miRNA Arrays, qRT-PCR	Metastatic disease	[135,141]
miR-642	↑	Oncogenic				Proliferative activity	[135]

Forkhead Box Protein O1A (FoxO1a), phosphatase and tensin homolog (PTEN), alpha thalassemia/mental retardation syndrome x-linked (ATRX), epithelial-mesenchymal transformation (EMT), immunohistochemistry (IHC)

1.4.2.3. miRNA as a therapeutic marker in PanNETs

miRNAs coordinate several biological processes by regulating the expression of thousands of distinct genes. Personalized cancer treatment is now possible thanks to advancements in cancer profiling. The complexity of miRNA biology could potentially offer new pharmacological alternatives for the management of PanNET (**Table 7**.). Currently, miRNAs are used in two different treatment strategies [134]. The first approach uses miRNA antagonists to inhibit oncogenic miRNAs, such as antimiRs, locked nucleic acids (LNAs), or miRNA antagonists (antagomiRs). AntagomiRs are single-stranded RNA molecules that act by complementary base pairing with miRNAs and are 21–23 nucleotides in length. To achieve effective pharmacological inhibition of disease-associated miRNAs, miRNA antagonists contain chemical modifications to enhance binding affinity, confer nuclease resistance, and facilitate cellular uptake [147]. The second approach substitutes downregulated tumor-suppressor miRNA with miRNA mimics to restore their function [134].

Dettori et al. [148] investigated the therapeutic potential of an anti-miR-214 compound in PanNETs, melanoma, and triple-negative breast cancer using mice models. Fewer lymphatic and pulmonary metastases, as well as circulating tumor cells, were observed in tumors treated with anti-miR-214. Targeting Ras/Erk signalling, miR-431 is elevated in PanNETs and promotes carcinogenesis. Inhibition of miR-431 by locked nucleic acids leads to significant downregulation of Erk signalling and the invasiveness of PanNET cells [149].

miRNAs might be utilized as biomarkers for treatment response. The antitumoral effects of metformin on PanNET cell lines were investigated by Yamaha et al. [150], who also confirmed the presence of certain miRNA expression patterns connected with the metformin antitumor impact. A p53 downstream effector, miR-34a, exhibits tumor-suppressive characteristics via promoting cell-cycle arrest and apoptosis. PanNETs showed abnormal expression of miR-34a, which may also be a useful target for therapy [146]. Several studies reduced tumor proliferation and induced apoptosis using miR-34a mimics in lung, pancreas, gastric, neuroblastoma, colon, prostate, and melanoma, and similar results may be achieved in PanNETs [151]. Bai et al.[152] investigated the role of miR-224 in PanNET and elucidated its involvement in tumorigenesis through the downstream proprotein convertase subtilisin/kexin 9 (PCSK9)/glucocorticoid pathway. In addition, they demonstrated the therapeutic prospect of miR-224 by transfecting miR-224 antagomiR into

BON-1 cell lines, which significantly inhibited development and invasion, as well as induced apoptosis.

Table 7. **The therapeutic role of miRNAs in PanNETs** (adjusted from [134])

miRNA	Expression	Model	Treatment	Method	Outcomes	Ref. No.
miR-214	⬆	Mouse	miR-214 inhibition	qRT-PCR, *in vitro* and *in vivo* assays	Reduced tumor volume Decreased volume of peripancreatic lymphatic metastases Reduced tumor vascularization	[148]
miR-431	⬆	Cell lines	miR-431-targeted locked nucleic acids	luciferase assay, qRT-PCR, Western Blot, RPPA	Reduced invasiveness	[149]
miR-224	⬇	Cell lines	miR-224 antagomiR	luciferase assay, qRT-PCR, Western Blot, TUNEL, CCK-8 assay, ELISA	Promotes apoptosis Inhibits proliferation, invasion	[152]

Reverse phase protein array (RPPA), TdT-UTP nick-end labeling (TUNEL), Cell Counting Kit-8 (CCK-8)

1.5 miRNA vs. mRNA expression profiling

Understanding the biological function of mRNA and miRNA genes requires accurate quantification in cells and tissues. Expression profiling of miRNAs has led to the identification of miRNAs that regulate multiple cellular processes. Although the number of miRNAs is relatively limited compared to mRNAs and proteins, a single miRNA can regulate hundreds of mRNAs with effects on gene expression networks. miRNA expression patterns can therefore be used as intermediary means to study biological processes, since their expression is linked to hundreds of target mRNAs. As a result, miRNAs are being explored as molecules that can reprogram cell fate and initiate cancer development as well as biomarkers to identify various types of cancer and to predict their outcome [153].

miRNA expression levels and those of their target genes can be quantitatively measured to better understand the mechanisms behind human disease development and discover new drug targets [154]. The development of high-throughput methods for detecting miRNAs and measuring gene and miRNA expression changes has received considerable attention. Due to their unique properties, miRNAs pose more challenges for accurate detection and quantification than mRNAs [155]. Traditionally designed primers for reverse transcription and polymerase chain reaction do not anneal to mature miRNAs due to their length of 22 nucleotides. The short length of miRNAs also makes it difficult to design complementary microarrays and perform reliable amplification or labelling without introducing biases in the signal [106].

The ability to discriminate between forms with single-nucleotide differences is also essential in miRNA detection and quantification, as miRNAs within a family (for example, the let-7 family) differ by as little as a single nucleotide [153,156].

For reverse transcription, miRNAs are not able to bind primers using a universal primer-binding site, such as the poly(A) tail, as mRNAs do. Since miRNAs make up a small percentage of the total amount of RNA, they must be detected selectively in a background of other, diverse RNA species, including pri- and pre-miRNA precursors that contain miRNA sequences [106,153]. Due to miRNAs' short length, variance in GC content can lead to wide variations in melting temperatures for annealing reactions, creating miRNA-specific biases. There are currently three major approaches for miRNA detection and quantification: microarray hybridization, RT-qPCR, and next-generation sequencing (NGS) [106,157].

Microarrays represent the most common high-throughput approach for miRNA profiling [158]. This hybridization-based technique, however, does not allow for absolute quantification, identification of novel miRNAs, or detection of canonical miRNAs and their isomiRs, the importance of which has only become apparent in recent years [159–161]. Moreover, microarray-based methods usually require high RNA input, which may be a limitation for liquid biopsies, where the RNA concentration is quite low [162].

In comparison to microarrays, RT-qPCR provides absolute quantification, a wide dynamic range, and high sensitivity, and can be used with low-input RNAs [157,163]. Besides that, RT-qPCR is a gold standard method for target miRNA analysis due to its availability in many laboratories as well as non-demanding instrumentation [157].

NGS technology has enabled a more comprehensive understanding of transcriptomes. In addition to known miRNAs profiling, miRNA sequencing can also identify novel miRNAs that cannot be detected by qRT-PCR or microarray. The NGS technology offers precise identification of miRNA sequences by detecting miRNAs with as little as a single nucleotide variation in their sequence, as well as identifying isomiRs of varying lengths, compared to other miRNA expression profiling techniques such as microarrays and RT-qPCR. However, the drawbacks are the complex experimental workflow and challenging computational analysis [157]. Despite these challenges, NGS represents an increasingly attractive option for comprehensive mRNA and miRNA studies.

1.6 miRNA target identification and prediction

The functional miRNA analysis is crucial to the identification of the genes that are targeted by the miRNA. The best way to identify target miRNA-mRNA interactions is usually to use a computational prediction tool followed by experimental validation of these targets. There are several tools available for computational analysis, each with a different approach to predict miRNA targets, and the number is continually growing [164,165]. Based on the characteristics of the mRNA sequence or the interaction between miRNA and mRNA, these algorithms can be classified into two main categories: statistical inference and machine learning [164].

In the first scenario, various components are considered when studying miRNA-target interactions. This includes analysing pairings between the seed sequence of miRNAs and

mRNAs, conducting thermodynamic analysis to determine the free energy and stability of these pairs, assessing the conservation of target sequences, evaluating the structural accessibility of 3'-UTRs for miRNAs, and calculating the number of potential miRNA binding sites on mRNAs, as a single mRNA can be targeted by multiple miRNAs [164]. Review studies focused on miRNA-mRNA targets described multiple prediction tools based of statistical inference; however, only a few of them are still available such as TargetScan [166], RNAhybrid [167], PITA [168], microTAR[169], RNA22 [170], and PACMIT [171].

In the case of the machine learning approach miRNA target identification prioritizes experimentally validated interactions between miRNA and mRNA, focusing on biological relevance rather than sequence or thermodynamic stability. As a part of artificial intelligence, machine learning allows systems to continuously improve their prediction accuracy by learning from curated datasets. Algorithms are trained using confirmed miRNA-mRNA interactions as positive examples, along with artificially created negative instances. As a result, machine learning tools look for patterns that differentiate true targets from false ones. By leveraging acquired knowledge through iterative learning, these systems can make predictions about whether a target is legitimate or not on new data [164,172]. Several prediction databases of experimentally validated miRNA-mRNA target interactions are available including miRDB [173], MiRTarBase [174], DIANA-TarBase [175], and miRecords [176].

2 OBJECTIVES

General:

- Combine the transcriptome profiles to investigate the role of the mRNA and miRNA expression in the molecular pathogenesis, clinical presentation, and prognosis of PanNETs compared to non-diseased controls.

Specific:

- Perform RNA sequencing to identify differentially expressed mRNAs in PanNETs.
- Undertake a focused transcriptomic analysis of expression levels of important clinicopathological biomarkers in the RNA-sequencing data.
- Classify PanNET cohort samples into distinct molecular subtypes based on their unique transcriptomic profiles.
- Perform miRNA sequencing and identify differentially expressed miRNAs in PanNETs.
- Validate miRNA expression data using quantitative real-time PCR as well as analysis of publicly available dataset to ensure robustness and reliability of sequencing results.
- Investigate the dynamic interplay between miRNAs and mRNAs by creating miRNA-mRNA interaction network, identifying miRNAs targets, and performing functional enrichment analysis of them.

3 MATERIAL AND METHODS

3.1 Patient cohort/Study group

The PanNET tissue sections were provided by the Ontario Tumour Bank, which is supported by the Ontario Institute for Cancer Research through funding provided by the Government of Ontario. The clinical characteristics of the patient's tumor samples (n=6) are described in **Table 8.** and non-diseased tissues (n=7) in **Table 9**. Usage of the PanNET samples was approved for research purposes through the Queen's University Health Sciences & Affiliated Teaching Hospitals Research Ethics Board (PATH-145-14). Non-diseased pancreatic tissues were delineated from pancreatic adenocarcinoma tissues and obtained from the Surgical Pathology Archive in the Department of Pathology and Molecular Medicine at Queen's University. Samples were approved for research through the Research Ethics Board at Queen's University (PATH-145-14). Hematoxylin-eosin-stained tissue sections from each case were reviewed and graded by an experienced pathologist according to the ENETS adopted by the WHO classification in 2010.

Table 8. Clinical characteristics of the tumor samples included in this study

Sample ID	Type	Age	Gender	Site of primary tumor	Tumor size (cm)	Grade	Tumor	Node	Metastasis	Type of procedure	Sites of disease
P1	Tumor	60-64	Male	pancreas	5	I	TX	NX	MI	resection	primary, liver
P2	Tumor	40-44	Female	pancreas	13	I	T3	N0	M0	resection	local nodes, primary, soft tissue
P3	Tumor	60-64	Female	pancreas	3	X	T2, NOS	N0	M0	resection	primary
P4*	Tumor	60-64	Female	pancreas	4.5	X	TX	N1	M0	resection	local nodes, primary
P5	Tumor	45-49	Female	tail of pancreas	10	I	T3	N1	M0	resection	primary, others
P6	Tumor	80-84	Male	distal pancreas	4.2	I	T2, NOS	N1	M0	resection	local nodes, primary

* neuroendocrine VIP-secreting tumor, I - Grade I (Well differentiated), X – Unknown, T – Tumor, N – Node, M – Metastasis

Table 9. Clinical characteristics of the non-diseased tissues included in this study

Sample ID	Type	Age	Gender	Description
P7	non-diseased	65-69	Female	Mucinous adenocarcinoma arising in a tubulovillous adenoma (duodenum)
P8	non-diseased	85-89	Male	Ductal adenocarcinoma, moderately differentiated
P10	non-diseased	70-74	Female	Moderately to poorly differentiated ductal adenocarcinoma
P11	non-diseased	55-59	Female	Well to moderately differentiated ductal adenocarcinoma
P12	non-diseased	70-74	Male	Moderately to poorly differentiated ductal adenocarcinoma
P13	non-diseased	60-64	Male	Moderately differentiated ductal adenocarcinoma
P14	non-diseased	65-69	Female	Moderately differentiated ductal adenocarcinoma

3.2 Total RNA isolation

Two to five 5 µm sections of the six FFPE PanNETs were scraped from slides and deparaffinized using Paraffin Dissolver (Macherey Nagel, Düren, Germany). Additionally, seven FFPE blocks of non-diseased tissues were sectioned (5 sections of 5 µm) for RNA extraction. Total RNA, including small RNAs, was isolated from all PanNETs and non-diseased tissue samples in a single batch using the NucleoSpin totalRNA FFPE XS kit (Macherey Nagel) according to the manufacturer's protocol with the following modifications as recommended in the user instructions: (I) extension of the proteinase K digestion step to 90 minutes at 56 °C, and (II) inclusion of the optional on-column rDNase digestion step to eliminate residual DNA. The extracted RNA was eluted in 25 µL of RNase-free water. After the isolation, the samples were immediately processed or stored at -80 °C.

RNA quantity was determined using the Qubit RNA HS Assay Kit (Qubit 4 Fluorometer, Thermo Fisher Scientific, Waltham, MA, USA) and RNA quality was assessed using the Agilent High Sensitivity RNA ScreenTape kit (Agilent 4150 TapeStation, Agilent, Santa Clara, CA, USA). Samples with DV_{200} > 25 % were considered suitable for library preparation.

3.3 RNA library preparation and sequencing

Total RNA libraries were prepared using TAKARA SMARTer Stranded Total RNA-Seq kit v3 – Pico Input Mammalian (TAKARA Bio, Kusatsu-Shi, Shiga, Japan) according to the manufacturer's guidelines (**Figure 7**.), with specific modifications recommended for highly degraded FFPE specimens, including (I) total RNA input 10 ng, (II) DNase pretreatment step, (III) omission of the fragmentation step, (IV) performing 10 PCR cycles for the first PCR amplification step, and (V) conducting 10 PCR cycles for the second PCR amplification step. Briefly, total RNA was converted to cDNA and then TruSeq Unique dual index adapters (Illumina, San Diego, CA, USA) for Illumina sequencing with specific barcodes were added through first PCR to differentiate each sample after pooling. The PCR products were purified using NucleoMag beads (Macherey Nagel) and then ribosomal cDNA was depleted. After that, the cDNA fragments were further amplified by second PCR with primers universal to all libraries (TAKARA Bio). Lastly, the PCR products were purified once more using NucleoMag beads to yield the final library. The final libraries were eluted in 12 µL of 5mM Tris Buffer. The quantity and range of fragment sizes were evaluated using the

Qubit dsDNA HS kit (Thermo Fisher Scientific), with a Qubit 4 Fluorometer as well as the Agilent High Sensitivity DNA ScreenTape kit (Agilent) with an Agilent 4150 TapeStation. After the quality check, libraries were pooled based on the concentration of each sample and the library fragment range. The molarity of the prepared 5 nM pool was quantified using Agilent High Sensitivity DNA ScreenTape kit with an Agilent 4150 TapeStation and KAPA library quantification assay (Kapa Biosystems, Wilmington, MA, USA). Pooled libraries were spiked with 10 % PhiX (Illumina), as recommended by both Illumina and Takara, and sequenced by an Illumina NovaSeq 6000 platform on an SP patterned flow cell. Paired-end sequencing with a read length of 2 x 100 bp was performed, aiming for approximately 100 million reads per sample.

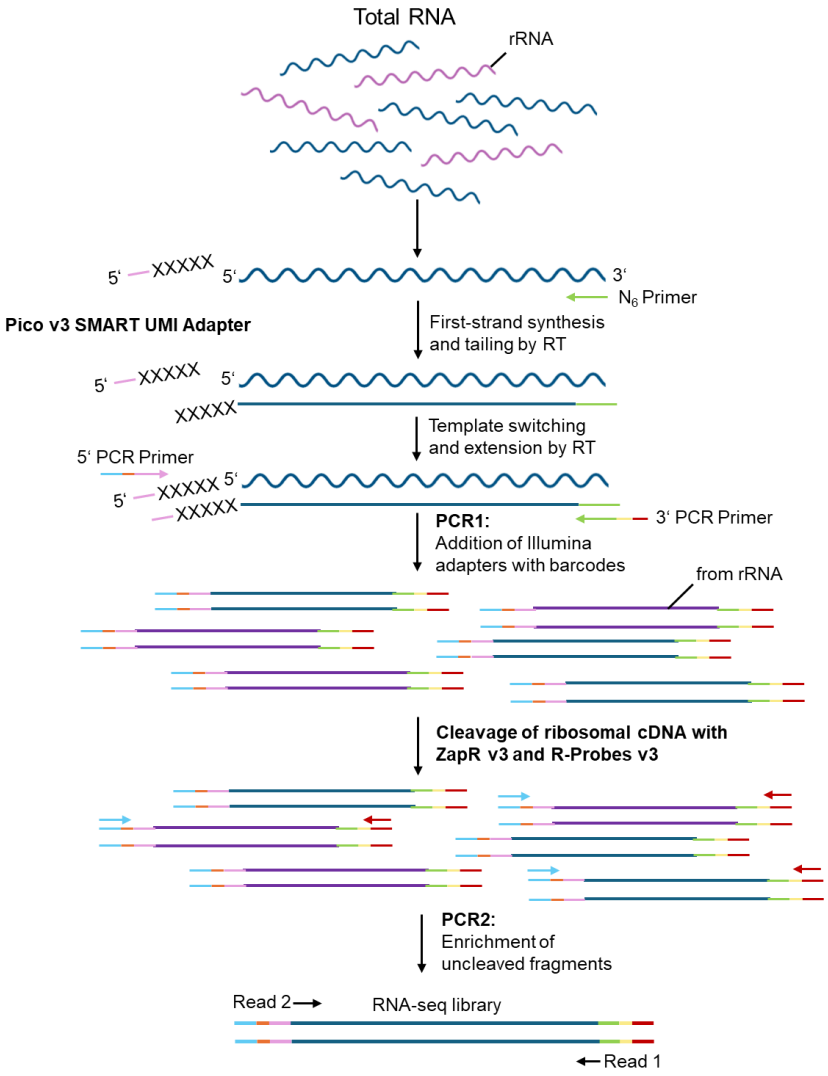

Figure 7. Overview of mRNA sequencing library preparation using the SMARTer Stranded Total RNA-Seq Kit v3 - Pico Input Mammalian (adjusted from the User Manual [177])

3.3.1 RNA sequencing data processing and differential expression analysis

The initial step in the RNA sequencing (RNA-seq) data processing workflow was the quality control (QC) of raw sequencing data using FastQC software v0.11.9 [178] to provide general descriptive statistics about sequence quality, identify duplicates, potential biases for downstream processing, sample outliers, and over-represented sequences or contaminants. The next step involved the removal of the adapter sequences using Cutadapt v3.4 [179]. Low quality bases were also trimmed off using UMI-tool v1.0.0 [180] since these could prevent proper read alignment to the reference genome. For alignment of our sequencing reads to the reference genome (GRCh38.104) the STAR aligner v2.7.7a [181] was used. Gene expression levels were quantified by counting reads mapped to each gene or transcript using FeatureCounts v1.5.2 [182]. For normalization to VST (variance stabilizing transformation) values and differential expression analysis, the DESeq2 v1.36.0 (R Package) [183] was used. Since all samples were prepared and sequenced in one batch, a tool for the elimination of the batch effect was not necessary.

Firstly, reads mapping to rRNA together with transcripts with less than five normalized counts in less than six samples (size of smaller group) were excluded. The final datasets consisted of 21,859 RNA transcript counts across the sample collection. Subsequently, DESeq2 [183] was used for differential expression (DE) analysis. Additionally, to enhance the accuracy of our analysis and remove false positive hits, DE analysis was performed a second time using the Wilcoxon rank-sum test [184]. In both cases, the significance level of DE was defined as $|\log_2(\text{fold change})| \geq 2$ and false discovery rate (FDR) adjusted P-value < 0.05. Differentially expressed genes (DEGs) fulfilled the following two requirements: (I) they were significantly differentially expressed in both analyses (i.e. the intersection of DESeq2 and Wilcoxon rank-sum test) and (II) the magnitude of their differential expression showed the same sign in both analyses, positive or negative difference compared to the non-diseased group. Then, the final DE intersection analyses were visualized as volcano plots of the DESeq2 data. For visualization of differences in expression patterns between tumor and non-diseased samples, principal component analysis (PCA) was used. The top 10% of up- and downregulated RNA transcripts were also hierarchically clustered and visualized as heatmaps. For hierarchical clustering, Euclidean distance and ward linkage criteria were used. To quantify the distinction between tumor and non-diseased, clusters silhouette score [185] was used. For PCA analysis, hierarchical clustering, and silhouette

score calculation, the scikit-learn (https://github.com/scikit-learn/scikit-learn) Python library was used. For scatter plot and heatmap visualization, seaborn (https://github.com/mwaskom/seaborn) and matplotlib (https://github.com/matplotlib/matplotlib) python libraries were used. Gene ontology (GO) annotation and Kyoto Encyclopedia of Genes and Genomes (KEGG) enrichment analysis were performed for up/downregulated DEGs by the Database for Annotation, Visualization, and Integrated Discovery (DAVID) annotation tool separately [186–188].

3.3.2 Focused analysis of expression levels of key clinicopathological markers

In clinical practice, several biomarkers are routinely studied for accurate PanNET diagnosis and management. RNA-seq data was scrutinized for the expression of key general biomarkers (*CHGA, PPY, ENO2, GNRH1*), specific biomarkers important for functioning tumors (*INS, IGF1, GCG, VIP, SST, PTHLH*), theranostic biomarkers (*SSTR1, SSTR2, SSTR3*), immunohistochemical tissue biomarkers (*MKI67, CHGA, SYP, PGR, CCND1, NESP55, CDX2, PAX8, PDX1)* as well as known molecular drivers (*DAXX, ATRX, TP53, RB1, MEN1, TSC1, TSC2, MGMT*). For this genes list, normalized gene expression values were filtered and compared between tumor and non-diseased group. Pearson correlation was used to assess significance. Balloon plot was used to visualize the data.

3.3.3 Molecular subtyping of PanNETs

A classification of PanNET into three different subtypes was carried out based on gene signatures taken from the study of Sadanandam et. al. [30]. This approach was divided into two steps. Firstly, genes with specific expression patterns for each of the pancreatic cancer subtypes were identified in the microarray dataset from the aforementioned study. The Kruskal-Wallis test (one-way ANOVA on ranks) was used to identify genes with specific expression patterns in subtypes (P-value <0.05) followed by a post-hoc Dunn test (P-value <0.05) to find genes with expression patterns exclusive to specific subtypes. Secondly, these groups of genes were used to interrogate their expression patterns in our RNA-seq data. Each sample was analysed separately. To compare microarray and RNA-seq expression data, we employed cosine similarity. A dimension reduction method, t-distributed stochastic neighbour embedding (t-SNE) [189], was used to visualize data points in low-dimensional space, with the goal being to preserve the patterns between data points from the original, high-dimensional space.

3.4 Small RNA library preparation and sequencing

Small RNA cDNA libraries were generated using QIAseq miRNA library kit (QIAGEN, San Diego, CA, USA), implementing 16 amplification cycles for 100 ng input, and 19 PCR cycles for 10 ng input. All steps from the procedure were performed according to the manufacturer's guidelines illustrated in **Figure 8**. Briefly, a pre-adenylated DNA adapter was ligated to the 3'end of all miRNAs. The 5' adaptor sequences were then added to the 5'end of the 3'-adaptor ligated small RNA molecules. The 3' and 5' adaptor ligated small RNAs were then reverse transcribed into cDNA while assigning a UMI (Unique Molecular Identifiers) to each miRNA molecule. UMI enables unbiased and accurate miRNome-wide quantification of mature miRNAs by NGS. During reverse transcription, a universal sequence is also added that is recognized by the sample indexing primers during library amplification. The libraries were purified using QIAseq Beads. Next, PCR amplification was performed using QIAseq miRNA NGS 48 Indexes (QIAGEN) to differentiate each sample after pooling. Lastly, the PCR products were purified once more using QIAseq Bead to yield the final library.

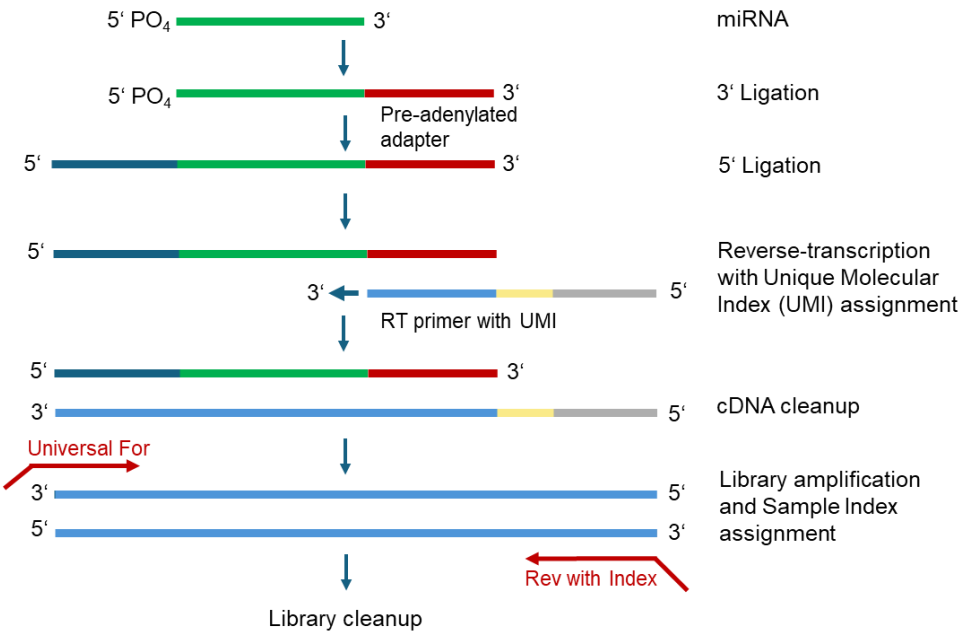

Figure 8. Overview of miRNA sequencing library preparation using the QIAseq miRNA Library Kit (adjusted from (189))

Libraries were pooled based on concentrations of each sample determined by Qubit 4 Fluorometer using Qubit dsDNA HS kit (Thermo Fisher Scientific), and based on library

fragment range determined by Agilent 4150 TapeStation using Agilent High Sensitivity DNA ScreenTape kit (Agilent). Sequencing was performed on Illumina NextSeq 500 using single-end high output mode with 75 cycles, 6nt index read mode with a sequencing depth of 10 million reads per sample.

3.4.1 Small RNA-seq data processing and differential expression analysis

Raw miRNA sequencing data were analysed using a Qiagen online tool called GeneGlobe (https://geneglobe.qiagen.com/us/analyze). Pre-configured pipelines for the analysis of miRNA sequencing data included steps for quality control, adapter trimming, alignment to reference sequences, and quantification of miRNA expression levels. Similar to RNA-seq, data processing for normalization to VST values and differential expression analysis via DESeq2 v1.36.0 was used [183] and elimination of the batch effect was not necessary. After filtering, the final miRNA dataset consisted of 437 miRNAs.

For miRNA-seq differential expression analysis, the same bioinformatic approaches were applied as mentioned previously for the RNA-seq data (Chapter: RNA sequencing data processing and differential expression analysis). Two methods were applied to identify differentially expressed miRNA genes (DEM): DESeq2 and Wilcoxon test with the same two criteria as for RNA-seq. The final DE intersection data points were visualized as volcano plots of the DESeq2 results. For visualization, PCA was used. For hierarchical clustering, all up- and downregulated miRNAs transcripts were included and visualized as heatmaps. Finally, to quantify the distinction between tumor and non-diseased, clusters silhouette score was applied.

3.4.2 Validation of miRNA expression

Relative expression of two miRNAs was analysed by means of the miRCURY LNA SYBR Green PCR kit and appropriate miRCURY LNA miRNA PCR assay primers (PCR assay for miR-216a-5p, PCR assay for miR-216b-5p, QIAGEN, Hilden, Germany) following the manufacturer's instructions. Master mix was made following the manufacturer's instructions with 3 µl of the diluted cDNA template added to each well with 7 µl of the master mix solution. All samples were run in triplicate. 5S rRNA and SNORD49A (QIAGEN, Hilden, Germany) were used as reference genes for expression analysis. Thermal cycling was performed on an AriaMx Real-Time PCR system (Agilent Technologies, California). The cycling conditions comprised initial heat activation at 95 °C for 2 minutes,

40 cycles at 95 °C for 10 seconds, and 56 °C for 60 seconds followed by a melt curve analysis. For the normalization of the expression level, we used comparative CT method. All Ct-values were normalized to an endogenous control (mean Ct value of 5S rRNA and SNORD49A), and ΔCt-values were calculated, where ΔCt = Ct (miRNA) − Ct (endogenous control) [191]. Relative expression values ($2^{-\Delta Ct}$) were plotted and compared. To verify mean differences among the groups, the normalized PCR data was analysed using a non-parametric statistical test, the Wilcoxon rank-sum test in GraphPad Prism v8.0.2. A two-sided $p < 0.05$ was considered statistically significant.

In the next step, publicly available dataset from Gene Expression Omnibus (GEO) database was used to verify the differential expression of the miR-216a-5p and miR-216b-5p. Preprocessing of miRNAs expression profiles from the GSE43796 dataset involved ensuring data quality and suitability for the next steps of the analysis. For the processing, quality assessment and differential expression analysis of Agilent miRNA array data the AgiMicroRna R package was applied [192]. First, background correction was performed using the limma package in R to remove non-specific signals. Second, quantile normalization [193] was performed to normalize the distribution of miRNA expression in the samples. Third, probe summation was performed to average the signal intensity between multiple probes assigned to the same miRNA. These specific preprocessing steps prepared the data for robust statistical analysis and accurately determined the DE of the miRNA. Criteria for selection of DEM were |log2fold change (FC)| ≥ 2 and P-value < 0.01. For the comparison of the miRNA expression profile in 6 PNETs patients and 5 healthy controls, we used z-score normalization. In this technique, values are subtracted by the mean of the dataset and then divided by the standard deviation.

3.4.3 miRNA target identification and miRNA-mRNA interaction network

For the prediction of miRNA-mRNA pairs, the top three upregulated and downregulated miRNAs were selected. The miRNA's putative mRNA targets were predicted by the miRDB [173] *in silico* prediction tool with default settings. To identify miRNA-mRNA pairs of interest, lists of predicted targets were intersected with our set of DEGs. The predicted targets for the top three upregulated miRNAs were overlapped with the downregulated DEGs and conversely, predicted targets for the top three upregulated miRNAs were crossed with the downregulated DEGs. This approach allows robust investigation of miRNA-target interactions and reduces false positive DEGs. For visualization of predicted

miRNA-mRNA pairs as well as for degree calculation, the NetworkX (https://github.com/networkx/networkx) Python library was used.

3.4.4 Correlation of the miRNA-mRNA predicted targets

For correlation analysis of predicted targets, Pearson correlation and subsequent hierarchical clustering with ward linkage were used to determine whether the expression levels of top DE miRNAs and its mRNA targets show an inverse correlation.

3.4.5 GO term & KEGG pathway enrichment analysis

For functional analyses of the DEGs and predicted targets, GO analysis was used to sort genes into categories based on biological processes, cellular components, and molecular functions, and the KEGG analysis was used to analyse their molecular function and associated pathways. The online tool for GO [186,187] and KEGG analysis was the module combined with clusterProfiler [194], Pathview [195], and the Scientific and Research plot tool (SRplot) [196]. These results were clarified by the DAVID software [188]. In the current study, GO terms and signalling pathways with P-value < 0.01 and FDR < 0.05 were considered significantly enriched.

4 RESULTS

4.1 Differential expression analysis of mRNAs

First, PCA was used to investigate whether transcriptomic profiles differed between the two sample groups. The plot of PC1 (46.11% variance cover) and PC2 (13.53% variance cover) showed clear differences between tumor and non-diseased samples, with no overlapping samples between groups in PC1. Moreover, the clustering was not affected by the sex or age of patients (**Figure 9**.).

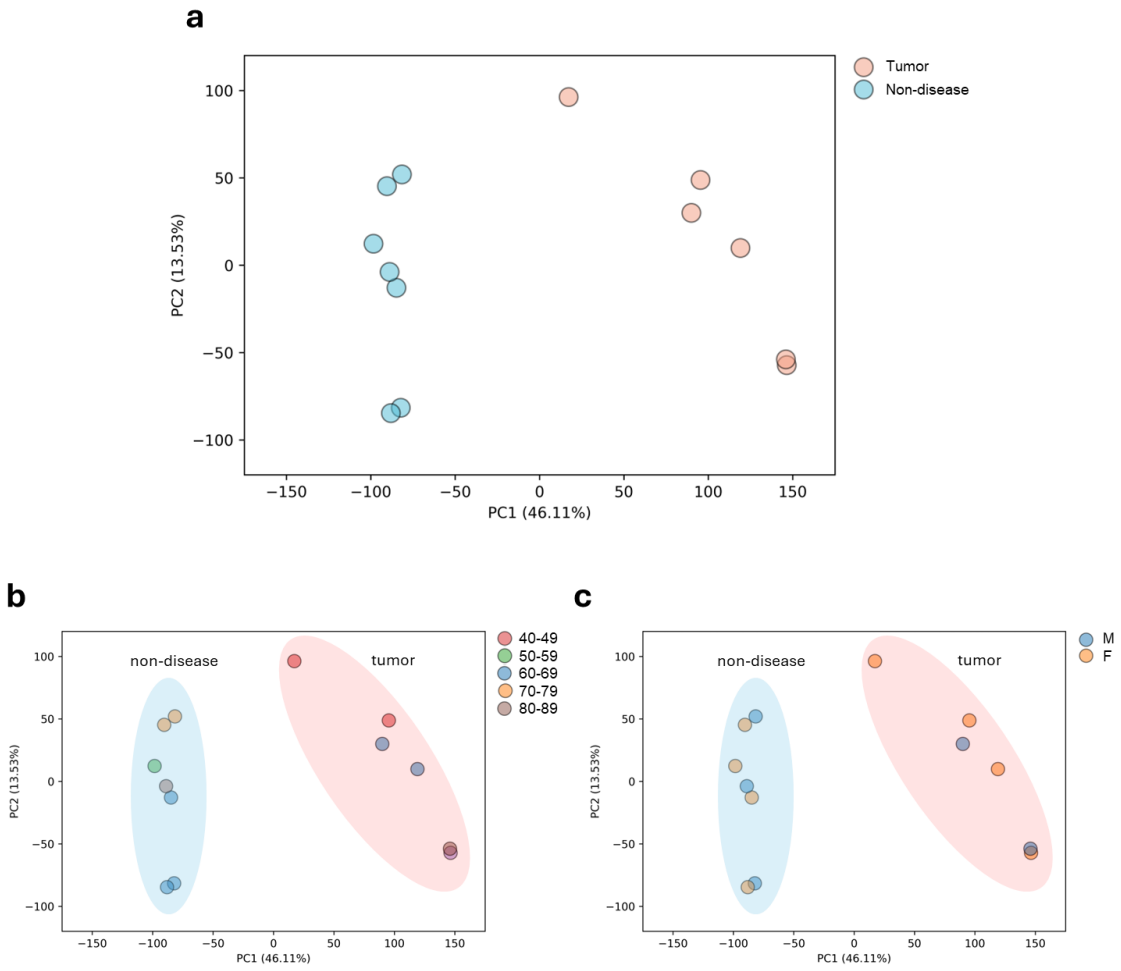

Figure 9. PCA of mRNA expression levels in tumor (n=6) and non-diseased (n=7) tissue samples. The PCA indicated a significant correlation with the disease status (**a**), regardless of age (**b**) or sex (**c**). Each dot represents a sample, and each color represents the type of the sample

To investigate differential expression patterns of mRNAs in tumor versus non-diseased groups, we took the intersection of the two DE analyses (DESeq2 and Wilcoxon

rank sum test), which revealed 1,417 (7.72 % of all analysed) DEGs. These were subsequently divided into 715 upregulated and 702 downregulated genes (**Figure 10**.). Hierarchical clustering of the top 10% upregulated and top 10% downregulated genes (72 and 70 genes respectively) showed clear separation by two clusters corresponding to tumor (light orange) and non-diseased (light blue) groups (**Figure 11**.). Unsupervised cluster analysis showed different clusters of tumor and non-diseased samples with a silhouette score of 0.75, indicating relatively well-separated clusters.

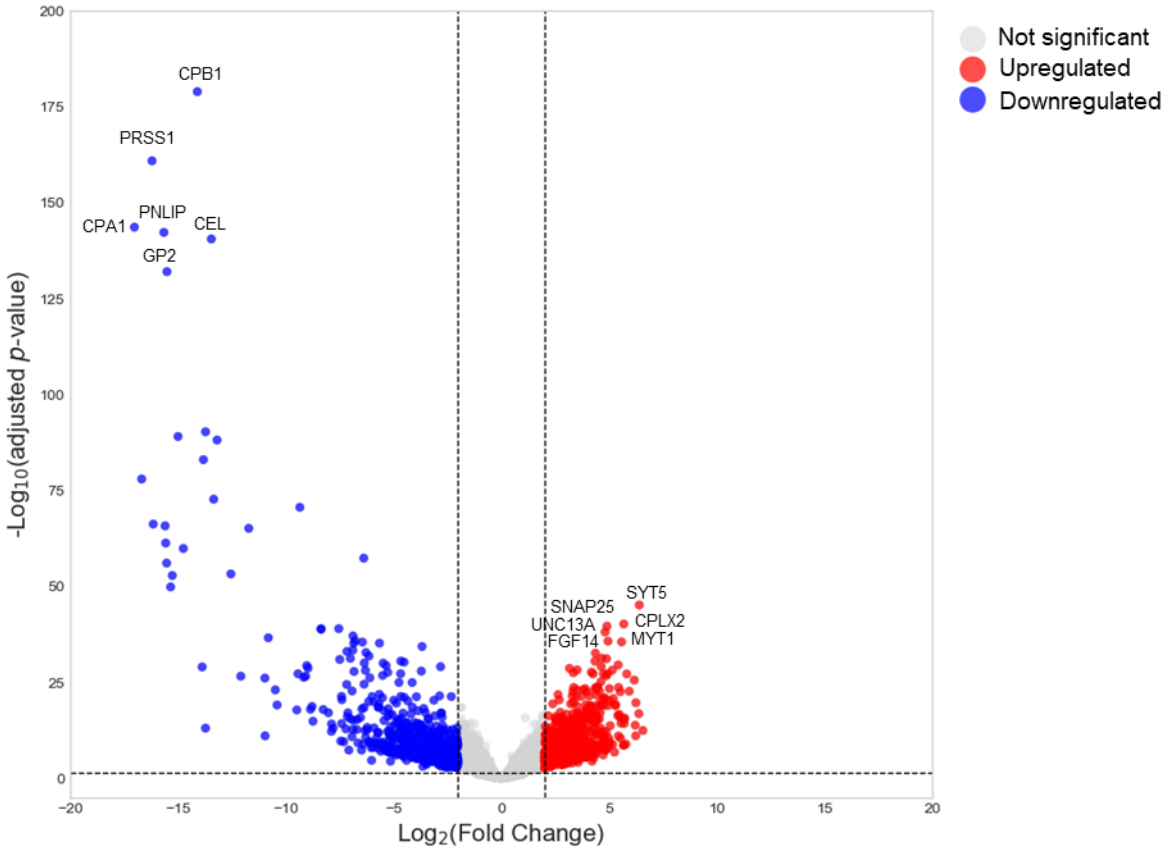

Figure 10. Volcano plot of intersection DE analysis of mRNA expression levels. The significance level was set to|Log2(fold change)| ≥ 2 and − Log10(adjusted P-value) < 0.05

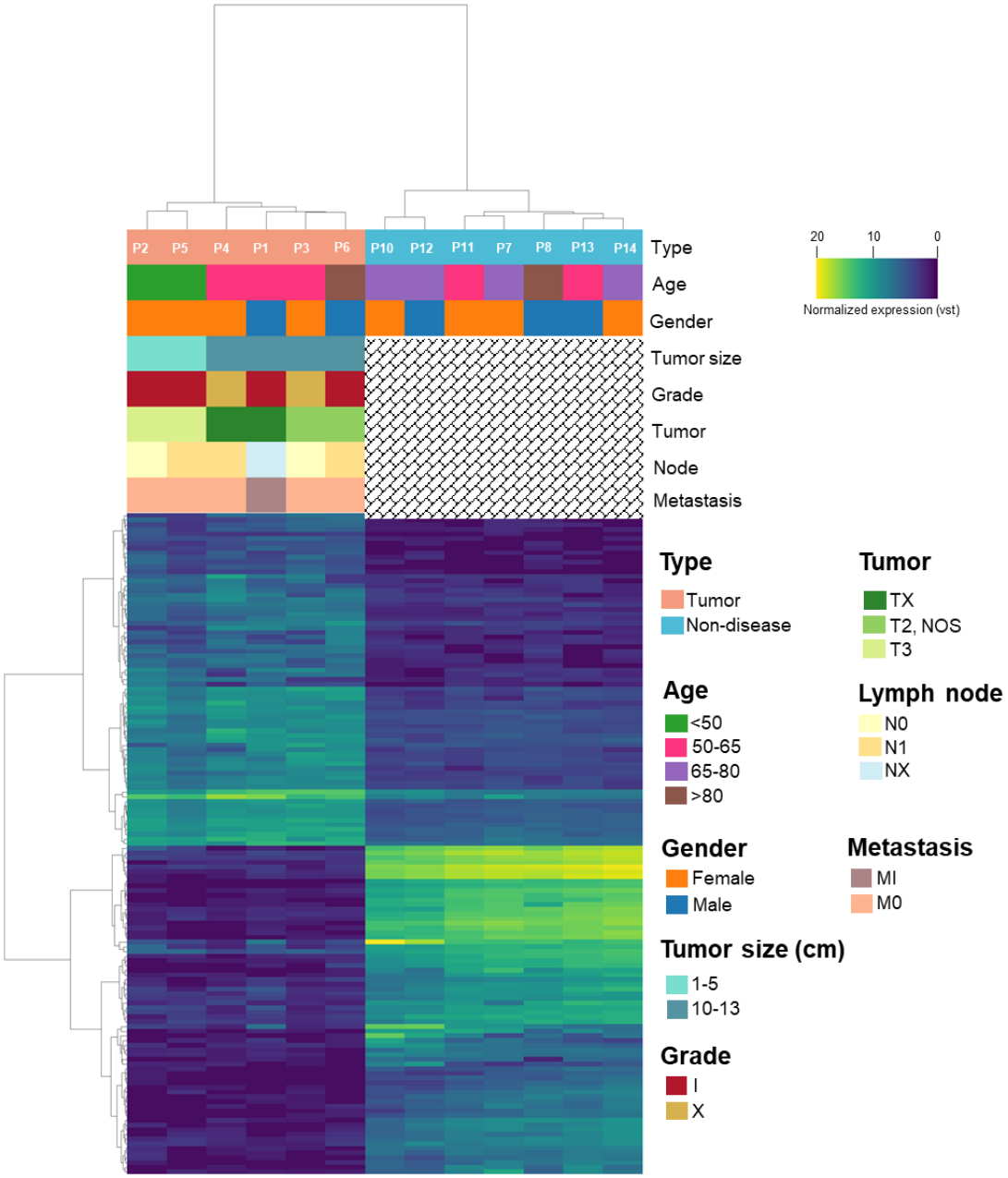

Figure 11. Hierarchically clustered heatmap of top 10% upregulated and downregulated genes based on their corresponding VST values

4.1.1 Functional enrichment analysis of differentially expressed mRNAs

To shed light on the functional characteristics of the DEGs, the upregulated and downregulated DEGs were analysed using GO and KEGG enrichment analyses separately. A list of the top 10 GO terms from the three categories of biological process (BP), cellular component (CC), and molecular function (MF) is presented in **Figure 12**. For the PanNET downregulated DEGs, the GO analysis showed that DEGs were significantly enriched in

digestion at the BP level, in extracellular exosome at the CC level, and in serine-type endopeptidase activity at the MF level. Furthermore, the enriched KEGG pathways of the downregulated DEGs included pathways involved in pancreatic secretion, protein digestion and absorption, maturity onset diabetes of the young, metabolism of xenobiotics by cytochrome P450, and metabolic pathways. For the PanNET upregulated DEGs, the GO analysis showed that DEGs were significantly enriched in the regulation of ion transmembrane transport at the BP level, in dendrite at the CC level, and in calcium ion binding at the MF level. Furthermore, the enriched KEGG pathways of the upregulated DEGs included pathways involved in the dopaminergic synapse, GABAergic synapse, circadian entrainment, glutamatergic synapse, and insulin secretion.

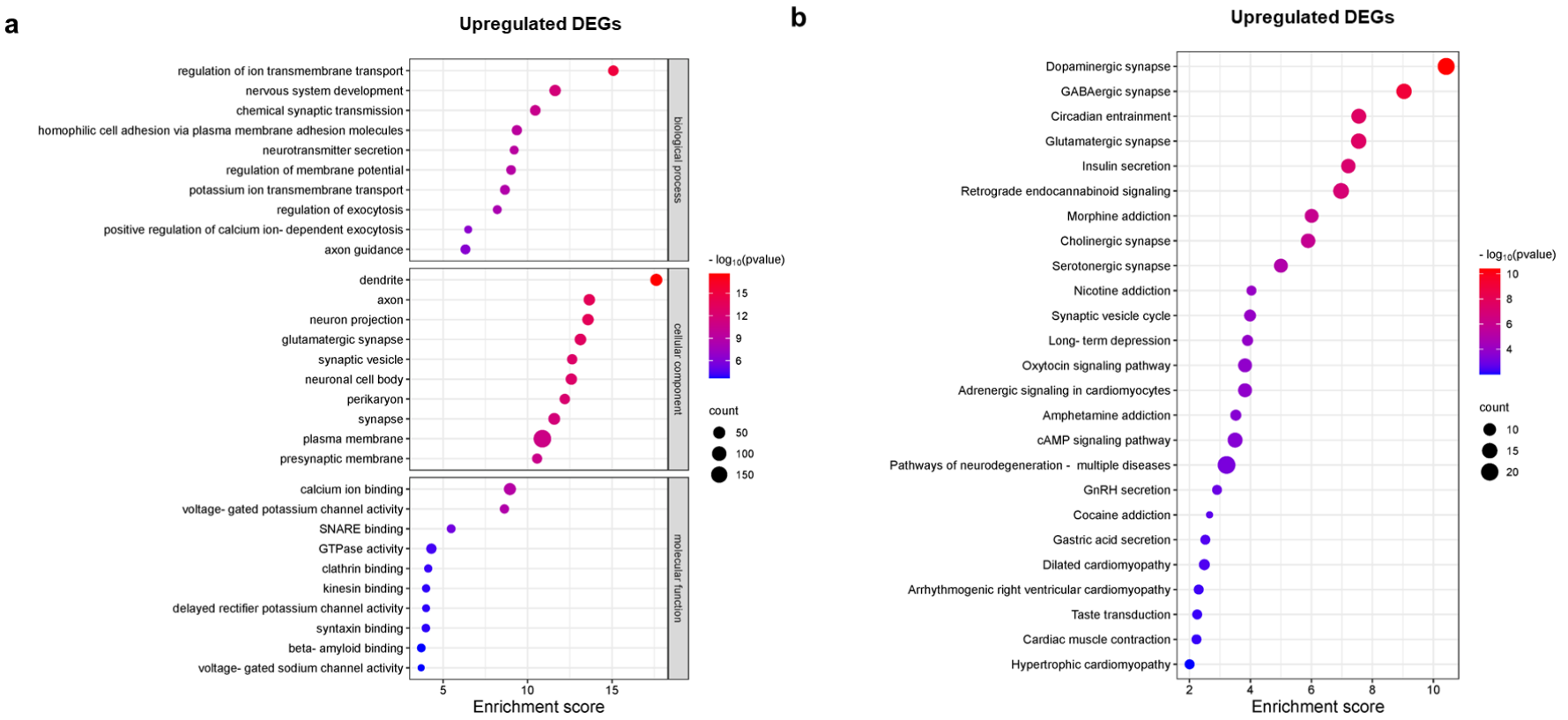
a
Upregulated DEGs
regulation of ion transmembrane transport
nervous system development
chemical synaptic transmission
homophilic cell adhesion via plasma membrane adhesion molecules
neurotransmitter secretion
regulation of membrane potential
potassium ion transmembrane transport
regulation of exocytosis
positive regulation of calcium ion- dependent exocytosis
axon guidance
biological process
dendrite
axon
neuron projection
glutamatergic synapse
synaptic vesicle
neuronal cell body
perikaryon
synapse
plasma membrane
presynaptic membrane
cellular component
calcium ion binding
voltage- gated potassium channel activity
SNARE binding
GTPase activity
clathrin binding
kinesin binding
delayed rectifier potassium channel activity
syntaxin binding
beta- amyloid binding
voltage- gated sodium channel activity
molecular function
5
10
15
Enrichment score
- log10(pvalue)
15
12
9
6
count
50
100
150
b
Upregulated DEGs
Dopaminergic synapse
GABAergic synapse
Circadian entrainment
Glutamatergic synapse
Insulin secretion
Retrograde endocannabinoid signaling
Morphine addiction
Cholinergic synapse
Serotonergic synapse
Nicotine addiction
Synaptic vesicle cycle
Long- term depression
Oxytocin signaling pathway
Adrenergic signaling in cardiomyocytes
Amphetamine addiction
cAMP signaling pathway
Pathways of neurodegeneration - multiple diseases
GnRH secretion
Cocaine addiction
Gastric acid secretion
Dilated cardiomyopathy
Arrhythmogenic right ventricular cardiomyopathy
Taste transduction
Cardiac muscle contraction
Hypertrophic cardiomyopathy
2
4
6
8
10
Enrichment score
- log10(pvalue)
10
8
6
4
count
10
15
20

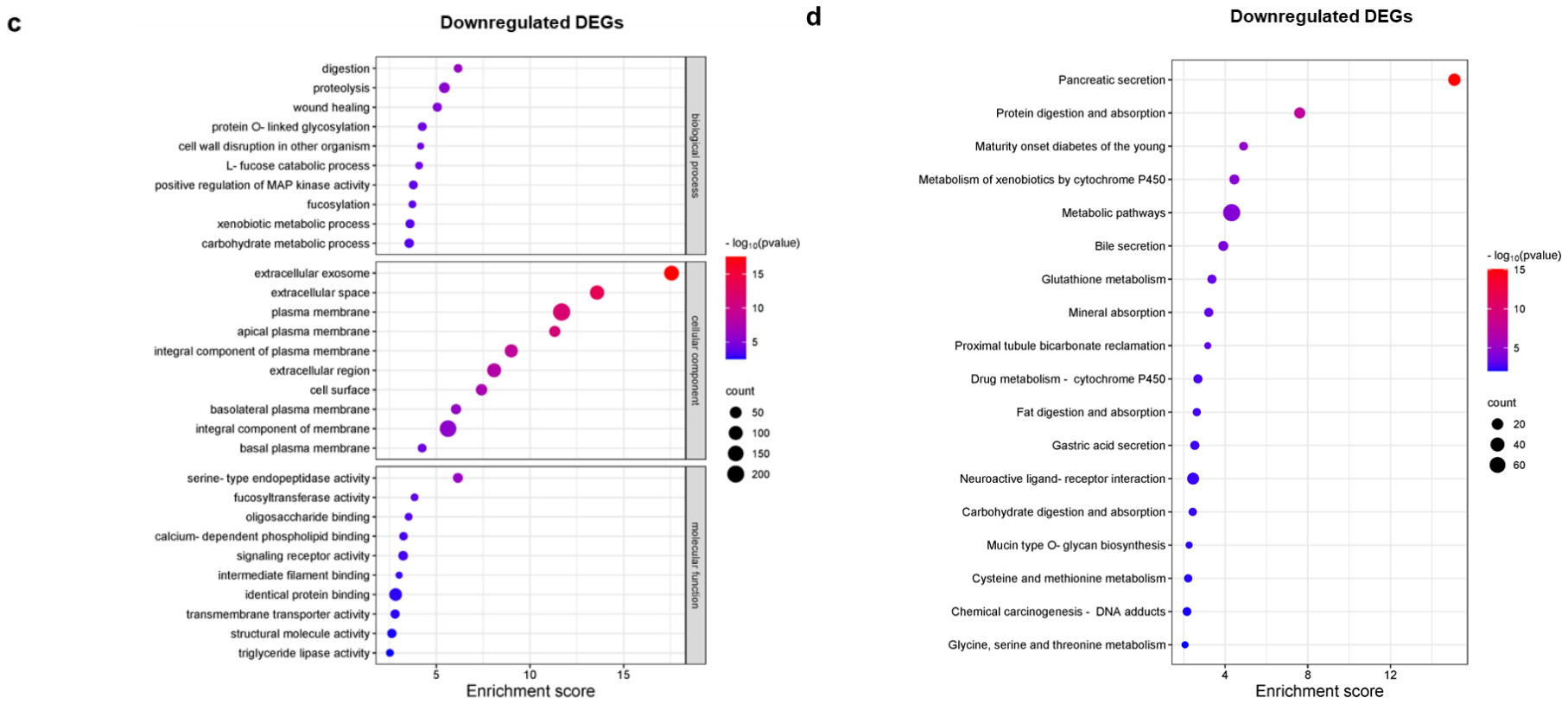

Figure 12. GO and KEGG functional enrichment analysis of 1,417 differentially expressed mRNAs. (**a**) GO analysis of upregulated DEGs, (**b**) Pathway enrichment analysis of upregulated DEGs, (**c**) GO analysis of downregulated DEGs, (**d**) Pathway enrichment analysis of downregulated DEGs (GO, Gene Ontology; DEGs, differentially expressed genes; KEGG, Kyoto Encyclopedia of Genes and Genomes)

4.2 Assessment of expression levels of important clinicopathological markers

From mRNA-seq data, the expression of known biomarkers, which are used in clinical practice for PanNETs management, was studied next. For this analysis, Person correlation was used to determine the significance of gene expression levels in comparison to non-diseased tissues. The balloon plot showed a few interesting findings that should be highlighted (**Figure 13**.). Commonly, CHGA and SYP were differentially expressed among tumors, when compared to control tissues, highlighting that RNA could be a surrogate analyte for these markers that are used to diagnose PanNETs with IHC (CHGA, $P<0.001$, SYP, $P<0.0001$). Similarly, SSTR1 ($P<0.01$) and SSTR2 ($P< 0.0001$), markers for treatment with somatostatin analogues, was differentially expressed in all tumors. Next, sample P4, which was diagnosed as a VIP-secreting tumor according to data from the biobank, gratifyingly displayed a significant increase in VIP RNA. Notably, results show increased expression of the INS marker in non-diseased samples compared to tumors ($P<0.001$). Finally, P3 and P6 tumor samples showed overexpression of glucagon (GCG). These results confirmed that mRNA expression data can provide valuable insights into the molecular characteristics of PanNETs, and potentially can serve as a complementary tool to traditional diagnostic and prognostic biomarkers.

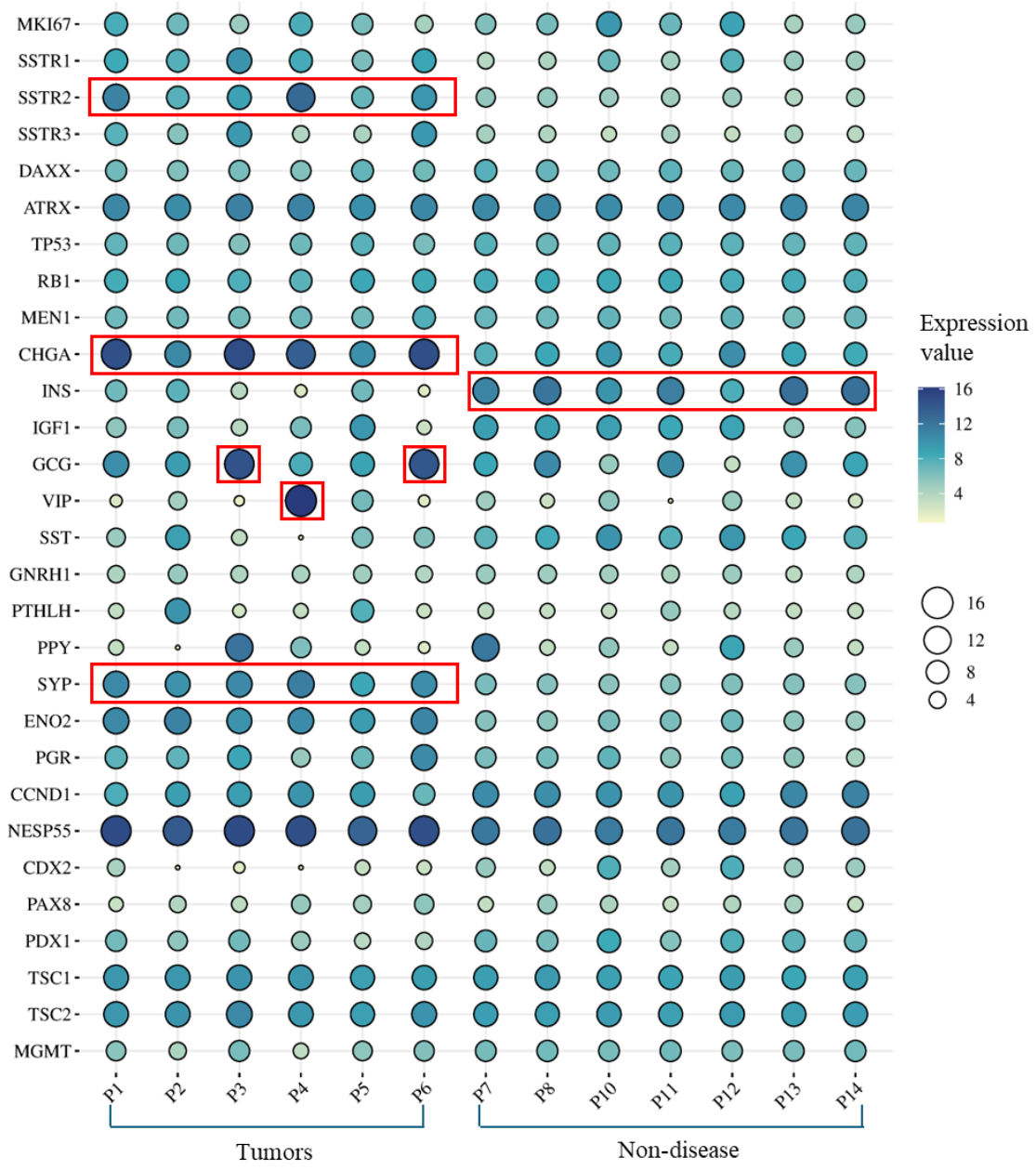

Figure 13. Analysis of mRNA expression data with comparison to clinicopathological data

4.3 Molecular subtyping of PanNETs

Statistical analysis of genes with subtype-specific expression patterns in microarray dataset

Sadanandam et. al [30] used median-centred microarray dataset of 221 genes for subtyping samples to Normal islet-like, (insulinoma-like), MLP (metastasis-like/primary) and Intermediate subtypes. To find genes with subtype specific expression patterns in the published dataset, we used the Kruskal-Wallis test (one-way ANOVA on ranks) (P-value <0.05) following the post-hoc Dunn test (P-value <0.05) on the publicly available data to find genes with expression patterns exclusive in specific subtypes. We found 10 genes for the

Insulinoma-like group, 29 genes for the MLP and 47 genes specific for the Intermediate group in Sadanandam's data. However, not all identified genes were detected in our RNA-seq data (**Figure 14**.). This may be caused by the fact that genes that had less than 5 counts in more than 3 samples were excluded from our RNA-seq dataset. In further analysis, we only worked with those genes which passed our rigorous filters. The final set thus consisted of 10 Insulinoma-like genes, 28 MLP genes and 43 genes for Intermediate (**Figure 15**.).

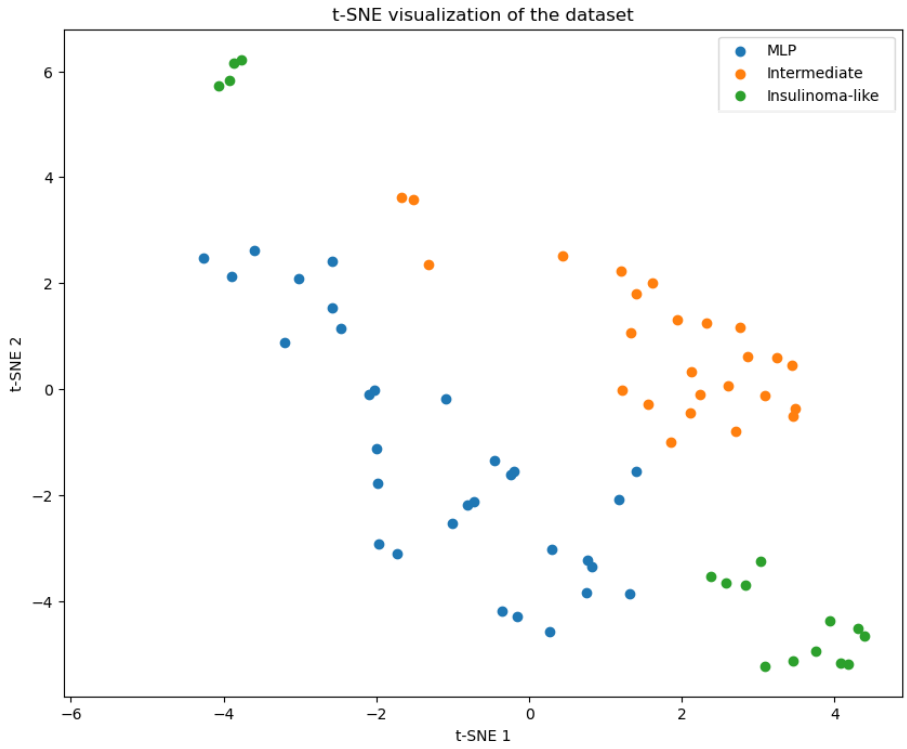

Figure 14. t-SNE visualization (with default hyperparameters) of Sadanandam´s cohort using 86 median-centred microarray genes

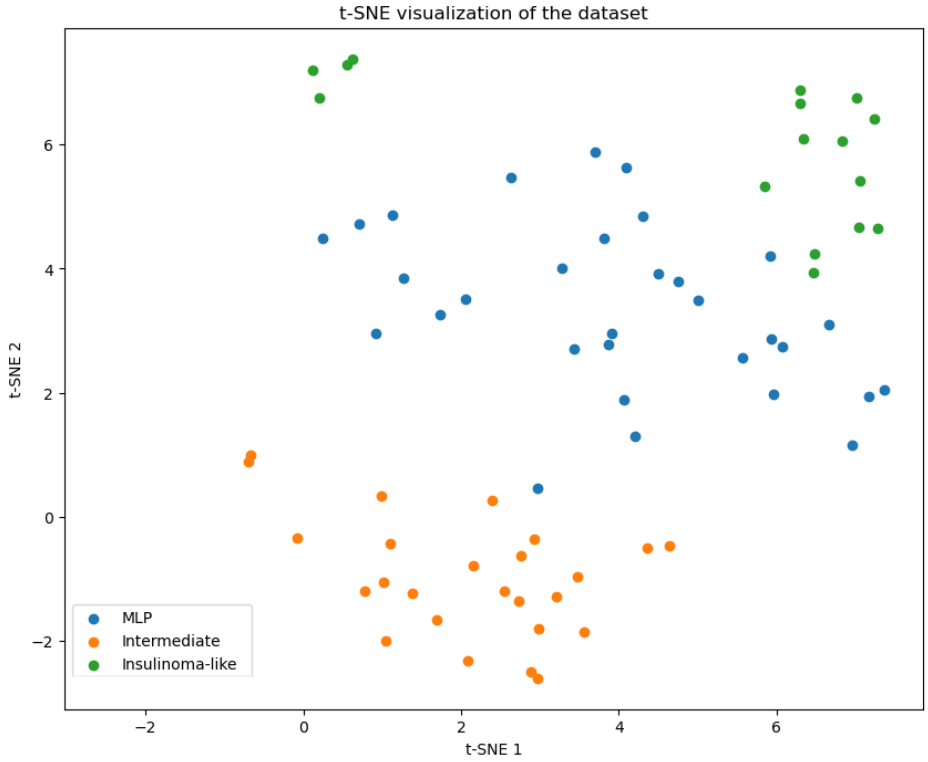

Figure 15. t-SNE visualization (with default hyperparameters) of Sadanandam´s cohort using 81 median-centred microarray genes, which were also detected in our RNA-seq data

Analysis of subtype specific gene patterns in RNA-seq samples and comparing microarray and RNA-seq results

Comparing microarray and RNA-seq expression patterns has two associated challenges. First, these are two different techniques with important technical differences (e.g. microarray has an upper limit of detection, which is imposed by the definite number of gene-specific probes on the array, whereas no such limit is to be expected in an NGS approach). Second, the original microarray dataset was median-centred. To compare microarray and RNA-seq expression patterns, the cosine similarity was employed between vectors: one vector represented by microarray data for each subtype and another by each RNA-seq sample. Each subtype vector was compared to each RNA-seq sample separately. Microarray subtype data included more than one sample. For this reason, the median value for each gene and each subtype was calculated to get 1D vector. Cosine similarity was in the range from -1 to 1 (-1 = strongly opposite vectors; 0 = orthogonal vector, data are independent; 1 = similar co-linear vectors). Values between 0 and 1 represent the degree of similarity. Values between 0 and -1 represent the opposite relationship between expressions (**Table 10**.).

Table 10. Subtyping of PanNET samples according to cosine similarity analysis

Subtypes/ RNA-seq samples	P1	P2	P3	P4	P5	P6
MLP	0.38	0.72	-0.8	0.04	0.8	-0.88
Intermediate	0.67	-0.24	0.09	-0.59	-0.53	0.36
Insulinoma-like	0.36	0.17	-0.09	-0.22	-0.3	-0.07

In order to subtype RNA-seq samples and demonstrate the cosine similarity results, t-sne median-centred RNA-seq data together with microarray dataset of 81 genes were plotted in **Figure 16**. P1, P2, and P5 samples showed affiliation to the same subtypes like in cosine similarity analysis (P1: 0.67 similarity with intermediate, P2: 0.72 and P5: 0.8 similarity with MLP subtype). Concordantly with the molecular data, P2 and P5 patients´ clinical presentation was the poorest in terms of disease onset and tumor size.

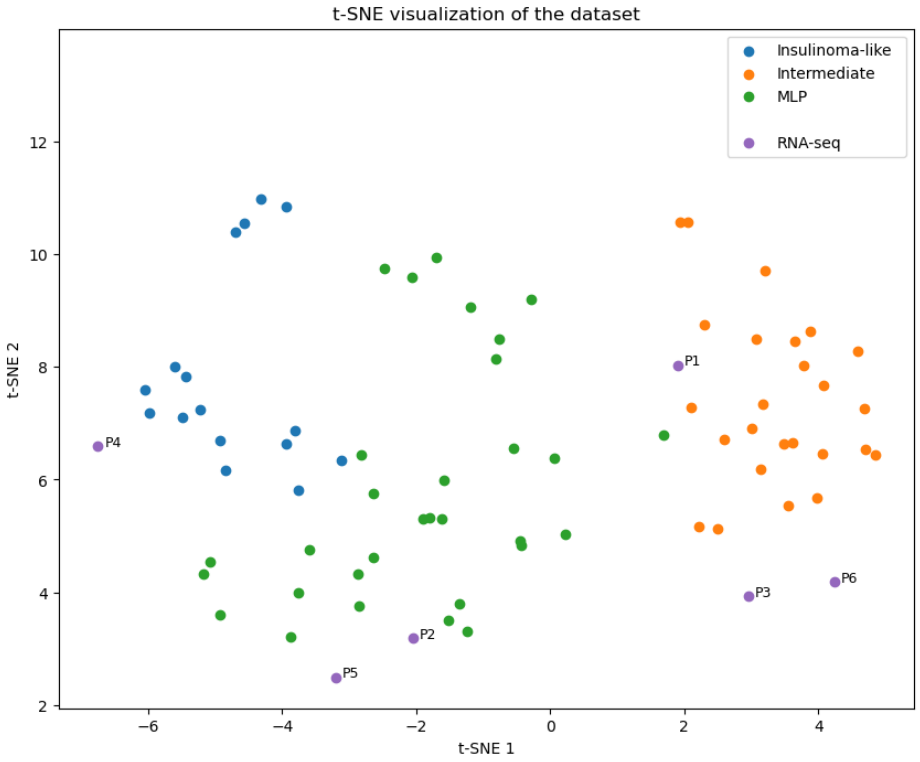

Figure 16. t-SNE visualization of RNA-seq samples and microarray cohort

4.4 Differential expression analysis of miRNAs

Similar to mRNA, PCA analysis of miRNome profiles showed clear differences in expression patterns between tumor and non-diseased groups in the first two dimensions, PC1 (49.43% variance covered) and PC2 (13.99% variance covered), which were independent of the patient's sex or age (**Figure 17**.).

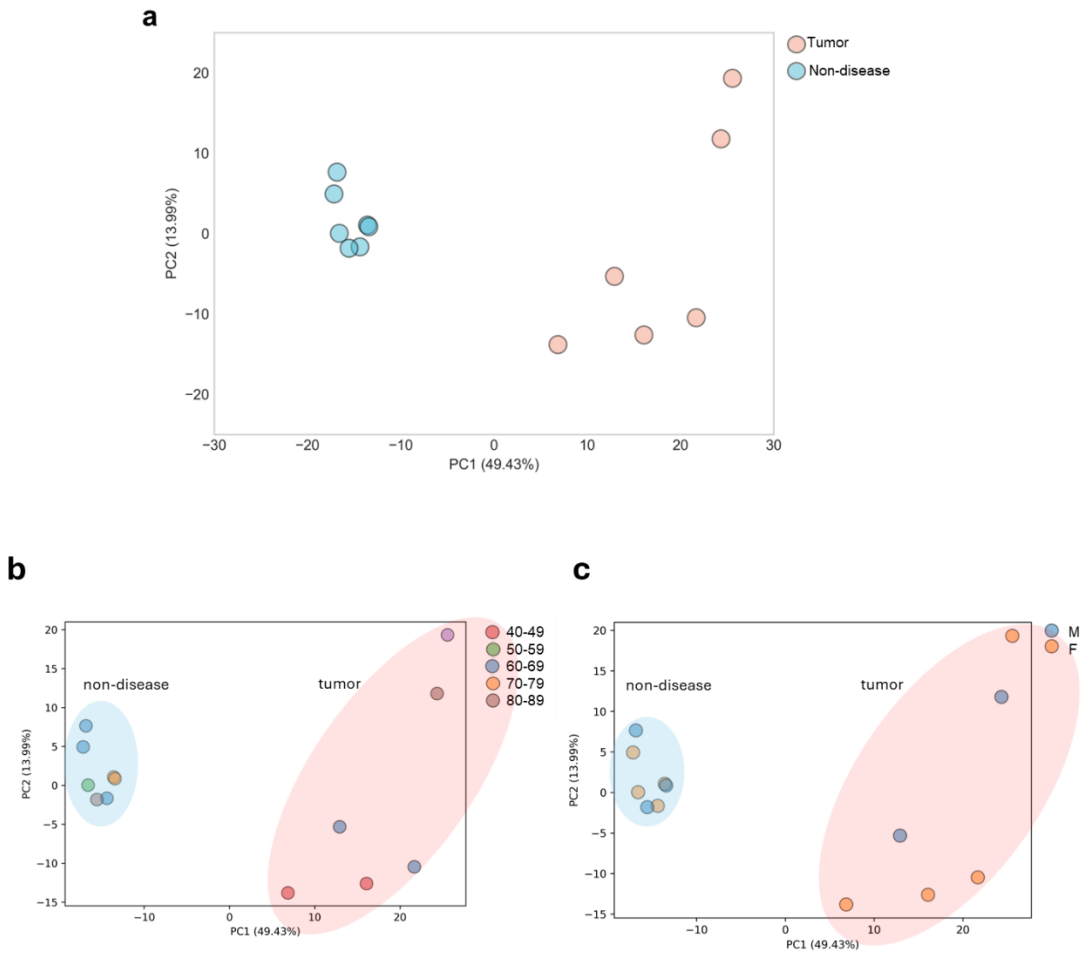

Figure 17. PCA of miRNA expression levels in tumor (n=6) and non-diseased (n=7) tissue samples. The PCA indicated a significant correlation with the disease status (**a**), regardless of age (**b**) or sex (**c**). Each dot represents a sample, and each color represents the type of the sample

To investigate differential expression patterns of miRNAs in tumor versus non-diseased groups, we again used the intersection of two DE analyses and found 60 (16.6 %) miRNAs with 41 and 19 miRNAs upregulated and downregulated, respectively (**Figure 198**.). Hierarchical clustering of all DEMs yielded two different clusters for tumor and non-

diseased samples, although the separation (0.57 silhouette score) was less defined than the clusters based on mRNA profiles (**Figure 19**.).

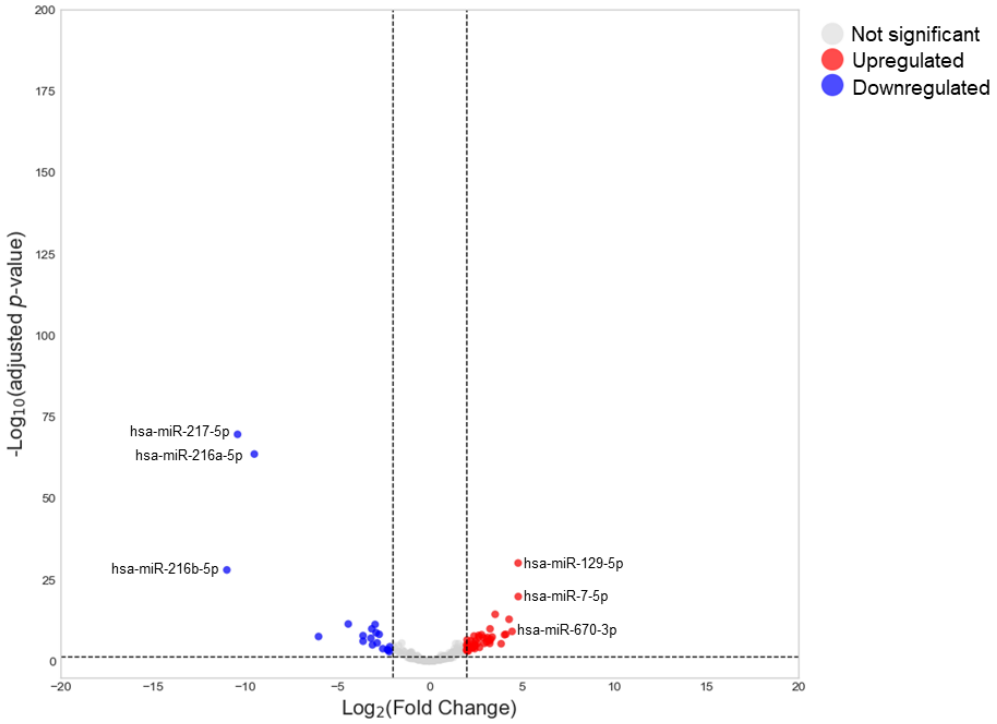

Figure 18. Volcano plot of intersection DE analysis of miRNA expression levels. The significance level was set to|Log2(fold change)| ≥ 2 and − Log10(adjusted P-value) < 0.05

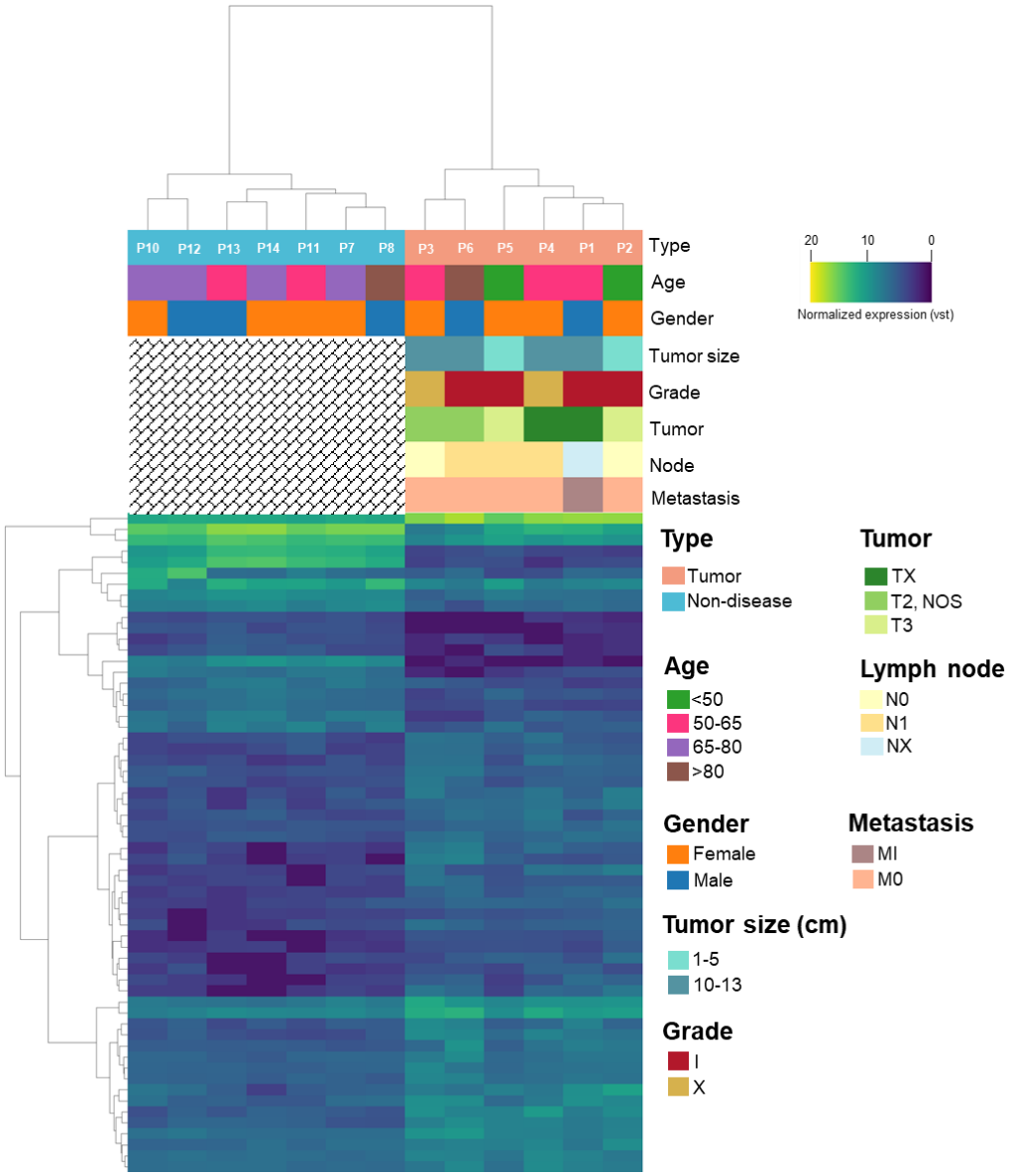

Figure 19. Hierarchically clustered heatmap of all (60) DEMs based on their corresponding VST normalized values

The miR-216 cluster (miR-216a, miR-216b, and miR-217), located in the same genomic region of chromosome 2 (2q16.1), were the most downregulated miRNAs in tumor versus non-diseased groups **(**

Table 11.); conversely, miR-670-3p, miR-129-5p, and miR-7-5p were the top upregulated miRNAs in tumor versus non-diseased groups (

Table 12.).

Table 11. Differential expression analyses results of the downregulated miRNA in PanNETs versus non-diseased samples

miRNA ID	log2FoldChange DESeq2	Padj DESeq2
hsa-miR-216b-5p	**-10.97**	1.09E-28
hsa-miR-217-5p	**-10.39**	2.64E-70
hsa-miR-216a-5p	**-9.48**	2.99E-64
hsa-miR-215-5p	-6.00	3.03E-08
hsa-miR-135b-5p	-4.39	4.25E-12
hsa-miR-148a-3p	-3.59	1.63E-08
hsa-miR-934	-3.59	8.08E-07
hsa-miR-148a-5p	-3.17	9.85E-08
hsa-miR-30c-2-3p	-3.12	1.34E-10
hsa-miR-561-5p	-3.08	1.10E-05
hsa-miR-30a-5p	-2.94	6.00E-12
hsa-miR-365a-3p	-2.88	2.06E-09
hsa-miR-130b-5p	-2.83	2.74E-06
hsa-miR-30a-3p	-2.72	6.49E-09
hsa-miR-548j-5p	-2.52	1.62E-04
hsa-miR-451a	-2.27	3.10E-04
hsa-miR-144-5p	-2.22	4.86E-04
hsa-miR-483-3p	-2.17	1.31E-03
hsa-miR-181a-2-3p	-2.15	4.34E-05

Table 12. Differential expression analyses results of the upregulated miRNA in PanNETs versus non-diseased samples

miRNA ID	log2FoldChange DESeq2	Padj DESeq2
hsa-miR-129-5p	**4.82**	1.65E-20
hsa-miR-7-5p	**4.81**	8.30E-31
hsa-miR-670-3p	**4.48**	8.09E-10
hsa-miR-874-3p	4.32	1.52E-13
hsa-miR-874-5p	4.15	6.26E-09

hsa-miR-129-1-3p	4.07	8.66E-09
hsa-miR-1224-5p	3.89	4.96E-06
hsa-miR-1180-3p	3.57	4.66E-15
hsa-miR-129-2-3p	3.41	4.10E-08
hsa-miR-3065-5p	3.33	2.02E-07
hsa-miR-642a-3p	3.29	1.34E-10
hsa-miR-210-3p	3.28	3.96E-06
hsa-miR-1179	3.26	6.61E-07
hsa-miR-488-3p	3.15	5.53E-08
hsa-miR-153-3p	3.11	1.57E-07
hsa-miR-487a-3p	3.11	1.51E-06
hsa-miR-3200-3p	2.99	3.57E-06
hsa-miR-323b-3p	2.92	6.52E-08
hsa-miR-132-3p	2.83	8.57E-09
hsa-miR-33b-5p	2.72	6.70E-05
hsa-miR-92b-3p	2.69	4.61E-08
hsa-miR-95-3p	2.67	1.37E-08
hsa-miR-212-3p	2.62	3.49E-06
hsa-miR-324-5p	2.49	7.81E-07
hsa-miR-1301-3p	2.47	2.17E-05
hsa-miR-1185-1-3p	2.46	1.62E-04
hsa-miR-539-3p	2.42	4.67E-06
hsa-miR-487b-3p	2.42	2.11E-08
hsa-miR-487a-5p	2.36	6.70E-05
hsa-miR-212-5p	2.35	6.97E-05
hsa-miR-485-5p	2.33	9.21E-05
hsa-miR-642a-5p	2.25	6.61E-07
hsa-miR-301a-3p	2.21	4.34E-05
hsa-miR-544a	2.20	5.24E-05
hsa-miR-1290	2.12	8.29E-04
hsa-miR-409-5p	2.09	5.73E-06
hsa-miR-652-3p	2.07	4.34E-05
hsa-miR-29b-2-5p	2.05	7.67E-04
hsa-miR-671-5p	2.05	3.40E-07
hsa-miR-598-3p	2.02	1.30E-05
hsa-miR-324-3p	2.01	3.99E-04

4.5 Validation of miRNA-seq results

In order to ensure the reproducibility and validity of differentially expressed miRNAs in PanNETs, we used RT-qPCR approach. Small RNA sequencing results were used to select miRNAs for verification analysis, specifically miR-216a-5p and miR-216b-5p. The Wilcoxon

rank-sum test confirmed that both miRNAs were significantly downregulated in the original sample cohort used for the study ($P < 0.001$ for both miR-216a-5p and miR-216b-5p). The boxplot shows the relative expression level of miR-216a/b-5p in tumor and non-diseased samples (**Figure 20**.).

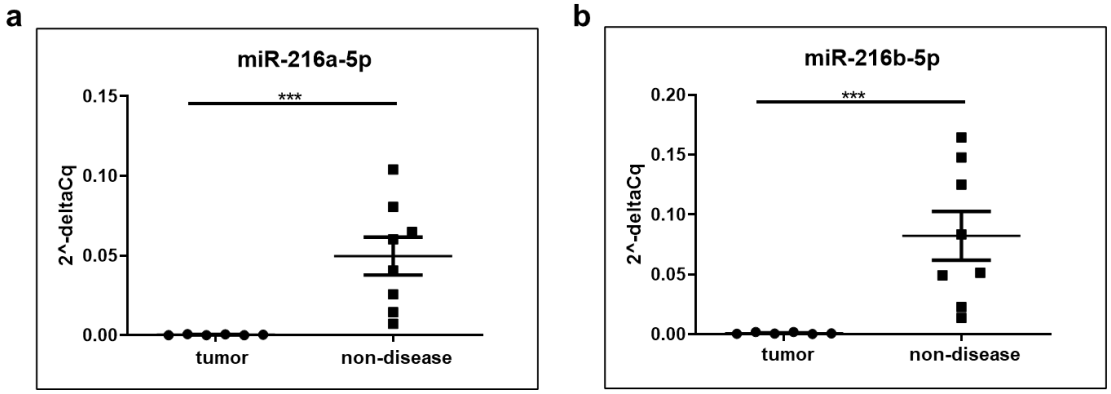

Figure 20. Relative expression of miR-216a-5p (a) and miR-216b-5p (b) in PanNETs compared to non-disease group by RT-qPCR

Our findings were further confirmed using GSE43796 dataset, which contains miRNA expression profile of 6 PNETs and 5 healthy controls. Z-score normalization and Wilcoxon rank-sum test were applied to calculate the significance of the aforementioned miRNAs in the disease ($P < 0.01$ for both miR-216a-5p and miR-216b-5p). The boxplots depicting Z-score of the tumors compared to control provided proof of the results from miRNA sequencing and the RT-qPCR, that indicated that miR-216a/b-5p may be a biomarker for differentiating PanNETs from healthy controls (**Figure 21.**).

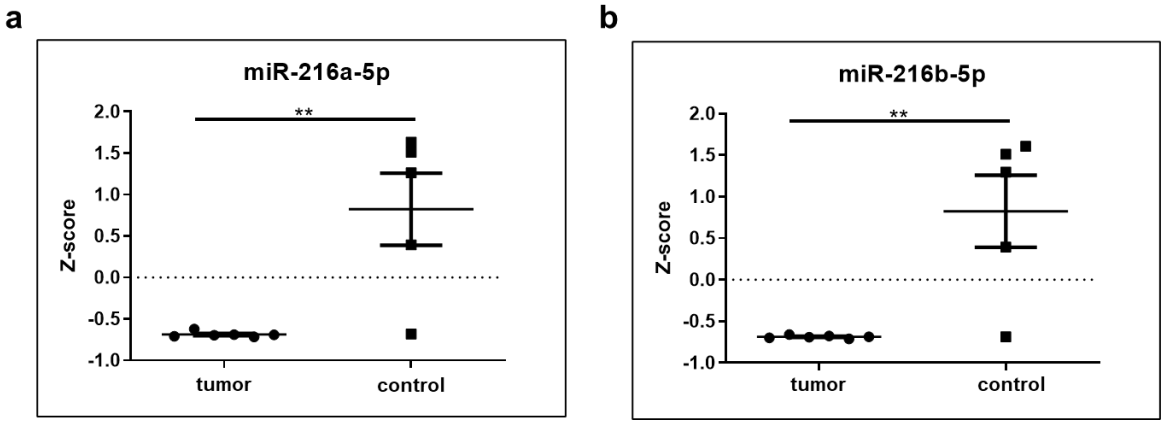

Figure 21. Expression level of miR-216a-5p (a) and miR-216b-5p (b) in PanNETs compared to healthy control using publicly available dataset

4.6 Construction of the miRNA-mRNA interaction network

Given that PanNETs can be stratified into molecular subtypes by their separate mRNA and miRNA profiles [30], it was decided to attempt to extend these findings by identifying miRNA-mRNA interaction networks using the top three upregulated miRNAs: 670-3p, 129-5p, and 7-5p as well as the top three downregulated miRNAs: 216a-5p, 216b-5p, and 217-5p. Thus, the miRDB [173] target prediction tool was used with default settings to generate a list of putative mRNA targets and we overlapped the list of putative mRNA targets with our list of DEGs. As a result, 54 unique targets were found for upregulated miRNAs and 35 unique targets for downregulated miRNAs. Upregulated miR-670-3p had the most targets (N=25), while downregulated miR-216a-5p had the least targets (N=7) in PanNETs versus non-diseased tissues (**Figure 22**.). The network of downregulated miRNAs consists of three distinct sub-networks with no shared targets among them, while our top upregulated miRNAs shared six mRNA targets, specifically *PKHD1* and *TSPAN6* between miR-670-3p and miR-129-5p. Also, miR-129-5p shares *TMEM97* and *PKP2* with miR-7-5p and miR-7-5p shares targets *IGSF3* and *TGFA* with miR-670-3p (**Figure 23.**).

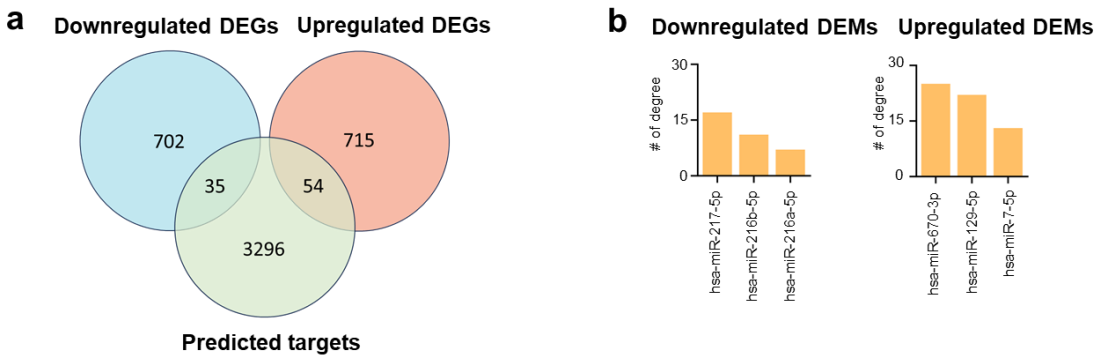

Figure 22. Predicted mRNA targets. (**a**) Venn diagram of the downregulated and upregulated DEGs and predicted targets. (**b**) Histograms of degree counts for top three downregulated DEMs (left) and top three upregulated DEMs (right)

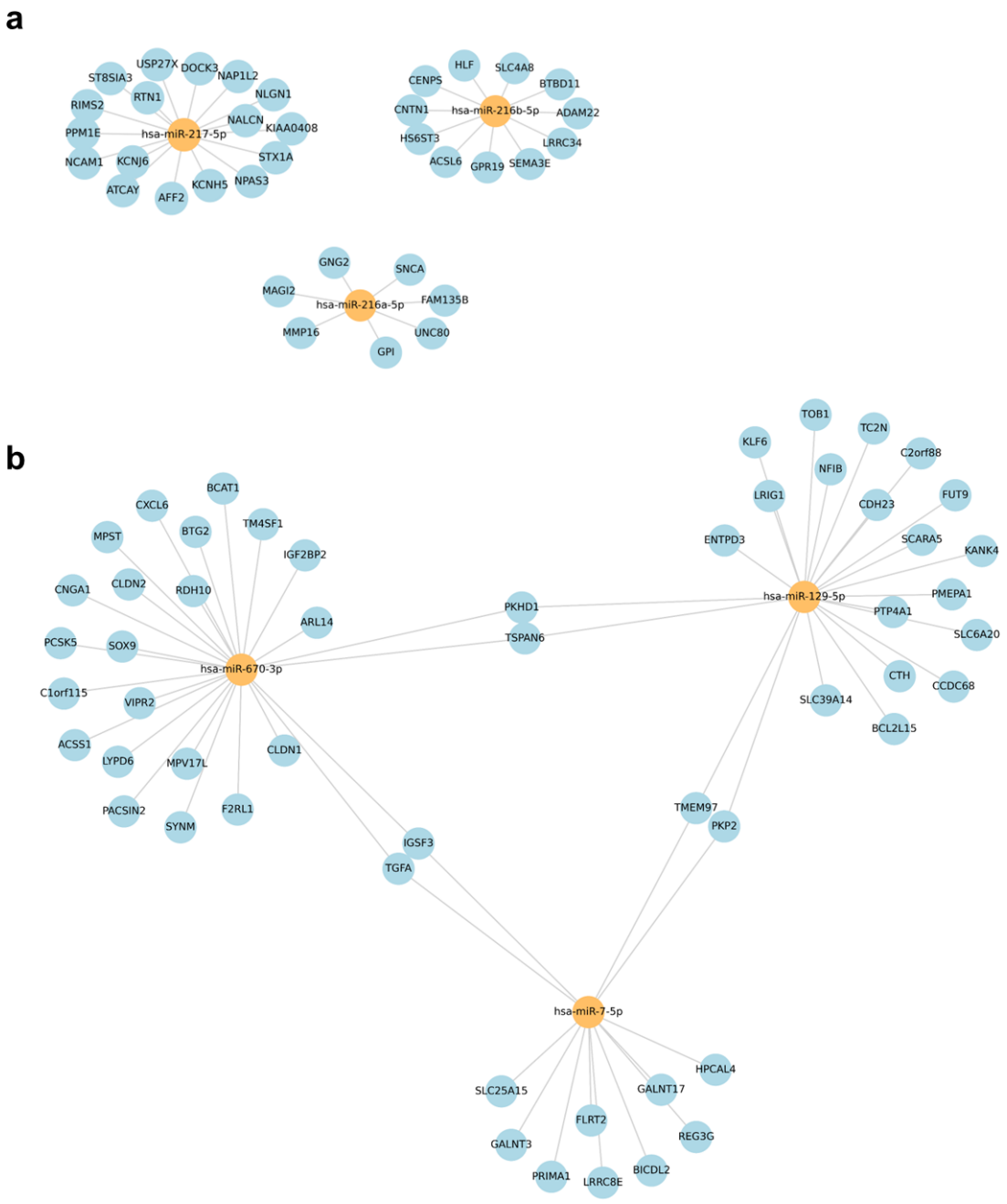

Figure 23. Predicted miRNA-mRNA interaction networks. (**a**) Network of top three downregulated DEMs with predicted upregulated mRNA. (**b**) Network of top three upregulated DEMs with predicted downregulated mRNA targets

4.7 Correlation of the miRNA-mRNA predicted pairs

For a more in-depth analysis of the relationships between expression patterns of miRNA-mRNA pairs, we calculated Pearson correlation coefficients between the selected

DEMs, and all their predicted mRNA targets (N=89), which participate in 95 interactions (**Figure 24**.).

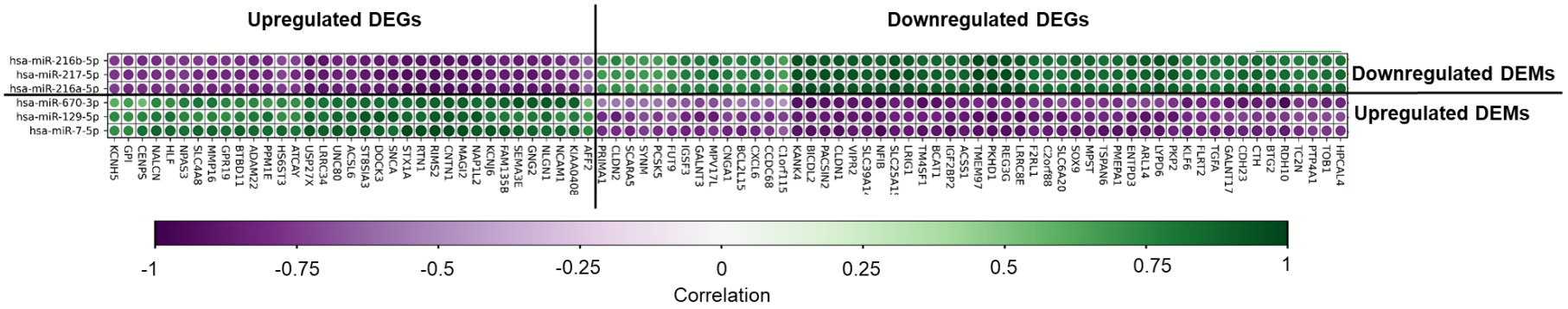

Figure 24. Hierarchically clustered correlation dot–plot between selected miRNAs and all their corresponding predicted mRNA pairs

Correlation between upregulated miRNAs and their downregulated mRNAs are generally strongly negative (R range -0.95, -0.47), with the highest anti-correlation for miR-670-3p/*RDH10* and miR-129-5p/*PKHD1* pairs and the smallest anticorrelation between the pairs miR-670-3p/*C1ORF115* and miR-670-3p/*CLDN2* (**Table 13.**).

Table 13. Predicted mRNA targets for upregulated miRNAs including the correlation statistics between gene and miRNA expression (Pearson's R and P-value), and results of the differential expression analyses between PanNETs and non-diseased samples

miRNA Name	Gene Symbol	Pearson's R	P-value correlation	log2FC DESeq2	padj DESeq2
hsa-miR-129-5p	*NFIB*	-0.88	5.47E-05	-2.27	5.90E-08
hsa-miR-129-5p	*KANK4*	-0.87	1.08E-04	-4.00	2.00E-14
hsa-miR-129-5p	*FUT9*	-0.68	1.01E-02	-3.90	8.80E-06
hsa-miR-129-5p	*PKHD1*	-0.94	1.84E-06	-6.91	2.00E-23
hsa-miR-129-5p	*CTH*	-0.76	2.43E-03	-3.36	3.60E-09
hsa-miR-129-5p	*PTP4A1*	-0.72	5.44E-03	-2.28	3.90E-04
hsa-miR-129-5p	*C2orf88*	-0.86	1.48E-04	-2.67	3.80E-09
hsa-miR-129-5p	*SCARA5*	-0.78	1.82E-03	-2.41	2.50E-04
hsa-miR-129-5p	*PMEPA1*	-0.82	6.27E-04	-2.49	2.70E-07
hsa-miR-129-5p	*SLC39A14*	-0.88	6.09E-05	-2.19	7.30E-08
hsa-miR-129-5p	*LRIG1*	-0.84	3.76E-04	-3.27	3.80E-11
hsa-miR-129-5p	*CDH23*	-0.72	5.23E-03	-2.68	5.40E-06
hsa-miR-129-5p	*KLF6*	-0.81	8.17E-04	-2.05	8.70E-05
hsa-miR-129-5p	*TC2N*	-0.70	7.18E-03	-3.52	3.20E-06
hsa-miR-129-5p	*BCL2L15*	-0.77	1.87E-03	-3.57	2.30E-09
hsa-miR-129-5p	*CCDC68*	-0.81	6.95E-04	-3.21	8.30E-08
hsa-miR-129-5p	*TMEM97*	-0.92	7.65E-06	-3.21	8.30E-08
hsa-miR-129-5p	*PKP2*	-0.89	5.29E-05	-2.37	6.90E-08
hsa-miR-129-5p	*SLC6A20*	-0.88	6.14E-05	-3.87	1.90E-10
hsa-miR-129-5p	*TSPAN6*	-0.81	8.02E-04	-2.11	2.90E-07
hsa-miR-129-5p	*ENTPD3*	-0.88	8.32E-05	-3.39	1.60E-08
hsa-miR-129-5p	*TOB1*	-0.70	7.31E-03	-2.24	3.60E-06
hsa-miR-7-5p	*REG3G*	-0.93	4.28E-06	-10.39	8.90E-20
hsa-miR-7-5p	*LRRC8E*	-0.92	9.33E-06	-3.86	4.80E-12
hsa-miR-7-5p	*HPCAL4*	-0.78	1.83E-03	-2.50	1.90E-05
hsa-miR-7-5p	*GALNT3*	-0.83	4.82E-04	-2.30	2.10E-06
hsa-miR-7-5p	*BICDL2*	-0.92	9.06E-06	-2.75	7.50E-13
hsa-miR-7-5p	*TMEM97*	-0.91	1.17E-05	-5.50	1.80E-27
hsa-miR-7-5p	*SLC25A15*	-0.88	8.58E-05	-4.19	2.10E-17
hsa-miR-7-5p	*GALNT17*	-0.87	1.34E-04	-2.13	5.40E-05
hsa-miR-7-5p	*TGFA*	-0.87	1.28E-04	-2.20	1.70E-05

hsa-miR-7-5p	*FLRT2*	-0.85	2.65E-04	-3.05	1.30E-05
hsa-miR-7-5p	*PKP2*	-0.82	5.82E-04	-2.37	6.90E-08
hsa-miR-7-5p	*IGSF3*	-0.83	4.93E-04	-2.43	9.70E-06
hsa-miR-7-5p	*PRIMA1*	-0.79	1.32E-03	-3.04	5.60E-06
hsa-miR-670-3p	*MPST*	-0.75	3.37E-03	-2.38	2.00E-12
hsa-miR-670-3p	*IGSF3*	-0.67	1.26E-02	-2.43	9.70E-06
hsa-miR-670-3p	*PACSIN2*	-0.90	2.57E-05	-2.21	1.10E-10
hsa-miR-670-3p	*IGF2BP2*	-0.87	1.00E-04	-3.15	3.40E-07
hsa-miR-670-3p	*ARL14*	-0.71	6.30E-03	-5.72	1.20E-12
hsa-miR-670-3p	*MPV17L*	-0.69	8.87E-03	-2.26	1.20E-04
hsa-miR-670-3p	*F2RL1*	-0.76	2.77E-03	-2.28	1.20E-08
hsa-miR-670-3p	*LYPD6*	-0.73	4.83E-03	-3.40	4.10E-16
hsa-miR-670-3p	*C1orf115*	-0.47	1.07E-01	-2.30	1.60E-04
hsa-miR-670-3p	*BTG2*	-0.85	2.03E-04	-3.07	5.80E-07
hsa-miR-670-3p	*VIPR2*	-0.90	3.51E-05	-3.05	3.10E-08
hsa-miR-670-3p	*CLDN2*	-0.57	4.08E-02	-7.30	3.40E-10
hsa-miR-670-3p	*SOX9*	-0.78	1.58E-03	-2.86	9.40E-11
hsa-miR-670-3p	*TGFA*	-0.80	9.93E-04	-2.20	1.70E-05
hsa-miR-670-3p	*PKHD1*	-0.85	2.17E-04	-6.91	2.00E-23
hsa-miR-670-3p	*TSPAN6*	-0.77	2.24E-03	-2.11	2.90E-07
hsa-miR-670-3p	*TM4SF1*	-0.92	1.04E-05	-3.37	7.60E-07
hsa-miR-670-3p	*CNGA1*	-0.64	1.97E-02	-2.08	1.30E-05
hsa-miR-670-3p	*BCAT1*	-0.91	1.94E-05	-3.31	1.10E-06
hsa-miR-670-3p	*CXCL6*	-0.60	2.94E-02	-3.64	1.70E-05
hsa-miR-670-3p	*PCSK5*	-0.58	3.60E-02	-3.17	2.80E-06
hsa-miR-670-3p	*SYNM*	-0.59	3.26E-02	-2.64	3.00E-05
hsa-miR-670-3p	*ACSS1*	-0.83	4.33E-04	-2.08	1.60E-11
hsa-miR-670-3p	*RDH10*	-0.95	5.10E-07	-2.15	5.40E-04
hsa-miR-670-3p	*CLDN1*	-0.89	4.39E-05	-4.62	1.60E-12

The strongest anti-correlation between downregulated miRNAs and their upregulated mRNAs (R range -0.93, -0.64), was observed in the pairs miR-217-5p/*RIMS2* and miR-216a-5p/*MAGI2*, while the weakest anti-correlation was seen in the miR-217-5p/*AFF2* and miR-216b-5p/*HS6ST3* (**Table 14**.). Counterintuitively, all up- and downregulated miRNAs have some putative mRNA targets that are expressed in the same direction (i.e., both upregulation of the miRNA and its putative target), suggesting that regulation at the transcript level may occur through an indirect mechanism or direct regulation may not result in degradation of the mRNA transcript, but rather translational repression.

Table 14. Predicted mRNA targets for downregulated miRNAs, including the correlation statistics between gene and miRNA expression (Pearson's R and P-value), and results of the differential expression analyses between PanNETs and non-diseased samples

miRNA Name	Gene Symbol	Pearson's R	P-value correlation	log2FC DESeq2	padj DESeq2
hsa-miR-216b-5p	*HLF*	-0.75	2.90E-03	2.35	6.00E-07
hsa-miR-216b-5p	*ACSL6*	-0.83	4.50E-04	2.99	6.40E-08
hsa-miR-216b-5p	*SEMA3E*	-0.87	1.20E-04	3.37	2.90E-09
hsa-miR-216b-5p	*BTBD11*	-0.80	1.01E-03	4.77	1.60E-11
hsa-miR-216b-5p	*GPR19*	-0.77	2.05E-03	2.45	3.40E-05
hsa-miR-216b-5p	*HS6ST3*	-0.71	6.83E-03	3.31	2.00E-07
hsa-miR-216b-5p	*SLC4A8*	-0.76	2.78E-03	2.77	5.20E-07
hsa-miR-216b-5p	*ADAM22*	-0.83	4.41E-04	2.50	1.40E-07
hsa-miR-216b-5p	*LRRC34*	-0.90	3.39E-05	2.48	3.50E-10
hsa-miR-216b-5p	*CENPS*	-0.80	9.35E-04	2.20	1.80E-04
hsa-miR-216b-5p	*CNTN1*	-0.92	1.14E-05	3.98	3.40E-23
hsa-miR-217-5p	*RIMS2*	-0.93	3.33E-06	4.45	2.80E-24
hsa-miR-217-5p	*DOCK3*	-0.90	3.17E-05	3.70	7.30E-12
hsa-miR-217-5p	*USP27X*	-0.88	8.10E-05	2.83	2.00E-14
hsa-miR-217-5p	*KCNJ6*	-0.85	2.53E-04	4.34	5.70E-16
hsa-miR-217-5p	*KCNH5*	-0.76	2.51E-03	2.84	3.70E-04
hsa-miR-217-5p	*NPAS3*	-0.75	3.47E-03	2.48	5.90E-07
hsa-miR-217-5p	*KIAA0408*	-0.81	7.56E-04	2.76	6.00E-06
hsa-miR-217-5p	*NAP1L2*	-0.92	7.61E-06	2.54	2.10E-15
hsa-miR-217-5p	*STX1A*	-0.93	4.56E-06	2.83	1.00E-16
hsa-miR-217-5p	*NALCN*	-0.79	1.37E-03	2.74	3.60E-07
hsa-miR-217-5p	*NLGN1*	-0.86	1.91E-04	2.87	2.20E-08
hsa-miR-217-5p	*NCAM1*	-0.83	5.09E-04	2.74	9.80E-07
hsa-miR-217-5p	*ATCAY*	-0.80	1.08E-03	5.54	4.20E-11
hsa-miR-217-5p	*ST8SIA3*	-0.88	8.15E-05	3.48	2.70E-13
hsa-miR-217-5p	*PPM1E*	-0.82	5.37E-04	2.75	2.00E-07
hsa-miR-217-5p	*RTN1*	-0.92	8.58E-06	4.42	2.20E-22
hsa-miR-217-5p	*AFF2*	-0.64	1.81E-02	2.23	1.50E-04
hsa-miR-216a-5p	*FAM135B*	-0.89	5.48E-05	3.71	4.50E-11
hsa-miR-216a-5p	*MAGI2*	-0.93	4.09E-06	3.22	4.40E-20
hsa-miR-216a-5p	*SNCA*	-0.88	6.35E-05	2.71	1.60E-07
hsa-miR-216a-5p	*UNC80*	-0.86	1.91E-04	3.79	3.40E-13
hsa-miR-216a-5p	*GNG2*	-0.90	3.56E-05	2.80	2.50E-08
hsa-miR-216a-5p	*GPI*	-0.80	1.16E-03	2.46	1.80E-06
hsa-miR-216a-5p	*MMP16*	-0.82	5.53E-04	2.60	5.20E-07

4.8 GO term & KEGG pathway enrichment analysis of target genes

To elucidate the potential function of 89 candidate target genes observed in our miRNA-mRNA interaction networks, GO and KEGG pathway enrichment analyses were performed. In biological processes, the enriched GO terms were associated with the regulation of synaptic vesicle cycle, positive regulation of exocytosis, and positive regulation of regulated secretory pathway (**Figure 25**.). These targeted genes were categorized into the Cell adhesion molecules pathway (*NLGN1, NCAM1, CNTN1, CLDN1*, and *CLDN2*), Cysteine and methionine metabolism (*MPST*, *CTH*, and *BCAT1*), Mucin and other type O-glycan biosynthesis (*GALNT17* and *GALNT3*), Ferroptosis (*SLC39A14* and *ACSL6*), Glycolysis/Gluconeogenesis (*ACSS1*/*GPI*) and Sulfur metabolism (*MPST*) by the KEGG pathway analysis (**Figure 26**.).

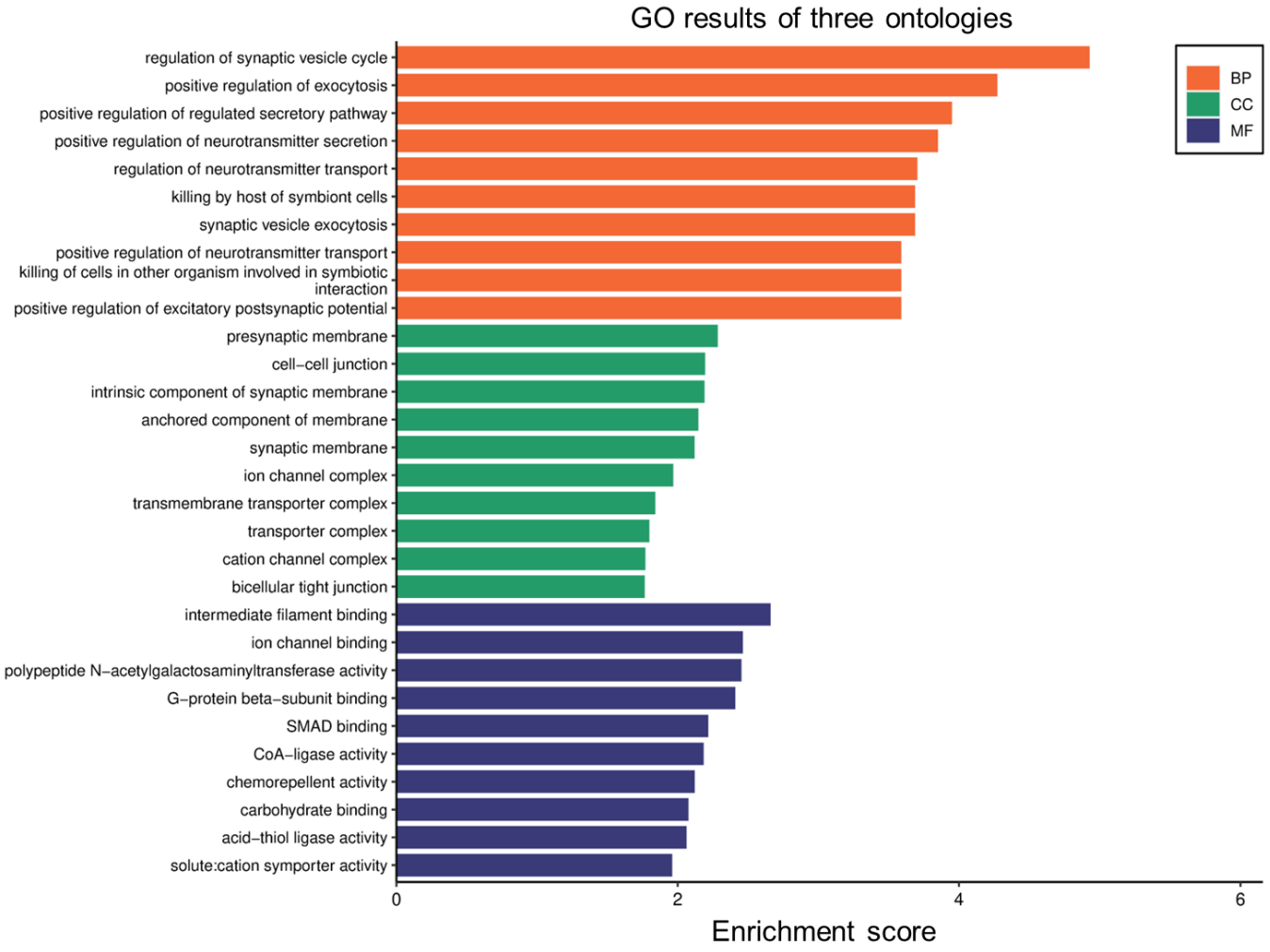

Figure 25. GO functional enrichment analysis of predicted mRNA targets (BP, biological process; CC, cellular component; MP, molecular function)

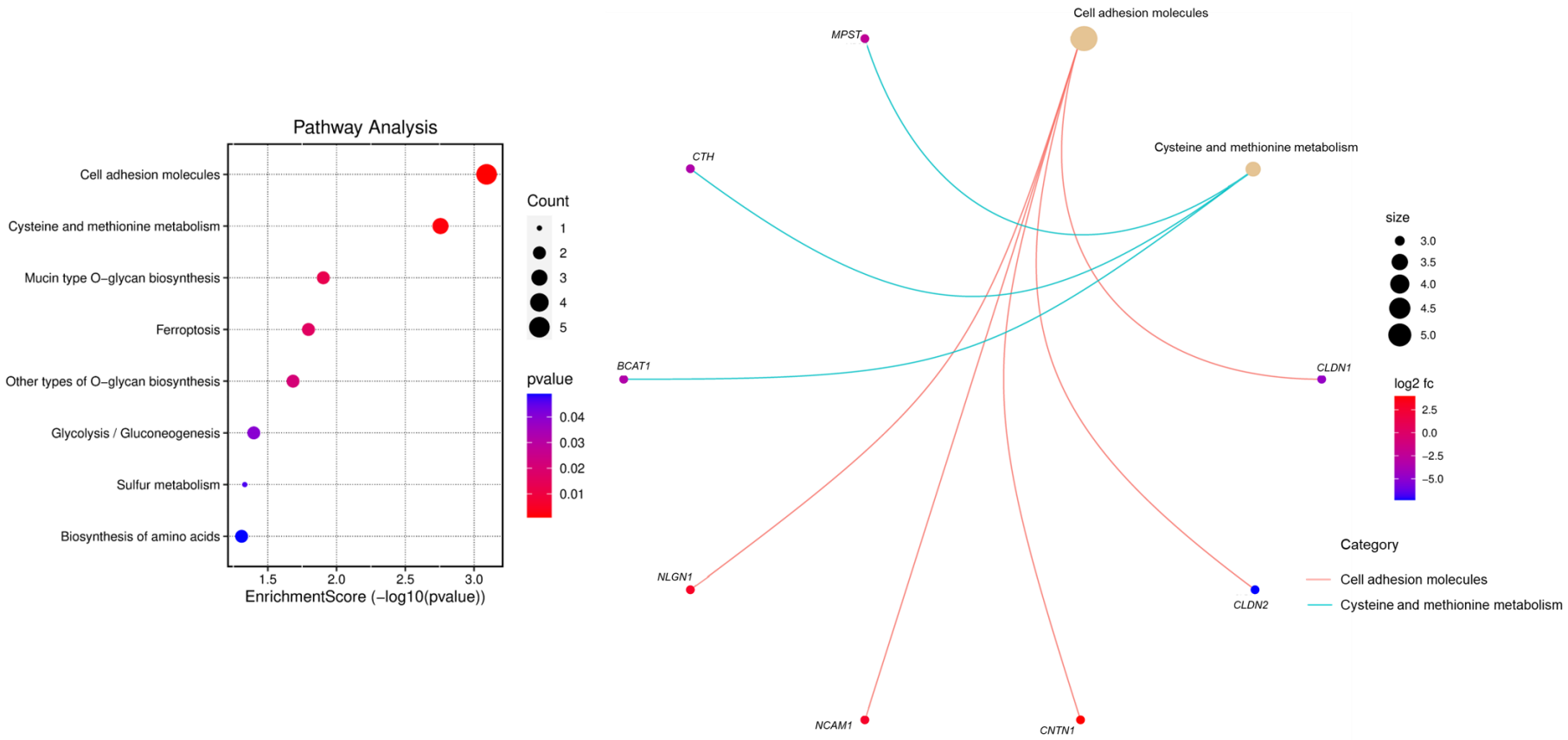

Figure 26. KEGG pathway analysis of the 89 predicted gene targets (dot plot on the left, network plot on the right). The size and color of the dots represent the amount of DEGs enriched in the pathway and enrichment significance

5 DISCUSSION

Neoplasms arising from neuroendocrine cells within pancreatic islets are known as pancreatic neuroendocrine tumors (PanNETs). Even though PanNETs are rare, comprising <2% of all pancreatic cancers, their incidence has increased in recent decades, emphasizing the need to understand their molecular, clinical, and pathological characteristics [197–199]. There is a wide spectrum of behaviours found among PanNETs, from indolent, slow-growing tumors to more aggressive and metastatic tumors. This poses two main challenges: (I) Due to PanNET's heterogeneity and unpredictable progression, their diagnosis and treatment can be complicated; (II) the molecular pathways involved in the development and progression of PanNETs are still unclear and specific biomarkers are limited or lacking. These challenges highlight the need for further mechanistic research and development of effective diagnostic and treatment strategies [200,201].

Current diagnostic biomarkers for PanNETs are limited to individual immunohistochemical markers and a handful of mutated genes [15], making it challenging to capture the complexity and heterogeneous nature of PanNETs. In this study, we sequenced both mRNA and miRNA, integrated these results with *in silico* miRNA target predictions, and identified novel dysregulated miRNA-mRNA interaction partners in PanNETs compared to non-diseased pancreatic samples. Our comprehensive analysis of PanNET coding and small non-coding transcriptomes provides valuable insights into regulatory mechanisms that may drive PanNET pathogenesis and reveals several novel biomarkers and potential therapeutic targets.

While emerging evidence underlines the importance of both mRNA and miRNA transcriptomes in PanNETs, to the best of our knowledge, there is only one study [202] describing pairwise next-generation sequencing analysis of mRNA/miRNAs and their interaction networks in PanNETs versus non-diseased tissues so far. Our approach extends these findings by (I) using a well described, homogeneous clinical cohort of low grade (G1), high risk (large tumor, node positive), well differentiated PanNETs, thus allowing us to identify factors that may drive progression; (II) conducting stringent differential expression analysis using two combined approaches to mitigate false positive DEGs; (III) categorizing PanNETs samples into molecular subtypes, which can lead to improvement of the appropriate therapeutic selection, (IV) highlighting important clinicopathological biomarkers on

transcriptomic level that correlated with clinical characteristics of PanNETs patients; and (V) performing transcriptome profiling of mRNA/miRNAs on identical RNA samples from the same patients, enabling robust investigation of miRNA-target interactions.

Using RNA sequencing, dysregulated genes were found in tumors compared to non-diseased tissues via differential mRNA expression analysis. At the biological processes level of the GO analysis, upregulated genes were significantly associated with ion transmembrane transport regulation, nervous system development and chemical synaptic transmission. Excessive ion transport regulation could promote uncontrollable cell growth and disrupt pancreatic endocrine cell function, affecting glucose metabolism. Metastasis formation may be influenced through changes in the nervous system development and synaptic transmission, which can alter tumor cell communication, adhesion and migration. The significant upregulation of genes associated with the regulation of dendrites, axons and neuronal projections at the cellular level may be related to the fact that PanNETs originate from neuroendocrine cells. These neuroendocrine cells have many of the hallmarks of neurons, such as membrane excitability, but are specialized not to secrete neurotransmitter into a synaptic cleft, but to secrete hormones into blood. The growth and behaviour of PanNETs can be affected by alterations in these processes, since they are important for neuronal communication and signalling through regulation of dendrites, axons and neuron projections [203].

At the molecular function level, the most upregulated genes were associated with the calcium ion binding. Neuroendocrine cells play a role in regulation of calcium ion flux as part of their physiological function [204]. These cells regulate hormone secretion through intricate calcium-dependent pathways, where calcium ions act as critical mediators of exocytosis. Dysregulation of calcium ion binding genes in PanNETs could disrupt these signalling cascades, leading to abnormal hormone secretion and dysregulated cellular functions characteristic of tumor growth. Additionally, calcium signalling pathways are integral to the control of neuroendocrine cell excitability and responsiveness, processes fundamental to PanNET pathogenesis. Thus, the pronounced upregulation of calcium ion binding genes underscores their potential significance in driving the molecular mechanisms, underpinning PanNET development and progression.

Neurodegeneration pathways displayed the most upregulated genes in expression analyses, while dopaminergic synapse and GABAergic synapse were found to be the most significant, suggesting a possible relationship between neurodegenerative processes and PanNETs tumorigenesis. Pancreatic neuroendocrine tumors arise from neuroendocrine cells that have similar characteristics with neurons, and thus disturbances in such genes may indicate underlying abnormalities in these endocrine cells leading to cancer development. Additionally, numerous neurodegenerative pathways are known to involve apoptosis, oxidative stress and protein misfolding, all of which are associated with cancer initiation and progression. Hence, the upregulation of genes associated with neurodegeneration pathways in PanNETs may reflect shared molecular mechanisms between neurodegenerative diseases and cancer.

On the other hand, the most representative and significant downregulated genes were determined to be a part of the pancreatic secretion and metabolic pathways. The pancreatic secretion pathways play a key role in the production and release of digestive enzymes, and hormones such as insulin and glucagon, crucially involved in glucose metabolism and the overall metabolic homeostasis. The downregulation of these pathways may result in diminishing hormone secretion and metabolic imbalance typically associated with PanNET patients, reinforcing the importance of the link between PanNET development and pancreatic dysfunction.

Although RNA-seq allows the assessment of multiple biomarkers simultaneously in multiple samples, quantitative measurements of gene expression levels and comparison of their gene expression allows for precise and reproducible assessment of biomarker expression. This quantitative data can better reflect the dynamic range of gene expression compared to semi-qualitative methods like IHC. In addition, RNA-seq provides a comprehensive molecular profile of the sample, in contrast to other routine techniques, which may be limited by the number of biomarkers. While RNA-seq offers numerous advantages for biomarker assessment in PanNETs, there are also some disadvantages compared to routinely used methods. RNA-seq is generally more expensive and technically complex than traditional methods. Analysing the data requires specialized equipment, bioinformatics expertise, and substantial computational resources. RNA-seq workflows often encompass multiple steps, including sample preparation, sequencing, and data analysis, which can extend the overall turnaround time. Furthermore, to ensure cost-efficiency, samples from

several patients are often aggregated before analysis, making this process less than ideal for studying rare tumor types.

In this study, mRNA expression of individual biomarkers in PanNETs was examined and compared with clinical data to gain a deeper understanding of the molecular characteristics of this disease and their correlation with clinical features and prognosis. Significantly increased levels of CHGA and SYP in PanNETs compared to normal controls indicate higher production of neuroendocrine cells in these tumors which is characteristic of PanNETs. The higher levels of CHGA and SYP could potentially be used to identify pancreatic neuroendocrine tumors and predict their aggressiveness, progression, etc. These findings could play a significant role in patient stratification for those with PanNETs and may help with the management of the disease. Furthermore, the significantly increased expression of SSTR2 in PanNETs compared to non-diseased controls suggests an interesting finding. Since SSTR2 is a receptor for somatostatin, an inhibitor of various hormones' release and cell growth regulation, there might be increased sensitivity to somatostatin in PanNETs, which has potentially important therapeutic implications. Increased SSTR2 expression could imply a better response to somatostatin analogues frequently used for managing PanNETs, thus mitigating symptoms and slowing down tumor growth. Finally, correlation analysis of mRNA expression data confirmed the clinicopathological characteristics of patient P4, diagnosed with a VIP-secreting tumor. Further specific information confirming the functional type of PanNETs included in the study is unfortunately not known, but the results of this study suggest that patients P3 and P6 might suffer from a very rare type of PanNET, glucagonoma.

Molecular subtyping is relevant for convenient therapeutic selection. For example, pathologically, 80% of all breast cancers are classified as invasive ductal carcinoma [205]. Yet, these tumors are classified into at least four subtypes using molecular classification methods, which mainly determine clinical and treatment decisions [206,207]. Multi-omics analyses have recently been combined to subtype PanNETs into unique subtypes using this type of molecular subtyping [205]. Using Sadanandam's cohort [30] and advanced statistical analyses, it was possible to categorize our patient samples according to Sadanandam's classification of PanNET subtypes. Two patients from our cohort were classified as MLP subtype, which corresponds to the most aggressive PanNET subtype and aligns with the clinical data. These two cases (P2 and P5) are younger patients with larger tumor size, suggesting tumor aggressiveness and worse prognosis. On the other hand, P1 was categorized

as intermediate subtype characterized by *MEN1* and *DAXX/ATRX* mutations [30]. Since the RNA sequencing does not allow to confirm the presence of the mutation, DNA sequencing such as target gene sequencing for specific mutation, would have to be used. Overall, the findings confirm the relevance and applicability of molecular diagnostics also in case of such rare tumors.

miRNA differential expression analysis using miRNA sequencing could potentially be used to showcase that not only mRNAs, but also miRNAs can serve to distinguish samples as either tumors or controls. The results of such an analysis revealed 41 significantly upregulated and 19 significantly downregulated miRNAs. In order to validate two of the top DEMs in PanNET and non-disease group, we used RT-qPCR method and publicly available dataset (GSE43796). Using mentioned approaches, a significant downreagulation of miR-216a-5p and miR-216b-5p in the disease was confirmed, which suggests their promising potential in PanNETs diagnosis.

When a miRNA is dysregulated, it will impact its direct target genes and subsequently affect the expression of the downstream genes through intracellular molecular regulatory networks, which would finally change the gene expression patterns in the cell. Therefore, a miRNA-mRNA regulatory network should be used to interpret the global transcriptional response to miRNA dysregulation. Identification of target genes of the aberrantly expressed miRNAs is important to understand the regulatory networks associated with PanNETs development. To construct a miRNA-mRNA regulatory network, we focused on the top three most downregulated (miR-216a-5p, miR-216b-5p, and miR-217-5p) and upregulated (miR-670-3p, miR-129-5p, and miR-7-5p) miRNAs. Next, a high probability mRNA targets were generated by crossing the lists of miRNAs *in silico* putative mRNA targets with PanNET-specific DEGs.

Although several studies have reported downregulation of the miR-216 family [202] and upregulation of miR-7-5p and miR-129-5p in neuroendocrine tumors (NETs) [141,208–210], including PanNETs, to the best of our knowledge, we are the first to extend these findings by highlighting the interconnections with mRNA targets, biological processes, and pathways. Our functional analyses of miRNA-mRNA networks yielded enriched GO terms that were consistent with aberrations in neuroendocrine cells and overactive secretion of bioactive hormones.

Based on the KEGG pathway analysis, the cell adhesion molecule pathway was enriched, including promising miRNA-mRNA pairs such as miR-217-5p/*NLGN1*, miR-217-5p/*NCAM1*, and miR-216b-5p/*CNTN1*. Tumor progression, metastasis, and interactions with the tumor microenvironment are all influenced by CAMs in NETs [211–213]. A member of the immunoglobulin superfamily (IgSF), *NCAM1* (Neural Cell Adhesion Molecule 1) and *CNTN1* (Contactin 1) are crucial for cell-cell interaction, neuronal development, and synaptic plasticity [214]. PanNETs can be distinguished from other pancreatic cancers using *NCAM1*, also known as *CD56*, as an IHC diagnostic and prognostic biomarker [215–218]. Tumors that lack *NCAM1* tend to grow rapidly and invade adjacent tissue as they play an important role in adhesion, detachment, and aggregation [217]. The invasive potential of PanNETs may be prevented by utilization of crucial therapeutic targets, such as the negative regulators of *NCAM1* (e.g. miR-217-5p).

A novel miRNA-mRNA interaction was detected herein between miR-670-3 and *CLDN1* and *CLDN2*, two claudins (CLDNs) that belong to the enriched cell adhesion molecule KEGG pathway. The dysregulation of CLDN expression is common in many cancers and contributes to tumor initiation, progression, metastasis, and treatment response. PDACs express *CLDNs -1, -4,* and *-7*, whereas PanNETs show high expression of *CLDNs -3* and *-7* and low expression of *CLDNs -1* and *-4* [219]. This suggests that distinct claudin signatures could be used as biomarkers and therapeutic targets to differentiate pancreatic cancers with different cellular origins (endocrine vs. exocrine). Furthermore, downregulation of *CLDN10, CLDN18, CLDN23* in our DEGs was found. As this is the first report of miR-670-3p upregulation in PanNETs, further validation is needed to confirm that claudins are targets of miR-670-3p and to understand the exact roles of each claudin isoform in pathogenesis of PanNET.

Novel pairs (miR-670-3/*BCAT1*, miR-670-3/*MPST*, miR-129-5p/*CTH*) that are important in the cysteine and methionine metabolism pathway were found by our miRNA-mRNA interaction networks, indicating alterations in metabolic processes in PanNETs. Cystathionine gamma-lyase (*CTH*) gene enrichment in glutathione synthesis in PanNETs and *BCAT1* expression were linked to intermediate patient outcomes, according to a recent multi-omic (transcriptomic and metabolomic) investigation of duodenopancreatic NETs [220]. The *CTH* gene has been explored in several tumor types, such as glioblastoma [221], lung adenocarcinoma [222], prostate cancer [223], and hepatocellular carcinoma [224];

nevertheless, its specific expression in PanNETs is unknown. While it is unclear whether *MPST* (also known as *3-MST*) contributes to PanNET pathogenesis, growing evidence indicates that *MPST* is upregulated in many cancers and may be a druggable target [225,226]. Overall, cysteine and methionine metabolism genes also influence redox balance, antioxidant defence, and cellular proliferation in cancer cells, all of which play critical roles in cancer pathogenesis [227]. These findings add to the growing body of evidence indicating unique metabolic gene programs in PanNETs and imply that aberrant regulation of genes and pathways involved in energy homeostasis may be related to disrupted expression of miRNA-mRNA networks.

Consistent with our findings, numerous publications demonstrate upregulated miR-7-5p in NETs [141,208–210]. NET patients have 48-fold higher miR-7 levels than non-NET controls [209], suggesting a neuroendocrine specificity of miR-7. Another study indicates that overexpression of miR-7-5p inhibits cell proliferation and induces apoptosis in GEP-NETs [228]. In pancreatic endocrine cells, miR-7 may affect pancreatic neuroendocrine progression by regulating the expression of regenerating islet-derived (Reg) gene family members. miR-7 specifically targets the expression of mouse Reg1 in islet β-cells and pancreatic acinar cells [210]. It's interesting to note that our data indicate a significant reduction in expression of Reg family members (*REG1A/B, REG3A/G*, and *REG4*), which may be related to miR-7-5p overexpression. Furthermore, we also show that *REG1A* and *CPA1* can be used to diagnose mixed pancreatic acinar cell carcinomas and acinar-neuroendocrine carcinomas [229]; notably, we indicate that *CPA1* is most likely to be reduced in PanNETs, which is consistent with the absence of *CPA1* immunohistochemistry [230]. Additionally, we discovered that miR-7-5p was a crucial component of a miRNA-mRNA interaction network that also comprised coregulation of *TGFA* and *IGSF3* with miR-670-3p and *TMEM97* and *PKP2* with miR-129-5p. Further research efforts should focus on elucidating the processes by which an upregulation of miR-7-5p expression might drive pancreatic cell type-specific gene networks (e.g., the Reg family), and how this could be utilized for therapeutic and diagnostic purposes.

The current study is inherently affected by several limitations and challenges. Firstly, the study’s sample size is relatively small, which may limit the validity of the findings. Publicly available datasets that include paired mRNA and miRNA sequencing data that are specifically associated with PanNETs are scarce, which impairs inter-study comparisons.

Moreover, the clinical and molecular characteristics of PanNETs display significant heterogeneity, which could affect the results. To overcome these challenges, studying PanNETs in larger and diverse cohorts allowing for building comprehensive datasets and robust comparisons need to be carried out to understand the biology of PanNETs. Secondly, although clinical data were integrated into the analysis, the study focused primarily on molecular profiling. Further validation of the clinical significance of the identified biomarkers and pathways is required in independent cohorts and functional studies.

There are several important demands for further investigation in PanNETs. Firstly, validation studies are important for larger, independent patient cohorts to verify identified biomarkers and pathways; the use of such techniques as qRT-PCR, western blots, microarrays, luciferase assays, etc. may confirm these findings. Further evaluation of the functionality of these markers and pathways should be based on *in vitro* and *in vivo* experiments validating the functional roles of abnormal genes in PanNET development. Studying how gene expression and molecular pathways change over time might lead to the identification of predictive biomarkers for disease progression or response to treatment. Combining various omics datasets like genomic, transcriptomic, proteomic, and metabolomic offers insight into PanNET biology and reveals new potential therapeutic targets. Lastly, translation of molecular discoveries into clinical application is required; hence, substantial collaborations between scientists, clinicians, and industry would have to be established. In turn, the resulting discoveries and development of biomarkers could be used in clinical practice to treat patients more effectively.

To sum up, present study provides valuable insights into the molecular landscape of PanNETs, highlighting dysregulation of key biological processes and signalling pathways. PanNET pathogenesis may be influenced by novel miRNA-mRNA pairs and interaction networks related to altered neuroendocrine function, cell adhesion, and metabolic pathways. In the future, further functional characterization of miRNA-mRNA networks and individual DEGs could lead to the identification of new biomarkers and therapeutic targets for PanNET management, leading to improved outcomes for patients.

6 CONCLUSIONS

My doctoral study research provides interesting contributions by integrating transcriptome profiling to gain a deeper understanding of the molecular pathogenesis, clinical presentation, and prognostic implications of PanNETs by analysing mRNA and miRNA expression in PanNETs compared to non-diseased tissues.

1. The first aim of the study was to uncover the complex molecular landscape of PanNETs using RNA sequencing. A comprehensive analysis revealed significant dysregulation of 715 upregulated and 702 downregulated genes. Their enrichment and pathway analysis provided insights into PanNET pathogenesis and disease progression mechanisms, highlighting processes such as ion transmembrane transport regulation, nervous system development, chemical synaptic transmission, digestion, and proteolysis to play a key role.
2. Next, expression levels of important clinicopathological biomarkers in patients cohort showed significant findings including increased expression of CHGA and SYP in disease, which confirms the potential of RNA as a surrogate diagnostic source. Additionally, SSTR1 and SSTR2 were also universally overexpressed in patients' samples. Increased expression of the INS marker was noted in non-disease samples compared to tumors. Finally, VIP RNA was significantly increased in P4 sample, in line with clinicopathological data, and overexpression of GCG was detected in P3 and P6 samples.
3. Another aim of the study was to classify PanNET samples into different molecular subtypes using transcriptomic profiles. Using gene signatures available from the literature and advanced two-stage statistical analysis, it was found that sample P1 showed similarity to the intermediate subtype, and samples P2 and P5 to the MLP subtype.
4. Using comprehensive analysis of miRNA sequencing data, 41 upregulated and 19 downregulated miRNAs were identified in PanNET compared to non-disease group.
5. Validation of top significantly differentially expressed miRNA, namely miR-216a-5p and miR-216b-5p, confirmed their downregulation in tumor samples compared to non-diseased individuals ($P < 0.001$ for both).
6. Lastly, by focusing on the top upregulated miRNAs - 670-3p, 129-5p and 7-5p, as well as the top downregulated miRNAs - 216a-5p, 216b-5p and 217-5p, network

analysis revealed common mRNA targets between upregulated miRNAs, such as *PKHD1* and *TSPAN6* between miR-670-3p and miR-129-5p, *TMEM97* and *PKP2* between miR-129-5p and miR-7-5p, and *IGSF3* and *TGFA* between miR-670-3p and miR-7-5p. Conversely, downregulated miRNAs formed separate subnetworks, indicating different regulatory mechanisms. Enrichment analysis of the 89 target genes revealed associations with crucial biological processes and pathways. Genes such as *NLGN1, NCAM1, CNTN1, CLDN1* and *CLDN2*, involved in cell adhesion molecules and genes *MPST*, *CTH*, and *BCAT1*, involved in cysteine and methionine metabolism, as well as genes associated with mucin biosynthesis, ferroptosis, glycolysis/gluconeogenesis, and sulfur metabolism provided valuable insights into the molecular mechanisms that contribute to PanNET's pathogenesis.

In conclusion, the study provided substantial insights into the molecular landscape of PanNETs that increased the understanding of their aetiology. Our miRNA-mRNA network analysis enabled the identification of different regulatory centres related to dysregulated miRNAs. Finally, by performing molecular classification of PanNET samples, establishing the relationship between our molecular tiers and major clinicopathological features, and further validation of selected miRNA expression, we managed to prove the robustness and potential diagnostic value of our study. If followed up by an extensive validation studies, these discoveries may directly contribute to the progress in the field of PanNET diagnostics and treatment, as well as further attempts aimed at developing new tools for PanNET prognosis.

7 LITERATURE

1. Gao HL, Wang WQ, Yu XJ, Liu L. Molecular drivers and cells of origin in pancreatic ductal adenocarcinoma and pancreatic neuroendocrine carcinoma. Exp Hematol Oncol. 2020 Oct 22;9:28.

2. Backx E, Coolens K, Van den Bossche JL, Houbracken I, Espinet E, Rooman I. On the Origin of Pancreatic Cancer: Molecular Tumor Subtypes in Perspective of Exocrine Cell Plasticity. Cell Mol Gastroenterol Hepatol. 2021 Dec 4;13(4):1243–53.

3. Sun J. Pancreatic neuroendocrine tumors. Intractable Rare Dis Res. 2017 Feb;6(1):21–8.

4. What Is a Pancreatic Neuroendocrine Tumor? [Internet]. [cited 2024 Jan 12]. Available from: https://www.cancer.org/cancer/types/pancreatic-neuroendocrine-tumor/about/what-is-pnet.html

5. Siegel RL, Miller KD, Jemal A. Cancer statistics, 2020. CA Cancer J Clin. 2020;70(1):7–30.

6. Christenson ES, Jaffee E, Azad NS. Current and emerging therapies for patients with advanced pancreatic ductal adenocarcinoma: a bright future. Lancet Oncol. 2020 Mar;21(3):e135–45.

7. Makohon-Moore A, Iacobuzio-Donahue CA. Pancreatic cancer biology and genetics from an evolutionary perspective. Nat Rev Cancer. 2016 Sep;16(9):553–65.

8. Basturk O, Tang L, Hruban RH, Adsay V, Yang Z, Krasinskas AM, et al. Poorly Differentiated Neuroendocrine Carcinomas of the Pancreas: A Clinicopathologic Analysis of 44 Cases. Am J Surg Pathol. 2014 Apr;38(4):437.

9. Zhuge X, Guo C, Chen Y, Feng L, Jia R, Zhao Y, et al. The Levels of Tumor Markers in Pancreatic Neuroendocrine Carcinoma and Their Values in Differentiation Between Pancreatic Neuroendocrine Carcinoma and Pancreatic Ductal Adenocarcinoma. Pancreas. 2018 Dec;47(10):1290.

10. Raphael MJ, Chan DL, Law C, Singh S. Principles of diagnosis and management of neuroendocrine tumours. CMAJ Can Med Assoc J. 2017 Mar 13;189(10):E398–404.

11. Hallet J, Law CHL, Cukier M, Saskin R, Liu N, Singh S. Exploring the rising incidence of neuroendocrine tumors: a population-based analysis of epidemiology, metastatic presentation, and outcomes. Cancer. 2015 Feb 15;121(4):589–97.

12. Leoncini E, Boffetta P, Shafir M, Aleksovska K, Boccia S, Rindi G. Increased incidence trend of low-grade and high-grade neuroendocrine neoplasms. Endocrine. 2017 Nov;58(2):368–79.

13. Dasari A, Shen C, Halperin D, Zhao B, Zhou S, Xu Y, et al. Trends in the Incidence, Prevalence, and Survival Outcomes in Patients With Neuroendocrine Tumors in the United States. JAMA Oncol. 2017 Oct 1;3(10):1335–42.

14. Das S, Dasari A. Epidemiology, Incidence, and Prevalence of Neuroendocrine Neoplasms: Are There Global Differences? Curr Oncol Rep. 2021 Mar 14;23(4):43.

15. Bocchini M, Nicolini F, Severi S, Bongiovanni A, Ibrahim T, Simonetti G, et al. Biomarkers for Pancreatic Neuroendocrine Neoplasms (PanNENs) Management—An Updated Review. Front Oncol. 2020 May 27;10:831.

16. Halfdanarson TR, Bamlet WR, McWilliams RR, Hobday TJ, Burch PA, Rabe KG, et al. Risk Factors for Pancreatic Neuroendocrine Tumors (PNETs): A Clinic-Based Case-Control study. Pancreas. 2014 Nov;43(8):1219–22.

17. Ben Q, Zhong J, Fei J, Chen H, Yv L, Tan J, et al. Risk Factors for Sporadic Pancreatic Neuroendocrine Tumors: A Case-Control Study. Sci Rep. 2016 Oct 26;6:36073.

18. Pavel M, Öberg K, Falconi M, Krenning EP, Sundin A, Perren A, et al. Gastroenteropancreatic neuroendocrine neoplasms: ESMO Clinical Practice Guidelines for diagnosis, treatment and follow-up†. Ann Oncol. 2020 Jul 1;31(7):844–60.

19. Oberg K. Pancreatic endocrine tumors. Semin Oncol. 2010 Dec;37(6):594–618.

20. Thakker RV, Newey PJ, Walls GV, Bilezikian J, Dralle H, Ebeling PR, et al. Clinical practice guidelines for multiple endocrine neoplasia type 1 (MEN1). J Clin Endocrinol Metab. 2012 Sep;97(9):2990–3011.

21. Scarpa A, Chang DK, Nones K, Corbo V, Patch AM, Bailey P, et al. Whole-genome landscape of pancreatic neuroendocrine tumours. Nature. 2017 Mar;543(7643):65–71.

22. Perren A, Couvelard A, Scoazec JY, Costa F, Borbath I, Delle Fave G, et al. ENETS Consensus Guidelines for the Standards of Care in Neuroendocrine Tumors: Pathology - Diagnosis and Prognostic Stratification. Neuroendocrinology. 2017 Feb 11;105(3):196–200.

23. Klimstra DS, Modlin IR, Coppola D, Lloyd RV, Suster S. The Pathologic Classification of Neuroendocrine Tumors: A Review of Nomenclature, Grading, and Staging Systems. Pancreas. 2010 Aug;39(6):707.

24. Fléjou JF. [WHO Classification of digestive tumors: the fourth edition]. Ann Pathol. 2011 Nov;31(5 Suppl):S27-31.

25. Liu TC, Hamilton N, Hawkins W, Gao F, Cao D. COMPARISON OF WHO CLASSIFICATIONS (2004, 2010), THE HOCHWALD GRADING SYSTEM, AJCC AND ENETS STAGING SYSTEMS IN PREDICTING PROGNOSIS IN LOCOREGIONAL WELL-DIFFERENTIATED PANCREATIC NEUROENDOCRINE TUMORS. Am J Surg Pathol. 2013 Jun;37(6):853–9.

26. Nagtegaal ID, Odze RD, Klimstra D, Paradis V, Rugge M, Schirmacher P, et al. The 2019 WHO classification of tumours of the digestive system. Histopathology. 2020;76(2):182–8.

27. Basturk O, Hong SM, Wood LD, Adsay NV, Albores-Saavedra J, Biankin AV, et al. A Revised Classification System and Recommendations From the Baltimore Consensus

Meeting for Neoplastic Precursor Lesions in the Pancreas. Am J Surg Pathol. 2015 Dec;39(12):1730–41.

28. Falconi M, Eriksson B, Kaltsas G, Bartsch DK, Capdevila J, Caplin M, et al. ENETS Consensus Guidelines Update for the Management of Patients with Functional Pancreatic Neuroendocrine Tumors and Non-Functional Pancreatic Neuroendocrine Tumors. Neuroendocrinology. 2016;103(2):153–71.

29. Ney A, Canciani G, Hsuan JJ, Pereira SP. Modelling Pancreatic Neuroendocrine Cancer: From Bench Side to Clinic. Cancers. 2020 Oct 28;12(11):3170.

30. Sadanandam A, Wullschleger S, Lyssiotis CA, Grötzinger C, Barbi S, Bersani S, et al. A Cross-Species Analysis in Pancreatic Neuroendocrine Tumors Reveals Molecular Subtypes with Distinctive Clinical, Metastatic, Developmental, and Metabolic Characteristics. Cancer Discov. 2015 Dec;5(12):1296–313.

31. Luley KB, Biedermann SB, Künstner A, Busch H, Franzenburg S, Schrader J, et al. A Comprehensive Molecular Characterization of the Pancreatic Neuroendocrine Tumor Cell Lines BON-1 and QGP-1. Cancers. 2020 Mar 14;12(3):691.

32. Saleh Z, Moccia MC, Ladd Z, Joneja U, Li Y, Spitz F, et al. Pancreatic Neuroendocrine Tumors: Signaling Pathways and Epigenetic Regulation. Int J Mol Sci. 2024 Jan;25(2):1331.

33. Mafficini A, Scarpa A. Genetics and Epigenetics of Gastroenteropancreatic Neuroendocrine Neoplasms. Endocr Rev. 2019 Jan 17;40(2):506–36.

34. Kulke MH, Hornick JL, Frauenhoffer C, Hooshmand S, Ryan DP, Enzinger PC, et al. O6-methylguanine DNA methyltransferase deficiency and response to temozolomide-based therapy in patients with neuroendocrine tumors. Clin Cancer Res Off J Am Assoc Cancer Res. 2009 Jan 1;15(1):338–45.

35. Waddell N, Pajic M, Patch AM, Chang DK, Kassahn KS, Bailey P, et al. Whole genomes redefine the mutational landscape of pancreatic cancer. Nature. 2015 Feb;518(7540):495–501.

36. Morrison AJ. Chromatin-remodeling links metabolic signaling to gene expression. Mol Metab. 2020 Mar 16;38:100973.

37. Zhang H, He J, Li J, Tian D, Gu L, Zhou M. Methylation of RASSF1A gene promoter is regulated by p53 and DAXX. FASEB J. 2013 Jan;27(1):232–42.

38. Tirosh A, Kebebew E. Genetic and epigenetic alterations in pancreatic neuroendocrine tumors. J Gastrointest Oncol. 2020 Jun;11(3):567–77.

39. Lin SY, Elledge SJ. Multiple Tumor Suppressor Pathways Negatively Regulate Telomerase. Cell. 2003 Jun 27;113(7):881–9.

40. Lamberti G, Brighi N, Maggio I, Manuzzi L, Peterle C, Ambrosini V, et al. The Role of mTOR in Neuroendocrine Tumors: Future Cornerstone of a Winning Strategy? Int J Mol Sci. 2018 Mar 6;19(3):747.

41. Jiao Y, Shi C, Edil BH, de Wilde RF, Klimstra DS, Maitra A, et al. DAXX/ATRX, MEN1 and mTOR Pathway Genes are Frequently Altered in Pancreatic Neuroendocrine Tumors. Science. 2011 Mar 4;331(6021):1199–203.

42. Missiaglia E, Dalai I, Barbi S, Beghelli S, Falconi M, della Peruta M, et al. Pancreatic Endocrine Tumors: Expression Profiling Evidences a Role for AKT-mTOR Pathway. J Clin Oncol. 2010 Jan 10;28(2):245–55.

43. Neychev V, Steinberg SM, Cottle-Delisle C, Merkel R, Nilubol N, Yao J, et al. Mutation-targeted therapy with sunitinib or everolimus in patients with advanced low-grade or intermediate-grade neuroendocrine tumours of the gastrointestinal tract and pancreas with or without cytoreductive surgery: protocol for a phase II clinical trial. BMJ Open. 2015 May 19;5(5):e008248.

44. Tang B, Li Y, Qi G, Yuan S, Wang Z, Yu S, et al. Clinicopathological Significance of CDKN2A Promoter Hypermethylation Frequency with Pancreatic Cancer. Sci Rep. 2015 Sep 4;5(1):13563.

45. House MG, Herman JG, Guo MZ, Hooker CM, Schulick RD, Lillemoe KD, et al. Aberrant Hypermethylation of Tumor Suppressor Genes in Pancreatic Endocrine Neoplasms. Ann Surg. 2003 Sep;238(3):423–32.

46. Serrano J, Goebel SU, Peghini PL, Lubensky IA, Gibril F, Jensen RT. Alterations in the p16INK4a/CDKN2A Tumor Suppressor Gene in Gastrinomas. J Clin Endocrinol Metab. 2000 Nov 1;85(11):4146–56.

47. Liu J, Xiao Q, Xiao J, Niu C, Li Y, Zhang X, et al. Wnt/β-catenin signalling: function, biological mechanisms, and therapeutic opportunities. Signal Transduct Target Ther. 2022 Jan 3;7:3.

48. Aoki K, Taketo MM. Adenomatous polyposis coli (APC): a multi-functional tumor suppressor gene. J Cell Sci. 2007 Oct 1;120(19):3327–35.

49. Arnold CN, Sosnowski A, Schmitt-Gräff A, Arnold R, Blum HE. Analysis of molecular pathways in sporadic neuroendocrine tumors of the gastro-entero-pancreatic system. Int J Cancer. 2007 May 15;120(10):2157–64.

50. Volodko N, Gordon M, Salla M, Ghazaleh HA, Baksh S. RASSF tumor suppressor gene family: Biological functions and regulation. FEBS Lett. 2014 Aug 19;588(16):2671–84.

51. Turner GB, Johnston BT, McCance DR, McGinty A, Watson RGP, Patterson CC, et al. Circulating markers of prognosis and response to treatment in patients with midgut carcinoid tumours. Gut. 2006 Nov;55(11):1586–91.

52. Califf RM. Biomarker definitions and their applications. Exp Biol Med. 2018 Feb;243(3):213–21.

53. Ma ZY, Gong YF, Zhuang HK, Zhou ZX, Huang SZ, Zou YP, et al. Pancreatic neuroendocrine tumors: A review of serum biomarkers, staging, and management. World J Gastroenterol. 2020 May 21;26(19):2305–22.

54. Sansone A, Lauretta R, Vottari S, Chiefari A, Barnabei A, Romanelli F, et al. Specific and Non-Specific Biomarkers in Neuroendocrine Gastroenteropancreatic Tumors. Cancers. 2019 Aug;11(8):1113.

55. Kanakis G, Kaltsas G. Biochemical markers for gastroenteropancreatic neuroendocrine tumours (GEP-NETs). Best Pract Res Clin Gastroenterol. 2012 Dec 1;26(6):791–802.

56. Modlin IM, Bodei L, Kidd M. Neuroendocrine tumor biomarkers: From monoanalytes to transcripts and algorithms. Best Pract Res Clin Endocrinol Metab. 2016 Jan 1;30(1):59–77.

57. Hofland J, Zandee WT, de Herder WW. Role of biomarker tests for diagnosis of neuroendocrine tumours. Nat Rev Endocrinol. 2018 Nov;14(11):656–69.

58. Smolkova B, Kataki A, Earl J, Ruz-Caracuel I, Cihova M, Urbanova M, et al. Liquid biopsy and preclinical tools for advancing diagnosis and treatment of patients with pancreatic neuroendocrine neoplasms. Crit Rev Oncol Hematol. 2022 Dec 1;180:103865.

59. van Adrichem RCS, Kamp K, Vandamme T, Peeters M, Feelders RA, de Herder WW. Serum neuron-specific enolase level is an independent predictor of overall survival in patients with gastroenteropancreatic neuroendocrine tumors. Ann Oncol. 2016 Apr 1;27(4):746–7.

60. Baudin E, Gigliotti A, Ducreux M, Ropers J, Comoy E, Sabourin JC, et al. Neuron-specific enolase and chromogranin A as markers of neuroendocrine tumours. Br J Cancer. 1998 Oct;78(8):1102–7.

61. Walter T, Chardon L, Chopin-laly X, Raverot V, Caffin AG, Chayvialle JA, et al. Is the combination of chromogranin A and pancreatic polypeptide serum determinations of interest in the diagnosis and follow-up of gastro-entero-pancreatic neuroendocrine tumours? Eur J Cancer. 2012 Aug 1;48(12):1766–73.

62. Ardill JES, Erikkson B. The importance of the measurement of circulating markers in patients with neuroendocrine tumours of the pancreas and gut. Endocr Relat Cancer. 2003 Dec 1;10(4):459–62.

63. Lokich JJ, Ganda OP, O'Hara CJ, Warren KW, Moertel CG, Klee G. Alpha-fetoprotein associated with islet cell tumors. Am J Clin Oncol. 1987 Apr;10(2):133–5.

64. Ramage JK, Davies AHG, Ardill J, Bax N, Caplin M, Grossman A, et al. Guidelines for the management of gastroenteropancreatic neuroendocrine (including carcinoid) tumours. Gut. 2005 Jun;54 Suppl 4(Suppl 4):iv1-16.

65. Jung JY, Kim YJ, Kim HM, Kim HJ, Park SW, Song SY, et al. Hepatoid carcinoma of the pancreas combined with neuroendocrine carcinoma. Gut Liver. 2010 Mar;4(1):98–102.

66. McIntire KR, Waldmann TA, Moertel CG, Go VL. Serum alpha-fetoprotein in patients with neoplasms of the gastrointestinal tract. Cancer Res. 1975 Apr;35(4):991–6.

67. Shah T, Srirajaskanthan R, Bhogal M, Toubanakis C, Meyer T, Noonan A, et al. Alpha-fetoprotein and human chorionic gonadotrophin-beta as prognostic markers in neuroendocrine tumour patients. Br J Cancer. 2008 Jul 8;99(1):72–7.

68. Kyriakopoulos G, Mavroeidi V, Chatzellis E, Kaltsas GA, Alexandraki KI. Histopathological, immunohistochemical, genetic and molecular markers of neuroendocrine neoplasms. Ann Transl Med. 2018 Jun;6(12):252.

69. de Herder WW, Niederle B, Scoazec JY, Pauwels S, Klöppel G, Falconi M, et al. Well-Differentiated Pancreatic Tumor/Carcinoma: Insulinoma. Neuroendocrinology. 2007 Feb 23;84(3):183–8.

70. Cryer PE, Axelrod L, Grossman AB, Heller SR, Montori VM, Seaquist ER, et al. Evaluation and management of adult hypoglycemic disorders: an Endocrine Society Clinical Practice Guideline. J Clin Endocrinol Metab. 2009 Mar;94(3):709–28.

71. Berna MJ, Hoffmann KM, Serrano J, Gibril F, Jensen RT. Serum gastrin in Zollinger-Ellison syndrome: I. Prospective study of fasting serum gastrin in 309 patients from the National Institutes of Health and comparison with 2229 cases from the literature. Medicine (Baltimore). 2006 Nov;85(6):295–330.

72. Berna MJ, Hoffmann KM, Long SH, Serrano J, Gibril F, Jensen RT. Serum gastrin in Zollinger-Ellison syndrome: II. Prospective study of gastrin provocative testing in 293 patients from the National Institutes of Health and comparison with 537 cases from the literature. evaluation of diagnostic criteria, proposal of new criteria, and correlations with clinical and tumoral features. Medicine (Baltimore). 2006 Nov;85(6):331–64.

73. Eldor R, Glaser B, Fraenkel M, Doviner V, Salmon A, Gross DJ. Glucagonoma and the glucagonoma syndrome – cumulative experience with an elusive endocrine tumour. Clin Endocrinol (Oxf). 2011;74(5):593–8.

74. Song X, Zheng S, Yang G, Xiong G, Cao Z, Feng M, et al. Glucagonoma and the glucagonoma syndrome. Oncol Lett. 2018 Mar;15(3):2749–55.

75. Mansour JC, Chen H. Pancreatic endocrine tumors. J Surg Res. 2004 Jul 1;120(1):139–61.

76. Martin S, Fica S, Parfeni O, Popa L, Manuc T, Rizea O, et al. Somatostatinoma and Neurofibromatosis Type 1-A Case Report and Review of the Literature. Diagnostics. 2020 Aug 21;10(9):620.

77. Öberg K, Knigge U, Kwekkeboom D, Perren A, ESMO Guidelines Working Group. Neuroendocrine gastro-entero-pancreatic tumors: ESMO Clinical Practice Guidelines for diagnosis, treatment and follow-up. Ann Oncol Off J Eur Soc Med Oncol. 2012 Oct;23 Suppl 7:vii124-130.

78. Luchini C, Pantanowitz L, Adsay V, Asa SL, Antonini P, Girolami I, et al. Ki-67 assessment of pancreatic neuroendocrine neoplasms: Systematic review and meta-analysis of manual vs. digital pathology scoring. Mod Pathol. 2022;35(6):712–20.

79. Li LT, Jiang G, Chen Q, Zheng JN. Ki67 is a promising molecular target in the diagnosis of cancer (Review). Mol Med Rep. 2015 Mar 1;11(3):1566–72.

80. La Rosa S. Diagnostic, Prognostic, and Predictive Role of Ki67 Proliferative Index in Neuroendocrine and Endocrine Neoplasms: Past, Present, and Future. Endocr Pathol. 2023;34(1):79–97.

81. Oberg K, Krenning E, Sundin A, Bodei L, Kidd M, Tesselaar M, et al. A Delphic consensus assessment: imaging and biomarkers in gastroenteropancreatic neuroendocrine tumor disease management. Endocr Connect. 2016 Sep;5(5):174–87.

82. Gupta M, Lloyd RV, Fischer-Colbrie R, Tischler AS, Dayal Y. Immunohistochemical expression of neuroendocrine secretory protein-55 (NESP-55) in pituitary adenomas. Endocr Pathol. 2011 Sep;22(3):150–4.

83. Tomita T. Significance of chromogranin A and synaptophysin in pancreatic neuroendocrine tumors. Bosn J Basic Med Sci. 2020 Aug;20(3):336–46.

84. Graham RP, Shrestha B, Caron BL, Smyrk TC, Grogg KL, Lloyd RV, et al. Islet-1 is a sensitive but not entirely specific marker for pancreatic neuroendocrine neoplasms and their metastases. Am J Surg Pathol. 2013 Mar;37(3):399–405.

85. Koo J, Mertens RB, Mirocha JM, Wang HL, Dhall D. Value of Islet 1 and PAX8 in identifying metastatic neuroendocrine tumors of pancreatic origin. Mod Pathol. 2012 Jun 1;25(6):893–901.

86. Tachibana T, Kasajima A, Aoki T, Tabata T, McNamara K, Yazdani S, et al. Progesteron receptor expression in insulin producing cells of neuroendocrine neoplasms. J Steroid Biochem Mol Biol. 2020 Jul 1;201:105694.

87. Roy PG, Thompson AM. Cyclin D1 and breast cancer. The Breast. 2006 Dec 1;15(6):718–27.

88. Chai SM, Brown IS, Kumarasinghe MP. Gastroenteropancreatic neuroendocrine neoplasms: selected pathology review and molecular updates. Histopathology. 2018;72(1):153–67.

89. Rodrigues M, Gabriel M, Heute D, Putzer D, Griesmacher A, Virgolini I. Concordance between results of somatostatin receptor scintigraphy with 111In-DOTA-DPhe 1-Tyr 3-octreotide and chromogranin A assay in patients with neuroendocrine tumours. Eur J Nucl Med Mol Imaging. 2008 Oct;35(10):1796–802.

90. Hope TA, Truillet C, Ehman EC, Afshar-Oromieh A, Aggarwal R, Ryan CJ, et al. 68Ga-PSMA-11 PET Imaging of Response to Androgen Receptor Inhibition: First Human Experience. J Nucl Med Off Publ Soc Nucl Med. 2017 Jan;58(1):81–4.

91. Sollini M, Erba PA, Fraternali A, Casali M, Di Paolo ML, Froio A, et al. PET and PET/CT with 68Gallium-Labeled Somatostatin Analogues in Non GEP-NETs Tumors. Sci World J. 2014 Feb 13;2014:194123.

92. Geijer H, Breimer LH. Somatostatin receptor PET/CT in neuroendocrine tumours: update on systematic review and meta-analysis. Eur J Nucl Med Mol Imaging. 2013 Oct;40(11):1770–80.

93. Squires MH, Volkan Adsay N, Schuster DM, Russell MC, Cardona K, Delman KA, et al. Octreoscan Versus FDG-PET for Neuroendocrine Tumor Staging: A Biological Approach. Ann Surg Oncol. 2015 Jul 1;22(7):2295–301.

94. Refardt J, Hofland J, Wild D, Christ E. New Directions in Imaging Neuroendocrine Neoplasms. Curr Oncol Rep. 2021 Nov 4;23(12):143.

95. Ehlers M, Allelein S, Haase M, Willenberg HS, Knoefel WT, Schott M. Circulating tumor cells in patients with neuroendocrine neoplasms. Horm Metab Res Horm Stoffwechselforschung Horm Metab. 2014 Sep;46(10):744–5.

96. Rizzo FM, Vesely C, Childs A, Marafioti T, Khan MS, Mandair D, et al. Circulating tumour cells and their association with bone metastases in patients with neuroendocrine tumours. Br J Cancer. 2019 Feb;120(3):294–300.

97. Oberg K, Modlin IM, De Herder W, Pavel M, Klimstra D, Frilling A, et al. Consensus on biomarkers for neuroendocrine tumour disease. Lancet Oncol. 2015 Sep;16(9):e435–46.

98. Khan MS, Tsigani T, Rashid M, Rabouhans JS, Yu D, Luong TV, et al. Circulating tumor cells and EpCAM expression in neuroendocrine tumors. Clin Cancer Res Off J Am Assoc Cancer Res. 2011 Jan 15;17(2):337–45.

99. Cowzer D, Shah RH, Chou JF, Kundra R, Punn S, Fiedler L, et al. Clinical utility of plasma cell-free DNA in pancreatic neuroendocrine neoplasms. Endocr Relat Cancer. 2024 Apr 1;31(4):e230292.

100. Malczewska A, Witkowska M, Makulik K, Bocian A, Walter A, Pilch-Kowalczyk J, et al. NETest liquid biopsy is diagnostic of small intestine and pancreatic neuroendocrine tumors and correlates with imaging. Endocr Connect. 2019 Mar 1;8(4):442–53.

101. Bodei L, Kidd MS, Singh A, van der Zwan WA, Severi S, Drozdov IA, et al. PRRT neuroendocrine tumor response monitored using circulating transcript analysis: the NETest. Eur J Nucl Med Mol Imaging. 2020 Apr;47(4):895–906.

102. Modlin IM, Kidd M, Oberg K, Falconi M, Filosso PL, Frilling A, et al. Early Identification of Residual Disease After Neuroendocrine Tumor Resection Using a Liquid Biopsy Multigenomic mRNA Signature (NETest). Ann Surg Oncol. 2021 Nov;28(12):7506–17.

103. Partelli S, Andreasi V, Muffatti F, Schiavo Lena M, Falconi M. Circulating Neuroendocrine Gene Transcripts (NETest): A Postoperative Strategy for Early Identification of the Efficacy of Radical Surgery for Pancreatic Neuroendocrine Tumors. Ann Surg Oncol. 2020 Oct;27(10):3928–36.

104. Takayanagi D, Cho H, Machida E, Kawamura A, Takashima A, Wada S, et al. Update on Epidemiology, Diagnosis, and Biomarkers in Gastroenteropancreatic Neuroendocrine Neoplasms. Cancers. 2022 Feb 22;14(5):1119.

105. Bartel DP. Metazoan MicroRNAs. Cell. 2018 Mar 22;173(1):20–51.

106. Bartel DP. MicroRNAs: genomics, biogenesis, mechanism, and function. Cell. 2004 Jan 23;116(2):281–97.

107. Wilczynska A, Bushell M. The complexity of miRNA-mediated repression. Cell Death Differ. 2015 Jan;22(1):22–33.

108. Hayes J, Peruzzi PP, Lawler S. MicroRNAs in cancer: biomarkers, functions and therapy. Trends Mol Med. 2014 Aug 1;20(8):460–9.

109. Huang W. MicroRNAs: Biomarkers, Diagnostics, and Therapeutics. In: Huang J, Borchert GM, Dou D, Huan J (Luke), Lan W, Tan M, et al., editors. Bioinformatics in MicroRNA Research [Internet]. New York, NY: Springer; 2017 [cited 2024 Apr 26]. p. 57–67. Available from: https://doi.org/10.1007/978-1-4939-7046-9_4

110. Wang J, Chen J, Sen S. MicroRNA as Biomarkers and Diagnostics. J Cell Physiol. 2016;231(1):25–30.

111. Liang Y, Ridzon D, Wong L, Chen C. Characterization of microRNA expression profiles in normal human tissues. BMC Genomics. 2007 Jun 12;8(1):166.

112. Schanen BC, Li X. Transcriptional regulation of mammalian miRNA genes. Genomics. 2011 Jan 1;97(1):1–6.

113. O'Brien J, Hayder H, Zayed Y, Peng C. Overview of MicroRNA Biogenesis, Mechanisms of Actions, and Circulation. Front Endocrinol. 2018;9:402.

114. MacFarlane LA, Murphy PR. MicroRNA: Biogenesis, Function and Role in Cancer. Curr Genomics. 2010 Nov;11(7):537–61.

115. Bedi K, Paulsen MT, Wilson TE, Ljungman M. Characterization of novel primary miRNA transcription units in human cells using Bru-seq nascent RNA sequencing. NAR Genomics Bioinforma. 2019 Oct 30;2(1):lqz014.

116. Ha M, Kim VN. Regulation of microRNA biogenesis. Nat Rev Mol Cell Biol. 2014 Aug;15(8):509–24.

117. Denli AM, Tops BBJ, Plasterk RHA, Ketting RF, Hannon GJ. Processing of primary microRNAs by the Microprocessor complex. Nature. 2004 Nov 11;432(7014):231–5.

118. Alarcón CR, Lee H, Goodarzi H, Halberg N, Tavazoie SF. N6-methyladenosine marks primary microRNAs for processing. Nature. 2015 Mar 26;519(7544):482–5.

119. Okada C, Yamashita E, Lee SJ, Shibata S, Katahira J, Nakagawa A, et al. A high-resolution structure of the pre-microRNA nuclear export machinery. Science. 2009 Nov 27;326(5957):1275–9.

120. Yoda M, Kawamata T, Paroo Z, Ye X, Iwasaki S, Liu Q, et al. ATP-dependent human RISC assembly pathways. Nat Struct Mol Biol. 2010 Jan;17(1):17–23.

121. Khvorova A, Reynolds A, Jayasena SD. Functional siRNAs and miRNAs exhibit strand bias. Cell. 2003 Oct 17;115(2):209–16.

122. Zhukova M, Schedl P, Shidlovskii YV. The role of secondary structures in the functioning of 3′ untranslated regions of mRNA. BioEssays. 2024;46(3):2300099.

123. Braun JE, Huntzinger E, Izaurralde E. A Molecular Link between miRISCs and Deadenylases Provides New Insight into the Mechanism of Gene Silencing by MicroRNAs. Cold Spring Harb Perspect Biol [Internet]. 2012 Dec [cited 2024 Apr 24];4(12). Available from: https://www.ncbi.nlm.nih.gov/pmc/articles/PMC3504443/

124. Buhagiar AF, Kleaveland B. To kill a microRNA: emerging concepts in target-directed microRNA degradation. Nucleic Acids Res. 2024 Feb 28;52(4):1558–74.

125. Stavast CJ, Erkeland SJ. The Non-Canonical Aspects of MicroRNAs: Many Roads to Gene Regulation. Cells. 2019 Nov 19;8(11):1465.

126. Zhou L, Lim MYT, Kaur P, Saj A, Bortolamiol-Becet D, Gopal V, et al. Importance of miRNA stability and alternative primary miRNA isoforms in gene regulation during Drosophila development. eLife. 7:e38389.

127. Zhang Z, Qin YW, Brewer G, Jing Q. MicroRNA degradation and turnover: regulating the regulators. Wiley Interdiscip Rev RNA. 2012;3(4):593–600.

128. Marzi MJ, Ghini F, Cerruti B, de Pretis S, Bonetti P, Giacomelli C, et al. Degradation dynamics of microRNAs revealed by a novel pulse-chase approach. Genome Res. 2016 Apr;26(4):554–65.

129. Di Leva G, Garofalo M, Croce CM. microRNAs in cancer. Annu Rev Pathol. 2014;9:287–314.

130. Hanahan D, Weinberg RA. Hallmarks of cancer: the next generation. Cell. 2011 Mar 4;144(5):646–74.

131. Peng Y, Croce CM. The role of MicroRNAs in human cancer. Signal Transduct Target Ther. 2016 Jan 28;1(1):1–9.

132. Esquela-Kerscher A, Slack FJ. Oncomirs — microRNAs with a role in cancer. Nat Rev Cancer. 2006 Apr;6(4):259–69.

133. Cortez MA, Bueso-Ramos C, Ferdin J, Lopez-Berestein G, Sood AK, Calin GA. MicroRNAs in body fluids--the mix of hormones and biomarkers. Nat Rev Clin Oncol. 2011 Jun 7;8(8):467–77.

134. Havasi A, Sur D, Cainap SS, Lungulescu CV, Gavrilas LI, Cainap C, et al. Current and New Challenges in the Management of Pancreatic Neuroendocrine Tumors: The Role of miRNA-Based Approaches as New Reliable Biomarkers. Int J Mol Sci. 2022 Jan 20;23(3):1109.

135. Thorns C, Schurmann C, Gebauer N, Wallaschofski H, Kümpers C, Bernard V, et al. Global microRNA profiling of pancreatic neuroendocrine neoplasias. Anticancer Res. 2014 May;34(5):2249–54.

136. Roldo C, Missiaglia E, Hagan JP, Falconi M, Capelli P, Bersani S, et al. MicroRNA expression abnormalities in pancreatic endocrine and acinar tumors are associated with

distinctive pathologic features and clinical behavior. J Clin Oncol Off J Am Soc Clin Oncol. 2006 Oct 10;24(29):4677–84.

137. Vicentini C, Calore F, Nigita G, Fadda P, Simbolo M, Sperandio N, et al. Exosomal miRNA signatures of pancreatic lesions. BMC Gastroenterol. 2020 May 6;20(1):137.

138. Matthaei H, Wylie D, Lloyd MB, Dal Molin M, Kemppainen J, Mayo SC, et al. miRNA biomarkers in cyst fluid augment the diagnosis and management of pancreatic cysts. Clin Cancer Res Off J Am Assoc Cancer Res. 2012 Sep 1;18(17):4713–24.

139. Kövesdi A, Kurucz PA, Nyírő G, Darvasi O, Patócs A, Butz H. Circulating miRNA Increases the Diagnostic Accuracy of Chromogranin A in Metastatic Pancreatic Neuroendocrine Tumors. Cancers. 2020 Sep 2;12(9):2488.

140. Panarelli N, Tyryshkin K, Wong JJM, Majewski A, Yang X, Scognamiglio T, et al. Evaluating gastroenteropancreatic neuroendocrine tumors through microRNA sequencing. Endocr Relat Cancer. 2019 Jan 1;26(1):47–57.

141. Zimmermann N, Knief J, Kacprowski T, Lazar-Karsten P, Keck T, Billmann F, et al. MicroRNA analysis of gastroenteropancreatic neuroendocrine tumors and metastases. Oncotarget. 2018 Jun 19;9(47):28379–90.

142. Grolmusz VK, Kövesdi A, Borks K, Igaz P, Patócs A. Prognostic relevance of proliferation-related miRNAs in pancreatic neuroendocrine neoplasms. Eur J Endocrinol. 2018 Oct 1;179(4):219–28.

143. Gill P, Kim E, Chua TC, Clifton-Bligh RJ, Nahm CB, Mittal A, et al. MiRNA-3653 Is a Potential Tissue Biomarker for Increased Metastatic Risk in Pancreatic Neuroendocrine Tumours. Endocr Pathol. 2019 Jun;30(2):128–33.

144. Cavalcanti E, Galleggiante V, Coletta S, Stasi E, Chieppa M, Armentano R, et al. Altered miRNAs Expression Correlates With Gastroenteropancreatic Neuroendocrine Tumors Grades. Front Oncol. 2020;10:1187.

145. Lee YS, Kim H, Kim HW, Lee JC, Paik KH, Kang J, et al. High Expression of MicroRNA-196a Indicates Poor Prognosis in Resected Pancreatic Neuroendocrine Tumor. Medicine (Baltimore). 2015 Dec 18;94(50):e2224.

146. Klieser E, Urbas R, Swierczynski S, Stättner S, Primavesi F, Jäger T, et al. HDAC-Linked 'Proliferative' miRNA Expression Pattern in Pancreatic Neuroendocrine Tumors. Int J Mol Sci. 2018 Sep 15;19(9):2781.

147. Krützfeldt J, Rajewsky N, Braich R, Rajeev KG, Tuschl T, Manoharan M, et al. Silencing of microRNAs in vivo with 'antagomirs'. Nature. 2005 Dec 1;438(7068):685–9.

148. Dettori D, Orso F, Penna E, Baruffaldi D, Brundu S, Maione F, et al. Therapeutic Silencing of miR-214 Inhibits Tumor Progression in Multiple Mouse Models. Mol Ther J Am Soc Gene Ther. 2018 Aug 1;26(8):2008–18.

149. Zhang T, Choi S, Zhang T, Chen Z, Chi Y, Huang S, et al. miR-431 Promotes Metastasis of Pancreatic Neuroendocrine Tumors by Targeting DAB2 Interacting

Protein, a Ras GTPase Activating Protein Tumor Suppressor. Am J Pathol. 2020 Mar 1;190(3):689–701.

150. Yamana H, Kato K, Kobara H, Fujihara S, Fujita K, Namima D, et al. Metformin Inhibits Proliferation and Tumor Growth of QGP-1 Pancreatic Neuroendocrine Tumor Cells by Inducing Cell Cycle Arrest and Apoptosis. Anticancer Res. 2020 Jan;40(1):121–32.

151. Hosseinahli N, Aghapour M, Duijf PHG, Baradaran B. Treating cancer with microRNA replacement therapy: A literature review. J Cell Physiol. 2018 Aug;233(8):5574–88.

152. Bai J, Na H, Hua X, Wei Y, Ye T, Zhang Y, et al. A retrospective study of NENs and miR-224 promotes apoptosis of BON-1 cells by targeting PCSK9 inhibition. Oncotarget. 2016 Dec 28;8(4):6929–39.

153. Pritchard CC, Cheng HH, Tewari M. MicroRNA profiling: approaches and considerations. Nat Rev Genet. 2012 Apr 18;13(5):358–69.

154. Liu J, Jennings SF, Tong W, Hong H. Next generation sequencing for profiling expression of miRNAs: technical progress and applications in drug development. J Biomed Sci Eng. 2011 Oct;4(10):666–76.

155. Wark AW, Lee HJ, Corn RM. Multiplexed detection methods for profiling microRNA expression in biological samples. Angew Chem Int Ed Engl. 2008;47(4):644–52.

156. Wyman SK, Knouf EC, Parkin RK, Fritz BR, Lin DW, Dennis LM, et al. Post-transcriptional generation of miRNA variants by multiple nucleotidyl transferases contributes to miRNA transcriptome complexity. Genome Res. 2011 Sep;21(9):1450–61.

157. Benesova S, Kubista M, Valihrach L. Small RNA-Sequencing: Approaches and Considerations for miRNA Analysis. Diagnostics. 2021 May 27;11(6):964.

158. Calin GA, Croce CM. MicroRNA signatures in human cancers. Nat Rev Cancer. 2006 Nov;6(11):857–66.

159. Koppers-Lalic D, Hackenberg M, de Menezes R, Misovic B, Wachalska M, Geldof A, et al. Non-invasive prostate cancer detection by measuring miRNA variants (isomiRs) in urine extracellular vesicles. Oncotarget. 2016 Apr 19;7(16):22566–78.

160. Telonis AG, Loher P, Jing Y, Londin E, Rigoutsos I. Beyond the one-locus-one-miRNA paradigm: microRNA isoforms enable deeper insights into breast cancer heterogeneity. Nucleic Acids Res. 2015 Oct 30;43(19):9158–75.

161. Telonis AG, Magee R, Loher P, Chervoneva I, Londin E, Rigoutsos I. Knowledge about the presence or absence of miRNA isoforms (isomiRs) can successfully discriminate amongst 32 TCGA cancer types. Nucleic Acids Res. 2017 Apr 7;45(6):2973–85.

162. Ono S, Lam S, Nagahara M, Hoon DSB. Circulating microRNA Biomarkers as Liquid Biopsy for Cancer Patients: Pros and Cons of Current Assays. J Clin Med. 2015 Oct 23;4(10):1890–907.

163. Valihrach L, Androvic P, Kubista M. Circulating miRNA analysis for cancer diagnostics and therapy. Mol Aspects Med. 2020 Apr;72:100825.

164. Riolo G, Cantara S, Marzocchi C, Ricci C. miRNA Targets: From Prediction Tools to Experimental Validation. Methods Protoc. 2020 Dec 24;4(1):1.

165. Liu B, Li J, Cairns MJ. Identifying miRNAs, targets and functions. Brief Bioinform. 2014 Jan 1;15(1):1–19.

166. Agarwal V, Bell GW, Nam JW, Bartel DP. Predicting effective microRNA target sites in mammalian mRNAs. Izaurralde E, editor. eLife. 2015 Aug 12;4:e05005.

167. Rehmsmeier M, Steffen P, Höchsmann M, Giegerich R. Fast and effective prediction of microRNA/target duplexes. RNA. 2004 Jan 10;10(10):1507–17.

168. Kertesz M, Iovino N, Unnerstall U, Gaul U, Segal E. The role of site accessibility in microRNA target recognition. Nat Genet. 2007 Oct;39(10):1278–84.

169. Krek A, Grün D, Poy MN, Wolf R, Rosenberg L, Epstein EJ, et al. Combinatorial microRNA target predictions. Nat Genet. 2005 May;37(5):495–500.

170. Miranda KC, Huynh T, Tay Y, Ang YS, Tam WL, Thomson AM, et al. A Pattern-Based Method for the Identification of MicroRNA Binding Sites and Their Corresponding Heteroduplexes. Cell. 2006 Sep 22;126(6):1203–17.

171. Marín RM, Šulc M, Vaníček J. Searching the coding region for microRNA targets. RNA. 2013 Jan 4;19(4):467–74.

172. Pattern Recognition and Machine Learning [Internet]. Springer New York; 2006 [cited 2024 Apr 24]. Available from: https://link.springer.com/deleted

173. Chen Y, Wang X. miRDB: an online database for prediction of functional microRNA targets. Nucleic Acids Res. 2020 Jan 8;48(D1):D127–31.

174. Chou CH, Shrestha S, Yang CD, Chang NW, Lin YL, Liao KW, et al. miRTarBase update 2018: a resource for experimentally validated microRNA-target interactions. Nucleic Acids Res. 2018 Jan 4;46(D1):D296–302.

175. Karagkouni D, Paraskevopoulou MD, Chatzopoulos S, Vlachos IS, Tastsoglou S, Kanellos I, et al. DIANA-TarBase v8: a decade-long collection of experimentally supported miRNA-gene interactions. Nucleic Acids Res. 2018 Jan 4;46(D1):D239–45.

176. Xiao F, Zuo Z, Cai G, Kang S, Gao X, Li T. miRecords: an integrated resource for microRNA-target interactions. Nucleic Acids Res. 2009 Jan;37(Database issue):D105-110.

177. SMARTer Stranded Total RNA-Seq Kit [Internet]. [cited 2024 May 30]. Available from: https://www.takarabio.com/products/next-generation-sequencing/rna-seq/legacy-rna-seq-kits/pico-input-strand-specific-total-rna-seq-for-mammalian-samples-v3

178. Babraham Bioinformatics - FastQC A Quality Control tool for High Throughput Sequence Data [Internet]. [cited 2024 Apr 26]. Available from: http://www.bioinformatics.babraham.ac.uk/projects/fastqc/

179. Martin M. Cutadapt removes adapter sequences from high-throughput sequencing reads. EMBnet.journal. 2011 May 2;17(1):10–2.

180. Smith T, Heger A, Sudbery I. UMI-tools: modeling sequencing errors in Unique Molecular Identifiers to improve quantification accuracy. Genome Res. 2017 Mar;27(3):491–9.

181. Dobin A, Davis CA, Schlesinger F, Drenkow J, Zaleski C, Jha S, et al. STAR: ultrafast universal RNA-seq aligner. Bioinformatics. 2013 Jan;29(1):15–21.

182. Liao Y, Smyth GK, Shi W. featureCounts: an efficient general purpose program for assigning sequence reads to genomic features. Bioinformatics. 2014 Apr 1;30(7):923–30.

183. Love MI, Huber W, Anders S. Moderated estimation of fold change and dispersion for RNA-seq data with DESeq2. Genome Biol. 2014 Dec 5;15(12):550.

184. Li Y, Ge X, Peng F, Li W, Li JJ. Exaggerated false positives by popular differential expression methods when analyzing human population samples. Genome Biol. 2022 Mar 15;23(1):79.

185. Shahapure KR, Nicholas C. Cluster Quality Analysis Using Silhouette Score. In: 2020 IEEE 7th International Conference on Data Science and Advanced Analytics (DSAA) [Internet]. 2020 [cited 2024 Jul 18]. p. 747–8. Available from: https://ieeexplore.ieee.org/document/9260048

186. The Gene Ontology Consortium, Aleksander SA, Balhoff J, Carbon S, Cherry JM, Drabkin HJ, et al. The Gene Ontology knowledgebase in 2023. Genetics. 2023 May 2;224(1):iyad031.

187. Ashburner M, Ball CA, Blake JA, Botstein D, Butler H, Cherry JM, et al. Gene ontology: tool for the unification of biology. The Gene Ontology Consortium. Nat Genet. 2000 May;25(1):25–9.

188. Sherman BT, Hao M, Qiu J, Jiao X, Baseler MW, Lane HC, et al. DAVID: a web server for functional enrichment analysis and functional annotation of gene lists (2021 update). Nucleic Acids Res. 2022 Jul 5;50(W1):W216–21.

189. Cieslak MC, Castelfranco AM, Roncalli V, Lenz PH, Hartline DK. t-Distributed Stochastic Neighbor Embedding (t-SNE): A tool for eco-physiological transcriptomic analysis. Mar Genomics. 2020 Jun 1;51:100723.

190. QIAseq miRNA Library Kit | microRNA Library Prep | QIAGEN [Internet]. [cited 2024 May 30]. Available from: https://www.qiagen.com/us/products/discovery-and-

translational-research/next-generation-sequencing/rna-sequencing/mirna-small-rnaseq/qiaseq-mirna-ngs

191. Schmittgen TD, Livak KJ. Analyzing real-time PCR data by the comparative CT method. Nat Protoc. 2008 Jun;3(6):1101–8.

192. Pedro Lopez-Romero <Plopez@Cnic. Es>. AgiMicroRna [Internet]. Bioconductor; 2017 [cited 2024 Jul 30]. Available from: https://bioconductor.org/packages/AgiMicroRna

193. Zhao Y, Wong L, Goh WWB. How to do quantile normalization correctly for gene expression data analyses. Sci Rep. 2020 Sep 23;10(1):15534.

194. Yu G, Wang LG, Han Y, He QY. clusterProfiler: an R Package for Comparing Biological Themes Among Gene Clusters. OMICS J Integr Biol. 2012 May;16(5):284–7.

195. Luo W, Brouwer C. Pathview: an R/Bioconductor package for pathway-based data integration and visualization. Bioinforma Oxf Engl. 2013 Jul 15;29(14):1830–1.

196. Tang D, Chen M, Huang X, Zhang G, Zeng L, Zhang G, et al. SRplot: A free online platform for data visualization and graphing. PloS One. 2023;18(11):e0294236.

197. Parbhu SK, Adler DG. Pancreatic neuroendocrine tumors: contemporary diagnosis and management. Hosp Pract. 2016 May 26;44(3):109–19.

198. Li D, Rock A, Kessler J, Ballena R, Hyder S, Mo C, et al. Understanding the Management and Treatment of Well-Differentiated Pancreatic Neuroendocrine Tumors: A Clinician's Guide to a Complex Illness. JCO Oncol Pract. 2020 Nov;16(11):720–8.

199. Amin MB, Greene FL, Edge SB, Compton CC, Gershenwald JE, Brookland RK, et al. The Eighth Edition AJCC Cancer Staging Manual: Continuing to build a bridge from a population-based to a more 'personalized' approach to cancer staging. CA Cancer J Clin. 2017 Mar;67(2):93–9.

200. Attaway CC, Yang Z, Wu RI. Diversity and pitfalls of pancreatic neuroendocrine tumors: A case series of cytologic-histologic correlation. Hum Pathol Rep. 2022 Jun 1;28:300630.

201. Werle SD, Ikonomi N, Lausser L, Kestler AMTU, Weidner FM, Schwab JD, et al. A systems biology approach to define mechanisms, phenotypes, and drivers in PanNETs with a personalized perspective. Npj Syst Biol Appl. 2023 Jun 3;9(1):1–17.

202. Zhou HQ, Chen QC, Qiu ZT, Tan WL, Mo CQ, Gao SW. Integrative microRNA-mRNA and protein-protein interaction analysis in pancreatic neuroendocrine tumors. Eur Rev Med Pharmacol Sci. 2016 Jul;20(13):2842–52.

203. Keener J, Sneyd J. Neuroendocrine Cells. In: Keener J, Sneyd J, editors. Mathematical Physiology: I: Cellular Physiology [Internet]. New York, NY: Springer; 2009 [cited 2024 May 16]. p. 385–426. Available from: https://doi.org/10.1007/978-0-387-75847-3_9

204. Scherübl H, Hescheler J, Bychkov R, Cuber JC, John M, Riecken EO, et al. Electrical activity and calcium channels in neuroendocrine cells. Ann N Y Acad Sci. 1994 Sep 15;733:335–9.

205. Yan J, Yu S, Jia C, Li M, Chen J. Molecular subtyping in pancreatic neuroendocrine neoplasms: New insights into clinical, pathological unmet needs and challenges. Biochim Biophys Acta BBA - Rev Cancer. 2020 Aug 1;1874(1):188367.

206. Al-thoubaity FK. Molecular classification of breast cancer: A retrospective cohort study. Ann Med Surg. 2019 Dec 6;49:44–8.

207. Inwald EC, Koller M, Klinkhammer-Schalke M, Zeman F, Hofstädter F, Gerstenhauer M, et al. 4-IHC classification of breast cancer subtypes in a large cohort of a clinical cancer registry: use in clinical routine for therapeutic decisions and its effect on survival. Breast Cancer Res Treat. 2015 Oct 1;153(3):647–58.

208. Heverhagen AE, Legrand N, Wagner V, Fendrich V, Bartsch DK, Slater EP. Overexpression of MicroRNA miR-7-5p Is a Potential Biomarker in Neuroendocrine Neoplasms of the Small Intestine. Neuroendocrinology. 2018;106(4):312–7.

209. Nanayakkara J, Tyryshkin K, Yang X, Wong JJM, Vanderbeck K, Ginter PS, et al. Characterizing and classifying neuroendocrine neoplasms through microRNA sequencing and data mining. NAR Cancer. 2020 Sep 1;2(3):zcaa009.

210. Downing S, Zhang F, Chen Z, Tzanakakis ES. MicroRNA-7 directly targets Reg1 in pancreatic cells. Am J Physiol-Cell Physiol. 2019 Aug;317(2):C366–74.

211. Ruan Y, Chen L, Xie D, Luo T, Xu Y, Ye T, et al. Mechanisms of Cell Adhesion Molecules in Endocrine-Related Cancers: A Concise Outlook. Front Endocrinol [Internet]. 2022 [cited 2024 Feb 21];13. Available from: https://www.frontiersin.org/journals/endocrinology/articles/10.3389/fendo.2022.865436

212. Ezzat S, Asa SL. The molecular pathogenetic role of cell adhesion in endocrine neoplasia. J Clin Pathol. 2005 Nov;58(11):1121–5.

213. Marques P, Barry S, Carlsen E, Collier D, Ronaldson A, Grieve J, et al. The expression of neural cell adhesion molecule and the microenvironment of pituitary neuroendocrine tumours. J Neuroendocrinol. 2021;33(12):e13052.

214. Pollerberg GE, Thelen K, Theiss MO, Hochlehnert BC. The role of cell adhesion molecules for navigating axons: Density matters. Mech Dev. 2013 Jun 1;130(6):359–72.

215. Tanigawa M, Nakayama M, Taira T, Hattori S, Mihara Y, Kondo R, et al. Insulinoma-associated protein 1 (INSM1) is a useful marker for pancreatic neuroendocrine tumor. Med Mol Morphol. 2018 Mar 1;51(1):32–40.

216. Liu B, Kudo A, Kinowaki Y, Ogura T, Ogawa K, Ono H, et al. A simple and practical index predicting the prognoses of the patients with well-differentiated pancreatic neuroendocrine neoplasms. J Gastroenterol. 2019 Sep;54(9):819–28.

217. Chen X, Guo C, Cui W, Sun K, Wang Z, Chen X. CD56 Expression Is Associated with Biological Behavior of Pancreatic Neuroendocrine Neoplasms. Cancer Manag Res. 2020 Jun 17;12:4625–31.

218. Li Y, Bi X, Zhao J, Huang Z, Zhou J, Li Z, et al. CEA Level, Radical Surgery, CD56 and CgA Expression Are Prognostic Factors for Patients With Locoregional Gastrin-Independent GNET. Medicine (Baltimore). 2016 May;95(18):e3567.

219. Borka K, Kaliszky P, Szabó E, Lotz G, Kupcsulik P, Schaff Z, et al. Claudin expression in pancreatic endocrine tumors as compared with ductal adenocarcinomas. Virchows Arch. 2007 Apr 26;450(5):549–57.

220. Jannin A, Dessein AF, Do Cao C, Vantyghem MC, Chevalier B, Van Seuningen I, et al. Metabolism of pancreatic neuroendocrine tumors: what can omics tell us? Front Endocrinol [Internet]. 2023 [cited 2024 Feb 21];14. Available from: https://www.frontiersin.org/journals/endocrinology/articles/10.3389/fendo.2023.1248575

221. Peleli M, Antoniadou I, Rodrigues-Junior DM, Savvoulidou O, Caja L, Katsouda A, et al. Cystathionine gamma-lyase (CTH) inhibition attenuates glioblastoma formation. Redox Biol. 2023 Jun 5;64:102773.

222. Ramadhan IA, Sulaiman LR, Salihi A. NOS3 and CTH gene mutations as new molecular markers for detection of lung adenocarcinoma. PeerJ. 2023 Dec 12;11:e16209.

223. Wang Y, Huang J, Chen W, Wang R, Kao M, Pan Y, et al. Dysregulation of cystathionine γ-lyase promotes prostate cancer progression and metastasis. EMBO Rep. 2019 Oct 4;20(10):e45986.

224. Xiang J, Wu X, Liu W, Wei H, Zhu Z, Liu S, et al. Bioinformatic analyzes and validation of cystathionine gamma-lyase as a prognostic biomarker and related to immune infiltrates in hepatocellular carcinoma. Heliyon. 2023 May 1;9(5):e16152.

225. Bonifácio VDB, Pereira SA, Serpa J, Vicente JB. Cysteine metabolic circuitries: druggable targets in cancer. Br J Cancer. 2021 Mar;124(5):862–79.

226. Szabo C. Gasotransmitters in cancer: from pathophysiology to experimental therapy. Nat Rev Drug Discov. 2016 Mar;15(3):185–203.

227. Lauinger L, Kaiser P. Sensing and Signaling of Methionine Metabolism. Metabolites. 2021 Jan 31;11(2):83.

228. Malczewska A, Kidd M, Matar S, Kos-Kudla B, Modlin IM. A Comprehensive Assessment of the Role of miRNAs as Biomarkers in Gastroenteropancreatic Neuroendocrine Tumors. Neuroendocrinology. 2018;107(1):73–90.

229. Said S, Kurtin PJ, Nasr SH, Graham RP, Dasari S, Vrana JA, et al. Carboxypeptidase A1 and regenerating islet-derived 1α as new markers for pancreatic acinar cell carcinoma. Hum Pathol. 2020 Sep;103:120–6.

230. Uhlig R, Contreras H, Weidemann S, Gorbokon N, Menz A, Büscheck F, et al. Carboxypeptidase A1 (CPA1) Immunohistochemistry Is Highly Sensitive and Specific for Acinar Cell Carcinoma (ACC) of the Pancreas. Am J Surg Pathol. 2022 Jan;46(1):97–104.